Regulation of polyamine biosynthesis
in *Saccharomyces cerevisiae*

Inaugural-Dissertation

zur

Erlangung des Doktorgrades
der Mathematisch-Naturwissenschaftlichen Fakultät

der Universität zu Köln

vorgelegt von

Palani Murugan Rangasamy

aus Tamilnadu, Indien

Köln, März 2005

1. Berichterstatter:

Prof. Dr. R. Jürgen Dohmen

2. Berichterstatter:

Prof. Dr. Thomas Langer

3. Berichterstatter:

Prof. Dr. Martin Scheffner

Table of Contents

Table of Contents

Appendix

Acknowledgements

Eidesstattliche Erklärung

Lebenslauf

1 Zusammenfassung

Polyamine sind essentielle organische Kationen mit vielfältigen zellulären Funktionen. Ihre Synthese wird durch eine „Feedback"-Regulation kontrolliert, deren hauptsächliches Ziel die Ornithindecarboxylase (ODC) ist. ODC ist das geschwindigkeitsbestimmende Enzym in der Polyaminbiosynthese. Es war bekannt, dass ODC in Säugerzellen durch ODC-Antizym inhibiert und der Ubiquitin-unabhängigen Proteolyse zugeführt wird. Die Synthese von Antizym in Säugerzellen beinhalten einen Polyamin-induzierten ribosomalen Leserastersprung. Hohe Polyamin-Konzentrationen inhibieren somit die *de novo* Synthese von Polyaminen, indem sie den Abbau von ODC induzieren. In dieser Arbeit wurde eine zuvor nicht bekannte Sequenz im Genom der Hefe *Saccharomyces cerevisiae* identifiziert, die für ein Antizym (Oaz1) in dieser Hefe kodiert. Sequenzelemente mit der Bezeichnung **OFRE** (*OAZ1* Frameshifting Repressor Element) und **OPRE** (*OAZ1* Polyamine Responsive Element), die für die Polyamine-Regulation des Leserastersprungs verantwortlich sind, wurden in der *OAZ1* mRNA kartiert. Der Abbau von ODC der Hefe durch das Proteasom benötigt Oaz1. Oaz1 vermittelt den Abbau von ODC, in dem es an dasselbe bindet, wodurch ein Abbausignal (**ODS** für „ODC degradation signal") am N-Terminus exponiert wird, dass in dieser Arbeit identifiziert wurde. Mit Hilfe von Testproteinen, die dieses neue ODS-Abbausignal trugen, konnte eine Rolle des Transportfaktors Rad23 entdeckt werden. Es konnte außerdem gezeigt werden, dass ODS in vivo mit verschiedenen Untereinheiten des „Lid"-Komplexes des 19S-Aktivatorkomplexes des 26S-Proteasoms interagiert. Mithilfe des neuen Hefemodellsystems für das Studium der Polyaminregulation konnte ein neuer Kontrollmechanismus identifiziert werden. Oaz1 wird selbst durch Ubiquitin-abhängige Proteolyse durch das Proteasom reguliert. Der Abbau von Oaz1 wird durch Polyamine inhibiert. Diese Beobachtungen führten zu einem Modell, in dem Polyamine ihre Synthese durch zwei Mechanismen hemmen. Zum einen stimulieren sie die Synthese durch Erhöhung der Häufigkeit des Leserastersprungs bei der Translation der *OAZ1*-mRNA, zum anderen inhibieren sie den Abbau von Oaz1.

Im zweiten Teil dieser Arbeit wurden sogenannte Peptid-Aptamere isoliert, die den Ubiquitin-vermittelten Abbau von Testsubstraten über das Proteasom inhibieren. Diese Aptamere inhibieren entweder die Ubiquitylierung oder direkt das Proteasom und führen so zu einer *in vivo* Stabilisierung der Testsubstrate. Testsubstrate mit dem ODS-

Abbaussignal (siehe oben) können wegen ihres Ubiquitin-<u>un</u>abhängigen Abbaus in der Zukunft eingesetzt werden, um weitere potentiell klinisch relevante Peptidinhibitoren zu identifizieren, die spezifisch die Funktion des Proteasoms stören.

2 Abstract

Polyamines are essential organic cations with multiple cellular functions. Their synthesis is controlled by a feedback regulation whose main target is ornithine decarboxylase (ODC), the rate-limiting enzyme in polyamine biosynthesis. In mammals, ODC has been shown to be inhibited and targeted for ubiquitin-independent degradation by ODC antizyme. The synthesis of mammalian antizyme was reported to involve a polyamine-induced ribosomal frameshifting mechanism. High levels of polyamine therefore inhibit new synthesis of polyamines by inducing ODC degradation. In this work, a previously unrecognized sequence in the genome of *Saccharomyces cerevisiae* encoding an orthologue of mammalian antizyme was identified. Synthesis of yeast antizyme (Oaz1) involves polyamine-regulated frameshifting. New elements, termed **OFRE** (*OAZ1* frameshifting repressor element) and **OPRE** (*OAZ1* polyamine responsive element) that are necessary for the polyamines to regulate frameshifting were mapped in the *OAZ1 mRNA*. Degradation of yeast ODC by the proteasome depends on Oaz1. Oaz1 mediates the degradation by binding to ODC thereby exposing a degradation signal at the N-terminus of ODC. Using the novel transplantable yeast ODC degradation signal (**ODS**) identified in this work a new possible role of the shuttle factor Rad23 in ODC degradation was identified. In addition, ODS is shown to interact with multiple 19S lid subunits in the proteasome. Using this novel model system for polyamine regulation another level of its control was discovered. Oaz1 itself is subject to ubiquitin-mediated proteolysis by the proteasome. Degradation of Oaz1, however, is efficiently inhibited by polyamines. I propose a model, in which polyamines inhibit their ODC-mediated biosynthesis by two mechanisms, the control of Oaz1 synthesis and inhibition of its degradation.

In a second part of the work, peptide aptamers were isolated that inhibit the ubiquitin-dependent turnover of test substrates of the proteasome. These aptamers appear to either inhibit ubiquitylation or the proteasome and thereby lead to a stabilization of test substrates. I Propose that ODS due to its ubiquitin-independent mode of degradation can be used as a tool in aptamer screens that are aimed at identifying additional peptide inhibitors of the proteasome with potential clinical relevance.

3 Introduction

Small molecules are very important for the existence of life. Examples are nucleotides, which makes up the genetic material, and the amino acids that are the building blocks of proteins. However there are many small molecules that are essential for life without having to attain a macromolecular form. To illustrate the later type of molecule, the polyamines are one of the best examples. Polyamines are essential for life and they are associated with all life forms ranging from the most primitive to the most elaborate ones. Many chemists have long back discovered polyamines, however their association with life became clear only in 1687 after Antonie Van Lewenhoeck's observation that the seminal fluid contains a slowly crystallizing substance that was later identified as the polyamine spermine phosphate (Lewenhoeck, 1678). Thereafter many studies have contributed to understanding the role of polyamines in the evolution and the existence of life (Cohen, 1998). Although it is far from clear what all the functions of polyamines are, certainly the most important ones are their association with DNA and RNA (Coffino, 2001b). This association stabilizes the structure of DNA and RNA. Polyamines neutralize the negative charges in DNA thereby allowing it to be condensed into the chromosomes. On the other side, abnormal levels of polyamines are also associated with many diseases including cancer. Many genetic studies in mammals have concluded that altering either synthesis or catabolism of polyamines leads to abnormalities which are described in later sections. Therefore understanding the molecular mechanisms regulating the polyamines level is critical in order to understand the patho-physiology of the polyamine associated abnormalities.

In the present work, I focused on understanding the important role of selective proteolysis in controlling a metabolic process in the unicellular fungus *Saccharomyces cerevisiae*.

3.1 Polyamines and their cellular functions

Polyamines are essential, organic, aliphatic polycations that are present in all the life forms ranging form prokaryotes to higher eukaryotes. There are many modified forms of polyamines detected in the cell, but putrescine, spermidine and spermine are the three most abundant and important natural polyamines (Figure 1). Polyamines have multiple functions. A substantial amount of polyamines are secreted into human and rat milk and also into the seminal fluid. Polyamines are also known to act as odors and to modulate taste (Cohen, 1998). Polyamines are essential for normal cell growth and viability (Coffino, 2001b). Although identifying the molecular functions of polyamines is not easy because of their importance in normal cell physiology, many studies have recognized their direct role in stabilization of chromatin and the cytoskeleton, as well as in processes ranging from DNA replication, transcription and translation, ion transport, to the regulation of cell growth and apoptosis (Childs et al., 2003) (Coffino, 2001b) (Wallace et al., 2003). Polyamines alter protein-protein interactions as well as proteins interactions with DNA and RNA (Childs et al., 2003).
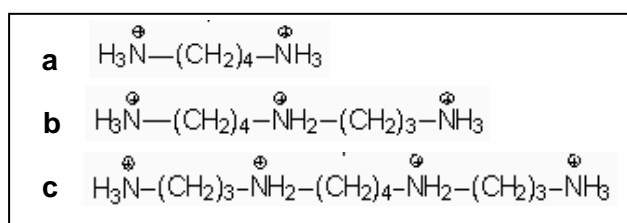
Fig. 1. Natural polyamines
(a) Putrescine
(b) Spermidine
(c) Spermine

Aside of the processes mentioned above, polyamines are associated with two rare physiological processes. The first one is hypusination, a rare posttranslational protein modification with an unusual amino acid hypusine (Shiba et al., 1971). In hypusination, the polyamine spermidine serves as the donor of an aminobutyl moiety which is attached to the lysine residue of eukaryotic translation initiation factor eIF-5A. Later the amino butyl group is converted to hypusine (Park et al., 1993). EIF-5A which is involved in RNA processing (Peebles et al., 1983) is the only known substrate for hypusination. Even though it is a rare modification, inhibition of hypusination is lethal in the yeast *S. cerevisiae* (Park et al., 1993). In a second process, polyamines control the +1 ribosomal frameshifting involved in decoding of ODC antizyme. Ribosomal

frameshifting is an important event in the auto-regulatory circuit of polyamine biosynthesis (Matsufuji et al., 1995). In addition, polyamines can inhibit eukaryotic transposable element (Ty1) propagation by altering the +1 frameshifting efficiency during the decoding of its RNA (Balasundaram et al., 1994).

3.2 Metabolism of polyamines

Polyamines can be synthesized as well as broken down or modified within the cell. Polyamine biosynthesis involves several enzymatic processes and they are highly conserved between higher and lower eukaryotes. Polyamine catabolism is also composed of several enzymatic processes and requires subcellular compartments for detoxification of toxic intermediates. Moreover polyamine catabolism also helps to interconvert the higher polyamines spermine and spermidine to the lower polyamine putrescine. Figure 2 depicts the general scheme of polyamine metabolism as it occurs in prokaryotes as well as in eukaryotes. Polyamines are synthesised from amino acid precursors in several enzymatic steps. Ornithine decarboxylase (ODC) is the rate-limiting enzyme in the biosynthesis of the polyamines spermine and spermidine (Coffino, 2001b) (Wallace et al., 2003). It catalyses the conversion of ornithine derived from arginine into the diamine putrescine. By addition of an aminopropyl group, putrescine is subsequently converted to spermidine by spermidine synthase. Spermine is derived from spermidine by the action of spermine synthase (Wallace et al., 2003).

Some plants and bacteria derive putrescine via an additional pathway that requires arginine decarboxylase (ADC) and agmatinase. The existence of this pathway in eukaryotes such as yeast and mammals, however, is not clear (Coffino, 2001b). In addition, polyamines are either interconverted or catabolized by the enzyme pair spermidine/spermine acetyl transferase (SSAT) and polyamine oxidase (PAO) (Wallace et al., 2003). Polyamine levels are furthermore controlled by their uptake or excretion into the environment (Cohen, 1998).

Introduction

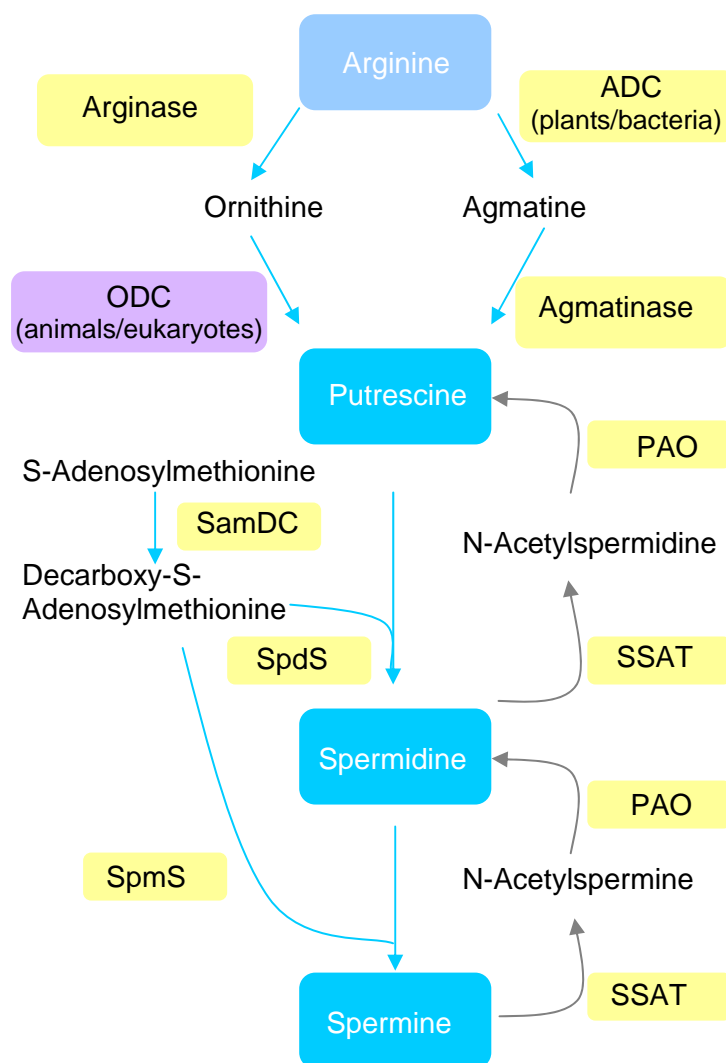---

Fig. 2. Polyamine metabolism
Polyamines are synthesized from the amino acid precursor arginine. In some plants and bacteria, arginine decarboxylase (ADC) converts arginine to agmatine, which is converted to the diamine putrescine by agmatinase. But in animals and other eukaryotes arginase initiates polyamine synthesis by producing ornithine from arginine, and ornithine decarboxylase (ODC) converts ornithine to putrescine. Afterwards the higher order polyamine spermidine is synthesized by addition of an aminopropyl group to putrescine by spermidine synthase (SpdS). Accordingly spermine synthase (SpmS) catalyses the addition of a second aminopropyl group to spermidine leading to spermine. The aminopropyl group is derived from S-adenosylmethionine by S-adenosylmethionine decarboxylase (SamDC). Polyamines are either interconverted or destroyed by spermidine/spermine acetylase (SSAT) and polyamine oxidase (PAO). ODC, SamDC and SSAT are three key rate-limiting enzymes in controlling the synthesis and catabolism of polyamines.

These processes are collectively important for polyamine homeostasis in the cell. Although polyamine transport has been well studied in bacteria, polyamine transport across the plasma membrane in eukaryotes is less clear (Igarashi and Kashiwagi, 1999).

In *S. cerevisiae*, however, polyamine transporters have been identified in the vacuolar membrane which may be important for either the storage or detoxification of polyamines (Tomitori et al., 1999). Although experimental evidences strongly suggest that polyamines are transported across the plasma membrane, there are no specific plasma membrane transporters known to be involved in polyamine transport. A report that described Tpo1 in *S. cerevisiae* as a plasma membrane polyamine transporter is controversial (Igarashi and Kashiwagi, 1999) (Albertsen et al., 2003) (Uemura et al., 2005).

3.3 Regulation of polyamine biosynthesis

The intracellular concentration of polyamine is controlled at several steps including their uptake, catabolism and their biosynthesis. In eukaryotes the regulation of biosynthesis is mainly achieved by controlling the cellular ODC activity via an unusual mechanism involving ODC antizyme (AZ) (Hayashi et al., 1996) (Coffino, 2001a). Higher levels of polyamine induce +1 ribosomal frameshifting during the decoding of *AZ mRNA* (Matsufuji et al., 1995). This in turn increases AZ levels in the cell. If present, AZ breaks ODC/ODC homodimers and forms ODC/AZ heterodimers. In the heterodimer, an ODC degradation signal is exposed which is recognised by the proteasome leading to loss of ODC and recycling of AZ (Figure 3).
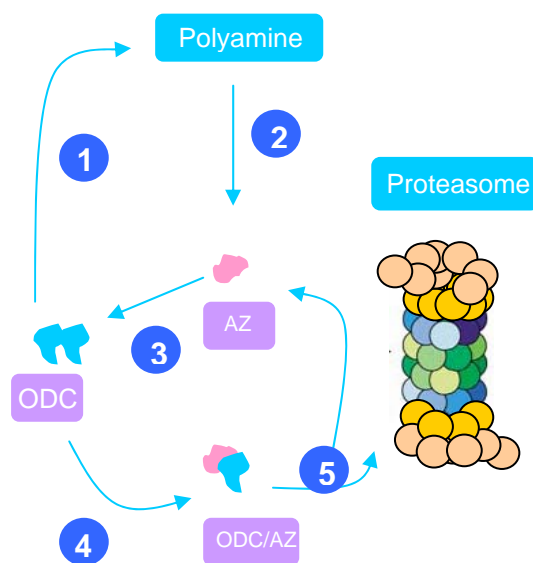
Fig. 3. Regulation of polyamine biosynthesis

Polyamine biosynthesis is mainly regulated by the degradation of ornithine decarboxylase (ODC) which is the rate-limiting enzyme in polyamine biosynthesis. 1.) ODC catalyses the conversion of ornithine to putrescine, which in turn increases the polyamine levels. 2.) Higher levels of polyamines induce the +1 ribosomal frameshifting thereby increasing the cellular antizyme (AZ) level. 3.) AZ disrupts ODC homodimers and inhibits ODC activity. 4 &5.) Antizyme forms ODC/AZ heterodimers, resulting in the degradation of ODC by the proteasome leaving the antizyme for recycling.

Proteasomal degradation usually requires ubiquitylation of substrates. ODC, however, is the only example where ubiquitin is not strictly required for its degradation (Murakami et al., 1992). Although the mechanism of regulation of polyamine biosynthesis is highly conserved, this complex regulation is mainly studied in mammals. A large number of biochemical and *in vivo* studies in mammals have revealed the importance of the components involved in regulating polyamine biosynthesis for normal cell physiology.

In the coming subsections, I will introduce the state of knowledge on ODC, ODC antizyme, ribosomal frameshifting and the ubiquitin proteasome system.

3.3.1 Ornithine decarboxylase (ODC)

Animals solely depend on ODC for polyamine biosynthesis, unlike plants and bacteria which have an additional pathway for synthesizing polyamines (Figure 2). The unicellular fungus *S. cerevisiae* also uses ODC for its polyamine biosynthesis and it is likely to remain the only pathway dedicated for polyamine biosynthesis since strains lacking the ODC encoding gene (*SPE1*) fail to grow when they are transferred to polyamine-free media (Schwartz et al., 1995). The active ODC enzyme is a homodimer and the crystal structures of C-terminally truncated mouse ODC (Kern et al., 1999) and of human ODC (Almrud et al., 2000) have been solved. Because ODC is the rate-limiting enzyme in polyamine biosynthesis, it was the target of many studies aimed to understand the role of polyamines. Initially an irreversible inhibitor of ODC, DFMO (DL-alpha-Difluoromethylornithine), has been used extensively for this purpose. Later genetic studies targeting ODC have shown that it is an important gene that is not only essential for cell physiology but also has a role during the development of multicellular organisms (Pendeville et al., 2001) . Firstly, the overexpression of ODC in mouse testis causes male sterility which resembles the 'Sertoli cells-only syndrome' that causes infertility in man (Halmekyto et al., 1991). Overexpression in the skin increases the spontaneous skin tumor development which can be prevented by using ODC inhibitor DFMO (Ahmad et al., 2001). Aside of tumor development this mouse also showed a very complex skin phenotype including complete and irreversible loss of hair, excessive skin wrinkling and enhanced nail growth (Megosh et al., 1995). Other studies have shown that overexpression also affects the central nervous system and the cardiac system (Shantz et al., 2001). On the other side, deletion of the ODC gene in mouse is embryonic lethal with the embryos not developing beyond day 3.5 (Pendeville et al., 2001). Interestingly, mammals have an ODC homolog called antizyme inhibitor, which is enzymatically inactive. However antizyme inhibitor has higher affinity towards antizyme than ODC. Therefore antizyme inhibitor is widely believed to inhibit antizyme activity when the polyamine levels are critically low thereby allowing ODC-mediated

biosynthesis to take place (Bercovich and Kahana, 2004). The mechanism controlling the level and the activity of the antizyme inhibitor, however, is not clear. In lower eukaryotes, a homolog of antizyme inhibitor has not been identified suggesting that other mechanisms govern the regulation of excess antizyme in those organisms. Since many studies in the transgenic mouse model suggest a direct role of ODC in tumor formation, this enzyme has become a potential target for tumor prevention especially in the skin where such treatment has been proven to be very effective (Feith et al., 2001). An interesting property of ODC is that it is degraded by the proteasome when it binds to ODC antizyme. Characterization of the 461 residue mouse ODC showed that 37 residues at the C-terminus contain the degradation signal that is exposed upon association with antizyme (Ghoda et al., 1989). Further characterisation revealed that residues between 117 and 140 are important for ODC association with antizyme (Kern et al., 1999).

The effects of lowering and increasing the intracellular production of polyamines have been extensively studied in transgenic models. In addition, abnormalities associated with abnormal polyamines levels are known to occur in humans (Janne et al., 2004). Inactivation of the ODC gene in mice e.g. led to embryonic lethality (Pendeville et al., 2001). In *S. cerevisiae* mutants lacking the *SPE1* gene encoding ODC are viable but cease to grow and become morphologically abnormal upon transfer to polyamine-free media (Schwartz et al., 1995). On the other side, elevated polyamine levels are usually linked to cancer. Consistent with that notion, mutations associated with hepatomas in humans have been mapped to the ODC degradation signal, which result in stabilization of ODC (Tamori et al., 1995). Lowering polyamine levels by the overexpression of SSAT (spermidine/spermine N-acetyl transferase) in the mouse led to hairlessness (Pietila et al., 1997) and female infertility (Min et al., 2002). Moreover, in humans the X-linked syndrome keratosis follicularis spinulosa decalvans (KFSD) affecting skin and eye is related to polyamines. The genetic alterations leading to this syndrome apparently include a duplication of a region on the X-chromosome that contains the SSAT gene (Gimelli et al., 2002). The relevant mutation in the human X-linked mental disorder Snyder-Robinson syndrome has recently been mapped to the spermine synthase gene (Cason et al., 2003) that is involved in the synthesis of the higher polyamine spermine.

3.3.2 ODC antizyme

The ODC <u>anti</u>-en<u>zyme</u> (antizyme) was first identified in mammals (Murakami et al., 1985), where it is now known to exist in several isoforms (AZ1, AZ2, AZ3, AZ4) (Heller et al., 1976) (Ivanov et al., 1998) (Ivanov et al., 2000b). Among those, AZ1 disrupts enzymatically active ODC homodimers by forming ODC/AZ heterodimers (Li and Coffino, 1992) (Mitchell and Chen, 1990). AZ1 binding moreover mediates ODC degradation by the 26S proteasome (Elias et al., 1995) (Li and Coffino, 1992) (Murakami et al., 1992). In contrast, binding of AZ2 does not result in degradation of ODC (Zhu et al., 1999). The molecular functions of AZ3, whose expression appears to be limited to the testis, and of AZ4 have not been analysed in detail (Ivanov et al., 2000b) (Coffino, 2001b). AZ1-dependent degradation of ODC was shown both *in vitro* and *in vivo* not to require its ubiquitylation (Rosenberg-Hasson et al., 1989) (Murakami et al., 1992). It was reported that instead a C-terminal degradation signal in ODC is exposed upon AZ1 binding that mediates binding to a ubiquitin recognition site in the 19S cap of the proteasome (Zhang et al., 2003). AZ levels increase with rising intracellular polyamine concentration. Polyamine-induction of AZ thus constitutes a feedback control in polyamine homeostasis. In mammals, it is shown that polyamines induce AZ levels by promoting +1 ribosomal frameshifting during the decoding of antizyme mRNA (Matsufuji et al., 1995). Although the function of ODC antizyme is conserved, its orthologues in mammals and *S. pombe* share very little sequence similarity (~10%) (Ivanov et al., 2000a). A few studies have concluded that mammalian antizyme is involved in other cellular process aside of its well known function of targeting ODC for ubiquitin-independent proteasomal degradation. Antizyme is known to be translocated into the nucleus during embryonic development (Gritli-Linde et al., 2001). Moreover antizyme forms a ternary complex with the transcription factor Smad1 and the proteasomal subunit HsN3 that is translocated into nucleus in response to bone morphogenetic protein receptor activation (Gruendler et al., 2001). In addition, a recent report showed a role of antizyme in targeting cyclin D1 for proteasomal degradation (Newman et al., 2004).

A mouse line overexpressing antizyme was shown to be less susceptible to skin tumorigenesis (Feith et al., 2001). Overexpression of antizyme in the fore-stomach also significantly reduced tumor formation and multiplicity (Fong et al., 2003). Based on these studies the authors have proposed that antizyme may represent a general *tumor repressor gene*. The carboxy-terminus of antizyme is involved in ODC interaction, but the amino-terminus of antizyme is required for inducing the degradation of ODC via an unknown mechanism (Li and Coffino, 1994). Many years after the identification of antizyme and after the discovery of mechanisms controlling its synthesis, it is still unclear how antizyme is removed from cells after ODC degradation. AZ1 degradation was reported to be inhibited by proteasome inhibitors in cell lines and the degradation also appears to require a functional ubiquitin activating enzyme (E1) suggesting that antizyme requires ubiquitin and the proteasome for its degradation (Gandre et al., 2002). However this study has not shown that ubiquitylation of antizyme is directly involved in its degradation by the proteasome leaving this process still unclear.

3.3.3 Programmed ribosomal frameshifting

Translational recoding such as hopping, programmed ribosomal frameshifting and termination codon suppression are the exceptions to the general dogma of protein synthesis (Namy et al., 2004). These poorly understood phenomenons in turn make the definition of the genetic code an incomplete process. Several genes in prokaryotes and eukaryotes have been reported to use translational recoding as a biological regulatory mechanism. Programmed ribosomal frameshifting is the translation recoding mechanism that is used as the molecular switch in regulating polyamine homeostasis (Matsufuji et al., 1995). During this event, the ribosome either moves forward (+1) or backward (-1) without the detachment of peptidyl tRNA thereby changing the coding frame. The former process is called the +1 programmed ribosomal frameshifting and the later is called -1 ribosomal frameshifting. The decoding of antizyme mRNA involves +1 ribosomal frameshifting and the decoding signal (5' UCC <u>UGA</u> U 3') is highly conserved in almost all known antizyme genes (Ivanov et al., 2004). In all species the antizyme is encoded by two overlapping ORFs (Figure 4A). ORF1 is short but contains

an AUG codon that initiates translation, whereas ORF2, which encodes a larger part of the antizyme lacks the proper initiation codon. The ribosome slips to the +1 frame during the decoding of antizyme mRNA in the "slippery site" or "frameshifting site" and continues then translation in ORF2 resulting in the functional antizyme. Interestingly, this process is induced by free polyamines via an unknown mechanism (Matsufuji et al., 1995). In vertebrates, all the known antizymes (AZ1, AZ2, AZ3 and AZ4) require +1 ribosomal frameshifting during their decoding and AZ1 has been widely used for the studies on the frameshifting mechanism. But despite major efforts the mechanism is still largely unknown (Namy et al., 2004). These studies, however, revealed that there are three elements in *AZ1 mRNA* that are required for +1 ribosomal frameshifting depicted in Figure 4B. The most important element required for the frameshifting is the UGA stop codon and its surrounding sequences of ORF1 which is the main part of the frameshifting signal.
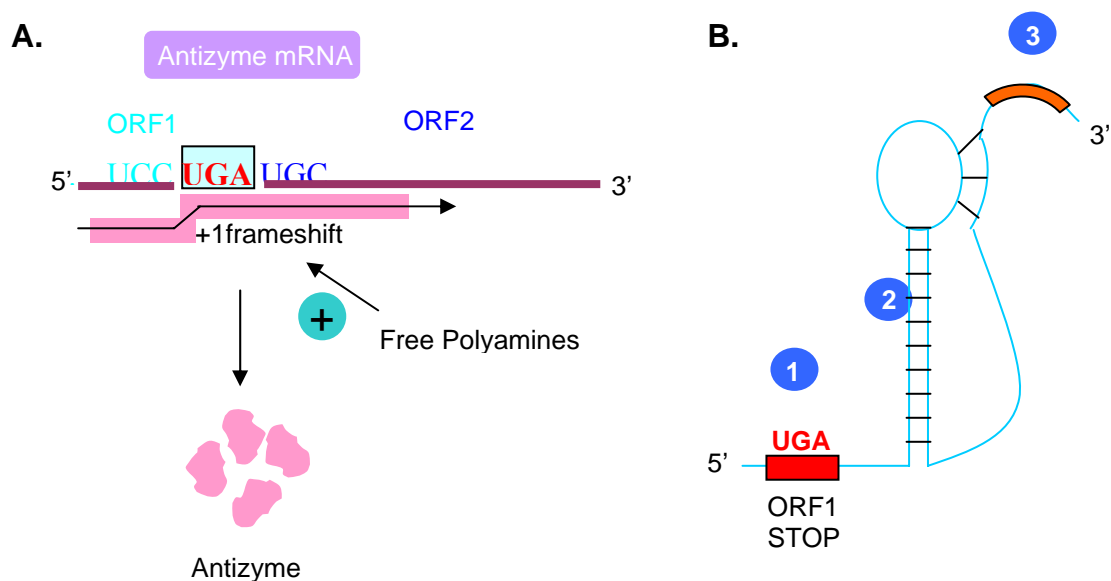
Fig. 4. +1ribosomal frameshifting in antizyme mRNA decoding
Decoding of ODC antizyme mRNA requires +1ribosomal frameshifting and this event is induced by free polyamines when present in excess. A. Antizyme is encoded by two ORFs (ORF1, ORF2) present in the same mRNA. Translation initiates from the AUG of ORF1, then the ribosome slips forward (+1) at the +1 frameshifting signal (5'UCC UGA UGC 3'). Thereby the translation continues into ORF2 without the detachment of the ribosome and peptidyl tRNA. +1 ribosomal frameshifting is induced by polyamines, which constitutes the auto-regulatory loop of regulating polyamine biosynthesis. B. AZ1 mRNA has been shown to have three important elements required for frameshifting, 1.) +1 ribosomal frameshifting signal that contains the UGA stop codon of ORF1 where the actual frameshifting occurs. 2.) A stem loop structure 3' to the frameshifting signal that forms a pseudoknot important for enhanced frameshifting, 3.) A sequence element 3' to the pseudoknot, which also influences the frameshifting efficiency. The polyamine responsive element however has not been identified.

An RNA pseudoknot that is 3' to the UGA stop codon of ORF1 is the second element which enhances the frameshifting efficiency of AZ1 by an unknown mechanism (Matsufuji et al., 1995). This element was identified in the vertebrate antizyme mRNA. But a recent study identified a new putative RNA pseudoknot in lower eukaryotes that enhances the frameshifting efficiency in these organisms as well (Ivanov et al., 2004). The third element, which is 3' to the pseudoknot, is also known to influence the frameshifting (Coffino, 2001b). Importantly none of these elements are known to be influenced by polyamines in order to induce the frameshifting. The mechanism underlying polyamine-mediated induction of +1 ribosomal frameshifting is therefore completely unknown as of yet.

3.3.4 Ubiquitin-proteasome system (UPS)

Proteolysis by the 26S proteasome is the main pathway for ATP-dependent non-lysosomal degradation of intracellular proteins in eukaryotes (Hershko and Ciechanover, 1998). Usually, the substrates destined for degradation by this multi-subunit protease are marked by the attachment of poly-ubiquitin chains, which are recognised by binding sites in the proteasome (Verma et al., 2004). Several exceptions to this principle of ubiquitin-dependent degradation by the proteasome have been reported. The first described and best-studied substrate of ubiquitin-independent degradation by the proteasome is ornithine decarboxylase (ODC) (Coffino, 2001b). Other examples are c-jun in mammals and Rpn4 in *S. cerevisiae* (Jariel-Encontre et al., 1995) (Xie and Varshavsky, 2001). In the latter two cases, however, ubiquitylation has been shown to be relevant to proteolysis *in vivo* (Ju and Xie, 2004) (Treier et al., 1994). The ubiquitin proteasome system therefore remains to be the major player in the selective proteolysis in eukaryotes.

3.3.4.1 The proteasome

The 26S proteasome is a ~2.0 MDa multi-subunit protease present in all eukaryotes, which has been studied and reviewed extensively (Heinemeyer et al., 2004) (Pickart and Cohen, 2004). The proteasomal protein turnover is a highly specific and regulated process. Unlike other proteases, the proteasome usually requires the substrate proteins to be modified by the attachment of ubiquitin. In eukaryotes, the proteasome is the most

important protease in the degradation of proteins that occur in the cytosol and in the nucleus (Hershko and Ciechanover, 1998). Protein degradation in general is an important mode of regulation of temporal processes such as the cell cycle. One specific feature of protein degradation is that it ensures that factors controlling such processes are eliminated irreversibly thereby allowing for a progression until a new cycle is reached (Peters, 2002). The proteasome is in addition important for protein quality control (Hampton, 2002). The proteasome is a fine complex molecular machine, which is composed of two particles, namely the 20S catalytic core and the 19S cap. The 20S proteasome (20S core) is a dimer of 14 different subunits. The 19S cap or regulatory particle is composed of 18 different subunits. The 20S particle is the catalytically active part, which degrades substrates that enters to its catalytic centre. The 19S caps in the 26S proteasome (Figure 5) are important for substrate recognition, unfolding and delivery to the catalytic centre, which is in the 20S core particle (Adams, 2003).
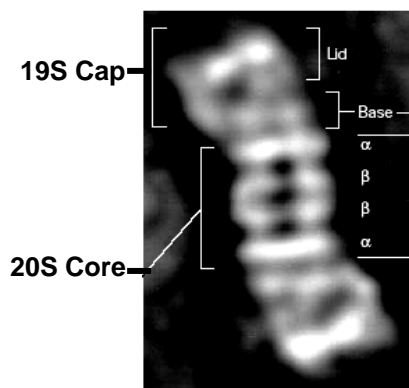
Fig. 5. The 26S proteasome
The proteasome is a multisubunit protease. The atomic electron micrograph (Glickman, et al, 1998) of *S. cerevisiae* proteasome shows that it contains a single 20S core with two 19S caps attached to both of its end. The 20S core contains two α and two β rings. The 19S cap contains a lid and a base. The base is attached to an α ring of the 20S core particle. The 19S cap regulates the entry of substrate to the proteasome and the 20S particle is responsible for degradation of the selected substrate.

3.3.4.1.1 The 20S proteasome

The 26S proteasome which is derived by the addition of two 19S regulators to the 20S proteasome, appears to be present only in eukaryotes. The 20S proteasome (20S core) in contrast, has been found in all phylae of life (Volker and Lupas, 2002). Unlike in eukaryotes, studies on the eubacterium *Mycobacterium smegmatis* and the archaeon *Thermoplasma acidophilum* showed that the proteasome is not essential for their viability (Knipfer and Shrader, 1997) (Ruepp et al., 1998). The precise function of the proteasome in those species is not clear. 20S proteasomes are composed of two types of subunits, α and β. In prokaryotes, proteasomes are either formed from one of two types

of α and β subunits (Heinemeyer et al., 2004). In contrast, eukaryotic 20S proteasome is composed of seven distinct α and seven distinct β subunits. The prokaryotic proteasome contains fourteen active sites compared to only six present in the β subunits of eukaryotic proteasome. Higher eukaryotes such as mammals, in addition, have a new type of proteasome that is called immunoproteasome. The immunoproteasome has three β subunits which are distinct from the normal proteasome. It has been implicated in antigen processing (Pamer and Cresswell, 1998) (Rock and Goldberg, 1999). 20S proteasomes are defined by a characteristic architecture, a stack of four heptameric rings with two outer α subunit rings and two central β subunit rings, which posses the catalytic centres. Eukaryotic proteasomes in comparison to prokaryotic ones have a high subunit complexity. The crystal structures of the yeast and the bovine particles have been solved, which confirmed that the topology is conserved from the yeast to the mammals (Bochtler et al., 1997; Unno et al., 2002). The crystal structure of yeast proteasome also revealed the specific subunits that possess peptidase activity. The β subunits β1/Pre3 mediates the post-acidic activity, β2/Pup1 has the trypsin-like activity and β5/Pre2 is responsible for chymotrypsin-like activity (Arendt and Hochstrasser, 1997; Heinemeyer et al., 1997).

The 20S proteasome biogenesis is fairly well studied in prokaryotes. Because, bacterial proteasomes lack the subunit complexity, there assembly and maturation is relatively simple. In contrast, proteasome biogenesis is very complex in eukaryotes because of its large number of distinct subunits. The assembly and maturation of 20S proteasome in the eukaryotes has been shown to involve a dedicated proteasome maturation factor termed Ump1 (Ramos et al., 1998). The Figure 6 shows the current model of 20S proteasome assembly and maturation in the yeast *S. cerevisiae*. First, the individual subunits assembled into a complex with Ump1 which is called 15S complex or half-proteasome. Then two half-proteasomes dimerise and form an intermediate with the Ump1 trapped within the complex. Conformational changes that coincide with dimerisation and that depend on Ump1 activate the catalytic centres, which in turn degrade Ump1 leading to the mature 20S proteasome. 19S activator complexes bind to 20S proteasomes in an ATP-dependent, poorly understood process that leads to the formation of 26S proteasome. In eukaryotes, it is also not clear if the 20S proteasome without the 19S cap plays a role in protein degradation. As only the 26S proteasome is

capable of degrading ubiquitylated proteins this form of the protease is essential for eukaryotic cells (Heinemeyer et al., 2004).
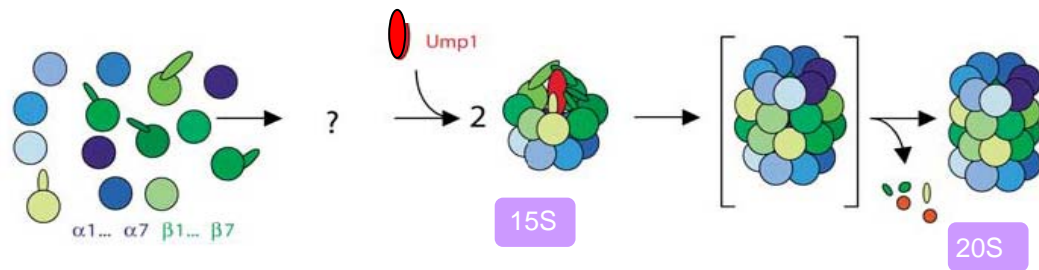
Fig. 6. 20S proteasome assembly and maturation in *S. cerevisiae*
The 20S proteasome assembly and maturation is a complex process. Individual α and β subunits form a 15S complex with the proteasome assembly and maturation factor Ump1. Later two 15S complexes associate to form an intermediate complex which contains Ump1. Finally conformational changes induce the activation of catalytic centers that in turn degrade Ump1. (modified from Heinemeyer et al, 2004)

3.3.4.1.2 The 19S regulatory particle

In eukaryotes, the 19S caps in the 26S proteasome are essential in controlling protein degradation. The 19S caps perform most of the sequential actions that are required for efficient protein turnover by the proteasome. They include recognition of ubiquitylated substrates, de-ubiquitylation, unfolding and delivery to the 20S catalytic centre (Pickart and Cohen, 2004). In the yeast *S. cerevisiae,* the 19S cap is composed of at least 19 different subunits, which are assembled into two sub-complexes. The base sub-complex contains six ATPases, and three non-ATPase subunits, the lid sub-complex contains ten non-ATPase subunits. The lid and the base are connected by a non-ATPase subunit Rpn10 (Regulatory Particle Non-ATPase). The base is attached to an α ring of the 20S core particle via its Rpt (Regulatory Particle ATPase) subunits (Glickman et al., 1998). Figure 7 is the schematic representation of the 19S cap subunits and their arrangements in the lid and base sub-complexes. One of the main functions of the 19S cap in the proteasome is to identify the polyubiquitylated proteins. This is thought to be achieved by the ability of the 19S cap subunits Rpn10 and Rpt5 to bind to the polyubiquitin chain with four or more ubiquitin molecules (Deveraux et al., 1994; Lam et al., 2002). The *S. cerevisiae* 19S cap interacts with several proteins which are not stoichiometric parts of the 26S proteasome including ubiquitin ligase (E3) such as Hul5 and the de-ubiquitylating enzyme Ubp6 (Leggett et al., 2002) (Verma et al., 2000). Another 19S lid

subunit, Rpn11, which contains a JAMM (or MPN+) domain has a Zn2+ dependent metalloprotease activity. Mutation of its active site residues leads to accumulation of polyubiquitin conjugates and causes cell death illustrating the essential role of de-ubiquitylation in proteasomal protein degradation (Maytal-Kivity et al., 2002; Verma et al., 2002; Yao and Cohen, 2002).
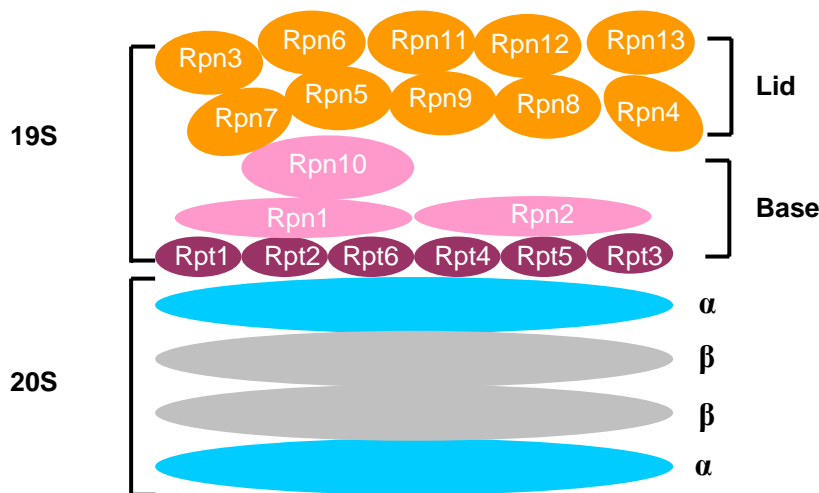
Fig. 7. 19S regulatory particle
The 19S cap contains at least 19 subunits. The subunits are arranged in two sub-complexes, the lid and the base. The base has six ATPases (Rpt1-6) that connect the 19S to the α ring of the 20S. These ATPases are also responsible for ATP hydrolysis and unfolding of substrates. The lid is composed of ten subunits, most of which are essential for proteasome activity. The lid and the base are connected by Rpn10, a non-ATPase in the base complex. Rpt5 and Rpn10 are the only two known multi-ubiquitin receptors in the proteasome.

The cooperation among these different factors in performing the sequential actions that are important for substrate delivery and the release of the polyubiquitin chains from the substrates is poorly understood. Another important function of the 19S base sub-complex is the unfolding and translocation of proteins to the 20S core active site chamber. This is an energy-dependent process that requires hydrolysis of ATP by the base sub-complex ATPases (Pickart and Cohen, 2004).

Several organic molecules are widely used as proteasome inhibitors in *in vitro* and *in vivo* studies. In humans, the proteasome has been shown to be an important target for treatment of diseases such as cancer (Adams, 2004). Molecules such as aclacinomycin A (Figueiredo-Pereira et al., 1996), bortezomib (PS-341) (Adams et al., 1998), benzamide (Lum et al., 1998), calpain inhibitors I and II (Orlowski et al., 1993), eponemycin (Meng et al., 1999), epoxomycin (Kim et al., 1999), lactacystin (Almond and Cohen, 2002) and MG132 (Elliott et al., 2003) have been shown to inhibit

proteasomal activity and are undergoing preclinical trails as drugs against several diseases (Adams, 2004). Among those, bortezomib (Valcade) is currently being used for treatment of refractory multiple myeloma in humans (Adams et al., 1998). The identification of novel proteasome inhibitors such as peptides that interfere with various aspects of its function (see below) could therefore potentially lead to a drug that can be used for treatment of several diseases in humans.

3.3.5 The peptide aptamers

Aptamers ('to fit' in greek) are novel biological tools that are based on biological macromolecules such as DNA, RNA or proteins. Peptide aptamers are selected from random peptides. The concept of peptide aptamers basically comes from antibodies. The antibodies have the ability to bind specifically to a large array of antigens despite having most of its structure unchanged. This specificity of the antibody binding to the antigen is due to the sequence variation in the VL and VH regions of the antibody that allows different conformations in that particular domain. Equally, peptide aptamers have been generated by the insertion of random peptide sequences into conformationaly stable proteins such as *E.coli* thioredoxin (Colas et al., 1996), green fluorescent protein (Abedi et al., 1998), retinol binding protein or the bilin binding protein (Beste et al., 1999; Skerra, 2000). Figure 8 illustrates the thioredoxin-based aptamer developed by John McCoy and Roger Brent. It contains a C-region that is the *E.coli* thioredoxin protein and the V-region which has inserted random peptides of 20 animo acid residues. Based on that design they constructed a library that can be expressed in the yeast *S. cerevisiae.* Using this library these authors were able to isolate peptide aptamers that specifically inhibit cyclin-dependent protein kinase 2 (Colas et al., 1996).
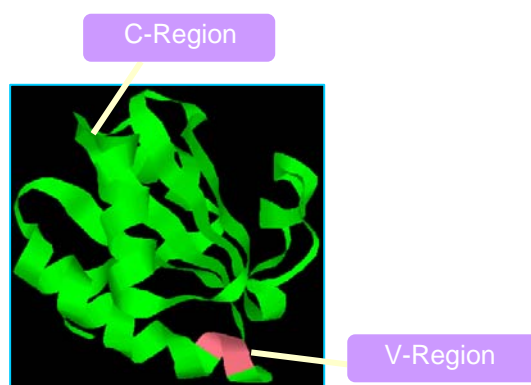
Fig. 8. Thioredoxin peptide aptamer
Shown is a thioredoxin peptide aptamer composed of two regions. The constant or C-region is the thioredoxin protein and the variable or V-region is the 20mer random peptide, which is inserted into thioredoxin active site.

3.3.5.1 Ubiquitylation

Ubiquitin is a 76 amino acid globular protein present in all eukaryotes. The multi-step attachment of ubiquitin to other proteins is called ubiquitylation (Hershko and Ciechanover, 1998). The best characterised role of ubiquitylation is to render proteins susceptible to degradation by the 26S proteasome. This occurs as a consequence of modification of proteins with chains of four or more ubiquitins linked through lysine 48 of ubiquitin. Protein modification by K63-linked ubiquitylation has roles that are independent of proteasomal degradation e.g. in protein kinase activation or in DNA repair.(Cheng et al., 2004; Hoege et al., 2002; Pickart, 2002) (Wang et al., 2001). In general, ubiquitylation occurs as a result of the sequential action of three classes of enzymes, E1 or ubiquitin activating enzyme, E2 or ubiquitin conjugating enzyme, and E3 or ubiquitin ligase (Figure 9). E1, the first enzyme in the ubiquitylation pathway forms a thiol-ester bond between its active site cysteine and the carboxy-terminus glycine of ubiquitin.
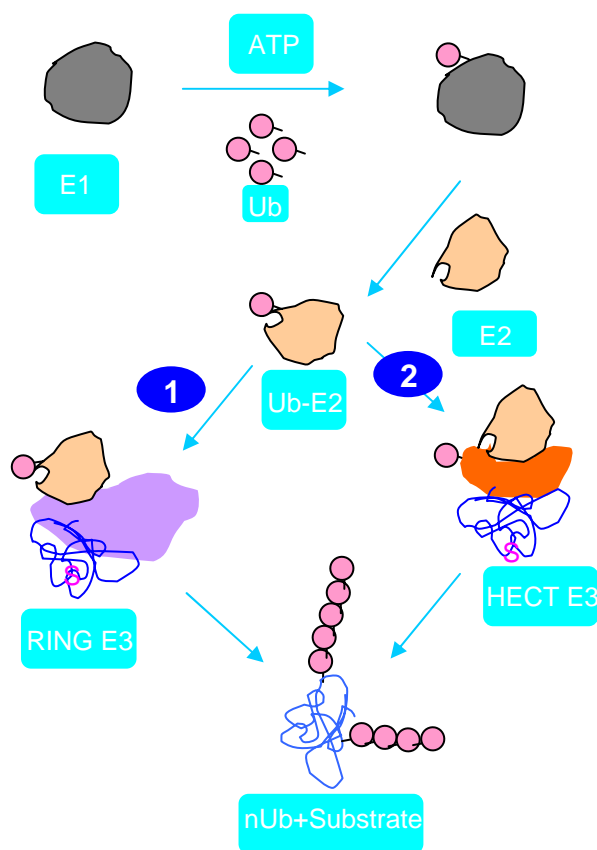
Fig. 9. Ubiquitylation
Ubiquitin activating enzyme (E1) activates free ubiquitin by forming a thiol-ester link with the C-terminal glycine of ubiquitin in the presence of ATP. Ubiquitin is then transferred to one of many ubiquitin conjugating enzymes (E2s). Later the Ub-E2 associates with substrate bound ubiquitin ligase (E3). 1.) The ubiquitin is directly transferred from E2 to the substrates in the case of RING E3-mediated ubiquitylation. 2.) Ubiquitin is transferred to the active-site cysteine residue of a HECT domain in case of HECT E3 before the ubiquitylation of the substrate. This process is repeated several times until the multi-ubiquitin chain is formed.

The activated ubiquitin on E1 is subsequently transferred to the active site cysteine of E2 by transesterfication. E3 binds ubiquitin-charged E2 and substrate and facilitates formation of an iso-peptide linkage between carboxy-terminal glycine of the ubiquitin and the ε-amino group of an internal lysine residue of the substrate, or an ubiquitin already attached to the protein (Hershko and Ciechanover, 1998). In rare instances ubiquitin is attached to the free α-amino group of the substrate rather than to an internal lysine (Aviel et al., 2000; Reinstein et al., 2000) (Doolman et al., 2004).

3.3.5.1.1 Ubiquitin activating enzyme (E1)

In the multistep ubiquitylation process, activation of ubiquitin is the initial reaction which is catalysed by the E1 or ubiquitin activating enzyme. In the yeast *S. cerevisiae,* E1 is encoded by a single and essential gene. Mammals are also widely believed to have only a single E1 which governs the ubiquitylation. Mammals E1, however, comes in two isoforms E1a and E1b (Handley-Gearhart et al., 1994) that are the result of the utilization of two translation initiation sites. In order to activate ubiquitin, E1 binds to MgATP and subsequently to ubiquitin forming an ubiquitin adenylate that serves as the donor of ubiquitin to the active cysteine in E1 (Haas and Rose, 1982; Hershko et al., 1983). Each fully loaded E1 carries two molecules of ubiquitin, one as a thiol-ester and the other as an adenylate. The activated ubiquitin is then transferred to the active site cysteine in E2. The carboxyl-terminal glycine of ubiquitin is essential for its activation by E1. The evolutionary conservation in activation for ubiquitin and other ubiquitin-like (UBL) protein modifiers is exemplified by the presence of a carboxyl-terminal glycine in the active forms of most UBLs, such as SUMO/Pic-1/Sentrin, Nedd8/Rub1, ISG15/UCRP and FAT10 (Hochstrasser, 2000; Raasi et al., 2001). In the case of SUMO and Nedd8 the activating enzymes are heterodimers, with the subunits displaying homology to the amino or carboxyl portions of the ubiquitin E1 (Tanaka et al., 1998).

3.3.5.1.2 Ubiquitin conjugating enzyme (E2)

After activation, ubiquitin is transferred to the ubiquitin conjugating enzyme (UBC) or E2. By sequence homology there are 13 known members of E2 family in the yeast *S. cerevisiae,* which are termed Ubc1-Ubc13, and there are at least 25 members in mammals. One of the yeast E2s (Ubc9) is specific for conjugation of SUMO, another one (Ubc12) is specific for Rub1, leaving 11 ubiquitin-specific E2s in this organism.

E2s have a ~150 amino acid, highly conserved core (UBC) domain that includes an invariant cysteine that accepts ubiquitin from E1. Some E2s have carboxy- and amino-terminal extensions, some have insertions in the core domain (Pickart, 2001). These extensions are believed to either facilitate or preclude interactions with specific E3.

3.3.5.1.3 Ubiquitin Ligase (E3)

Ubiquitin ligase or E3 is the third type of enzymes involved in ubiquitylation. E3 interacts directly with the substrate and the E2 thereby facilitating the transfer of ubiquitin to the substrate. Among the three classes of enzymes, E3s have more specificity towards the substrate than E2s and the E1. There are two known families of ubiquitin ligases in the cell. E3s of the first family have a characteristic RING (Really Interesting Gene) finger domain (Joazeiro and Weissman, 2000), which is highly conserved in those family members. E3s of the second family are characterized by the presence of a HECT (Homology to E6-AP Carboxy Terminus) domain (Huibregtse et al., 1995). This domain bears a conserved cysteine residue that forms a thioester with ubiquitin obtained from its Ubc enzymes (Scheffner et al., 1995). This class of E3s is named after its prototype cellular E6-AP, that is recruited by papilloma virus E6 to target the tumor suppresser p53 for degradation (Scheffner et al., 1994).

3.3.5.1.3.1   RING E3s

The family of RING type E3 enzymes is the largest so far. The characteristic RING finger ranges from 40 to 100 amino acids. The RING finger is defined by eight conserved cysteine and histidine residues that together coordinate two zinc ions in a cross-braced fashion [CX2CX(9–39)CX(1–3)HX(2–3)C/HX2CX(4–48)CX2C] (Borden and Freemont, 1996). The role of the RING finger in ubiquitylation became apparent several years ago with the determination that a small RING finger protein Rbx1, is essential for multi-subunit SCF (Skp1-Cul-F-box) complex E3 activity (Kamura et al., 1999), and the demonstration that a number of unrelated RING finger proteins all mediate ubiquitylation (Lorick et al., 1999). Since then, numerous RING finger proteins have been shown to mediate ubiquitylation. There are, however, a few RING finger proteins that neither mediate E2-dependent ubiquitin transfer by themselves nor cooperate with other RING fingers proteins in ubiquitylation when evaluated for auto ubiquitylation *in vitro* with a range of E2s. Whether the RING finger in those proteins

has functions unrelated to ubiquitylation remains to be determined. Two other motifs related to the RING finger are now implicated in ubiquitylation, the PHD finger and the U-box. The PHD finger is a RING finger variant that includes a cysteine rather than a histidine in the fourth predicted coordinating position and an invariant tryptophan before the seventh zinc-binding residue (Capili et al., 2001). Several herpes virus encoded PHD finger proteins have been implicated in ubiquitylation of major histocompatibility complex (MHC) class I molecules and membrane proteins in the endoplasmic reticulum and at the cell surface (Boname and Stevenson, 2001; Coscoy and Ganem, 2003; Coscoy et al., 2001). PHD finger-dependent E3 activities have been demonstrated for mammalian proteins such as MEKK1, which not only activates MAP kinase but also mediates its ubiquitylation (Lu et al., 2002). The U-box is distantly related to the RING finger in sequence but has no conserved zinc coordinating residues. The first U-box protein implicated in ubiquitylation was UFD2 (Koegl et al., 1999). Subsequently**,** CHIP (Carboxyl-terminus of Hsc70 Interacting Protein) was shown to be involved in the degradation of unfolded proteins by functioning as an E3 for Hsp70-interacting proteins (Jiang et al., 2001). Sequence analysis led to the realization that these proteins and others share conserved charged and polar residues and have a predicted structure resembling of RING finger (Aravind and Koonin, 2000). A number of other U-box proteins have now been shown to mediate ubiquitylation *in vitro* in a manner similar to RING finger E3s (Hatakeyama et al., 2001).

3.3.5.1.3.2   HECT E3s

This E3 family is defined by the HECT domain. It was identified as a consequence of the seminal discovery of E6-AP (E6-Associated Protein), as the mediator of HPV E6-dependent ubiquitylation of p53 (Scheffner et al., 1994). It was subsequently recognized that substantial homology to the carboxyl-terminal half of this molecule exists in a number of otherwise unrelated proteins (Huibregtse et al., 1995). This highly conserved ~350 amino acid domain is invariably located in the carboxyl-terminal portion of HECT proteins. A cysteine positioned about 35 amino acids upstream of the carboxyl-terminus accepts ubiquitin from bound E2, which is subsequently transferred to the substrate (Scheffner et al., 1995). This E3 family is smaller than the RING-type E3 family. In yeast, HECT family E3 ligases include Rsp5 and Ufd4.

3.3.5.2   *Substrate targeting to the proteasome*

The effect of ubiquitylation on protein stability is well studied. Polyubiquitin chains appear to specifically target the designated protein to the proteasome. It is widely believed that the proteasome has receptors that can bind to the ubiquitin chain thereby selecting substrates for subsequent degradation. The subunits Rpn10 and Rpt5 in the base of the 19S activator complex of the proteasome have been shown to bind to polyubiquitin chains (Pickart and Cohen, 2004) and are believed to act as polyubiquitin receptors on the proteasome. *In vivo* targeting of many physiological substrates of the proteasome, however, is not affected when the Rpn10 subunit is deleted suggesting that other binding sites are either more important or can complement for the loss of Rpn10 (Verma et al., 2004). In addition to the ubiquitin receptors on the proteasome, shuttle factors such as Rad23, Dsk2 and Ddi1 are known to bind polyubiquitin chains and the proteasome via their characteristic UbL and UBA (Ubiquitin Like and Ubiquitin Associated) domains (Madura, 2004) (Elsasser et al., 2004) (Verma et al., 2004) (Kim et al., 2004). The shuttle factors directly bind to the polyubiquitin chains via their UBA domains and associate with the proteasome via their UbL domains thereby bringing the substrate in close proximity to the proteasome (Madura, 2004). Proteasomes not only degrade proteins which are marked with ubiquitin, but also degrade ODC without ubiquitin both *in vivo* and *in vitro*. It is therefore important to know the targeting mechanism involved in ODC degradation. Surprisingly, ODC *in vitro* appears to utilise the same binding sites that are used by ubiquitylated proteins. Degradation of ODC by the proteasome was inhibited by the addition of oligo-ubiquitin chains (Zhang et al., 2003).

3.4 Aims of the current study

Many cellular processes are first identified and studied in unicellular model organisms such as *E.coli* and *S. cerevisiae*. Mainly because they are relatively easy to handle and to genetically manipulate and yet have mechanisms that are well conserved during the evolution of multi-cellular organisms. Although well conserved, the regulation of polyamine biosynthesis has been largely studied in mammals. These studies revealed that the failure to control polyamine levels is associated with many abnormalities including cancer in mouse as well as in humans. Molecular studies in higher eukaryotes are particularly challenging in humans because of their complexity and the technical limitations going along with it. As a consequence, many important molecular mechanisms governing the regulation of polyamines are still unknown. It is known that higher levels of polyamine induce +1 ribosomal frameshifting during the decoding of antizyme *mRNA*. Antizyme targets ODC, the rate-limiting enzyme in polyamine biosynthesis, for ubiquitin-<u>in</u>dependent proteasomal degradation thereby inhibiting the synthesis of polyamines. Interestingly, antizyme and its involvement in the regulation of polyamine synthesis is highly conserved between the unicellular fungus *Schizosaccharomyces pombe* and mammals. Regulation of polyamine biosynthesis in the yeast *S. cerevisiae,* the most elaborate unicellular eukaryotic model system, however, was not well understood at the onset of this study. The latter was mainly due to the absence of an identified antizyme-like protein in *S. cerevisiae*. Previous biochemical as well as bioinformatics approaches to identify antizyme in *S. cerevisiae* were not successful. The specific aims of this study were,

1.) to identify an antizyme orthologue in the unicellular fungus *S. cerevisiae*,

2.) to dissect the molecular mechanisms underlying the regulation of polyamine biosynthesis in *S. cerevisiae,* and

3.) to establish a new genetic screen to isolate inhibitors of selective proteolysis in *S. cerevisiae.*

4   Materials and Methods

4.1   Materials

4.1.1 *Saccharomyces cerevisiae* stains

Strain	Relevant Genotype	Source/Comment
BY4741	*MATa his3-Δ1 leu2Δ0 met15-Δ0 ura3-Δ0*	EUROSCARF ("wt")
BY4742	*MATα his3-Δ1 leu2-Δ0 lys2-Δ0 ura3-Δ0*	EUROSCARF ("wt")
Y02776	*oaz1-Δ::KanMX4 (=ypl052w-Δ)*	Derivative of BY4741, EUROSCARF
Y15034	*spe1-Δ::KanMX4 (="odc-Δ")*	Derivative of BY4742, EUROSCARF
Y04004	*doa4Δ::KanMX4 (="doa4-Δ")*	Derivative of BY4741, EUROSCARF
Y02894	*rpn10Δ::KanMX4 (="rpn10-Δ")*	Derivative of BY4741, EUROSCARF
Y00278	*rad23Δ::KanMX4 (="rad23-Δ")*	Derivative of BY4741, EUROSCARF
Y03240	*fes1Δ::KanMX4 (="fes1-Δ")*	Derivative of BY4741, EUROSCARF
Y00771	*hsc82Δ::KanMX4 (="hsc82-Δ")*	Derivative of BY4741, EUROSCARF
Y01052	*hsp82Δ::KanMX4 (="hsp82-Δ")*	Derivative of BY4741, EUROSCARF
PMY1	*ODC-ha$_3$::HISMX6*	Derivative of BY4741
PMY2	*ODC-ha$_3$::HISMX6 oaz1-Δ::KanMX4*	Derivative of BY4741
PMY17	*OAZ1-myc$_3$::HISMX6*	Derivative of BY4741
PMY15	*OAZ1-myc$_3$::HISMX6 spe1-Δ::KanMX4*	Derivative of Y15034

WGC4a	*MATα ura3 his3-11 leu2-3,112*	(Heinemeyer et al., 1991)
YHI29/1	*pre1-1*	Derivative of WGC4a (Heinemeyer et al., 1991)
YPH500	*MATα ade2-101 his3-Δ200 leu2-Δ1 lys2-801 trp1-Δ63 ura3-52*	(Sikorski and Hieter, 1989)
CMY762	*cim3-1*	Derivative of YPH500 (Ghislain et al., 1993)
ubc4 ubc5	*ubc4-Δ::HIS3 ubc5-Δ::LEU2*	(Seufert and Jentsch, 1990)
JD47-13C	*MATa his3-Δ200 leu2-3,112 lys2-801 trp1-Δ63 ura3-52*	(Ramos et al., 1998)
JD77-1-1	*uba1-Δ::HIS3 pRSts64-1(uba1-ts)*	Derivative of JD47-13C (McGrath et al., 1991)
PJ64-4A	*MATa his3-Δ200 leu2-3,1121 trp1-901 ura3-52 gal4-Δ gal80-Δ LYS2::GAL1-HIS3 GAL2-ADE2 met2::GAL7-lacZ*	(James et al., 1996)

4.1.2 *E.coli* stains

Strain Name	Relevant Genotype	Source/Comment
MC1061	hsdR2 hsdM+ hsdS+ araD139 Δ(ara-leu)7697Δ(lac)X74 galE15 galK16 rpsL (Strr) mcrA mcrB1	Lab Collection (E.c-252)
DH5α	F- φ80*lacZ*ΔM15 Δ(*lacZYA-arg*F)U169 *deo*R *rec*A1 *end*A1 *hsd*R17(rk-, mk+) *pho*A*sup*E44 *thi*-1 *gyr*A96 *rel*A1 λ-	Lab Collection (E.c-253)

4.1.3 Plasmids

Plasmid Name	Details	Source/Comment
pMY2	C-terminal 3x-Ha (chromosomal)	(Knop et al., 1999)
pMY5	C-terminal 3x-Myc (chromosomal)	(Knop et al., 1999)
YEp96	P_{CUP1}, *Ub,* 2μ/TRP1	(Ellison and Hochstrasser, 1991)
YEp105	P_{CUP1}, *myc-Ub,* 2μ/TRP1	(Ellison and Hochstrasser, 1991)
pJM2	P_{GAL}, *TrxA,* 2μ/TRP1	(Colas et al., 1996)
pJM3	P_{GAL}, *NL-TrxA,* 2μ/TRP1	(Colas et al., 1996)
pGAD-Rpn/t	*Proteasome subunit two-hybrid vectors*	(Cagney et al., 2001)
pRS316	CEN/URA3	(Sikorski and Hieter, 1989)
YcpLac33	CEN/URA3	(Gietz and Sugino, 1988)
YcpLac111	CEN/LEU2	(Gietz and Sugino, 1988)
pGAD-C2	*GAL4-AD,* 2μ/LEU2	(James et al., 1996)
pGBD-C2	*GAL4-BD,* 2μ/TRP1	(James et al., 1996)
pPM52	P_{CUP1}, *flag-His$_6$-OAZ1-ha$_2$,* CEN/URA3	Current study
pPM53	P_{CUP1}, *flag-His$_6$-OAZ1-if-ha$_2$,* CEN/URA3	Current study
pPM54	P_{CUP1}, *flag-His$_6$-YPL052W-ha$_2$,* CEN/URA3	Current study
pPM58	P_{CUP1}, *OAZ1-if-ha$_2$,* CEN/URA3	Current study
pPM64	P_{CUP1}, *ODC-ha$_3$,* CEN/LEU2	Current study
pPM67	P_{SPE1}, *ODC-ha$_3$,* CEN/LEU2	Current study
pPM84	P_{CUP1}, *myc$_2$-OAZ1-ha$_2$,* CEN/URA3	Current study
pPM85	P_{CUP1}, *myc$_2$-OAZ1-if-ha$_2$,* CEN/URA3	Current study

pPM92	P_{CUP1}, *myc$_2$-OAZ1-ha$_2$*, CEN/URA3	Current study
pPM94	P_{CUP1}, *OAZ1-if-ha$_2$*, CEN/URA3	Current study
pPM96	P_{CUP1}, *ODC-ha$_2$*, CEN/LEU2	Current study
pPM104	P_{GAL}, *OAZ1-if-ha$_2$*, CEN/URA3	Current study
pPM106	P_{CUP1}, *ODC-ΔN1 (47aa form N-ter)-ha$_2$*, CEN/LEU2	Current study
pPM107	P_{CUP1}, *ODC-ΔN2 (63aa from N-ter)-ha$_2$*, CEN/LEU2	Current study
pPM108	P_{CUP1}, *ODC-ΔC1 (11aa from C-ter)-ha$_2$*, CEN/LEU2	Current study
pPM109	P_{CUP1}, *ODC-ΔC2 (49aa from C-ter)-ha$_2$*, CEN/LEU2	Current study
pPM110	P_{CUP1}, *ODC-ΔC3 (102aa from C-ter)-ha$_2$*, CEN/LEU2	Current study
pPM111	P_{CUP1}, *ODC-ΔC4 (125aa from C-ter)-ha$_2$*, CEN/LEU2	Current study
pPM112	P_{CUP1}, *ODC-ΔC5 (175aa from C-ter)-ha$_2$*, CEN/LEU2	Current study
pPM113	P_{CUP1}, *OAZ1-if-ΔN1 (13aa from N-ter) -ha$_2$*, CEN/URA3	Current study
pPM114	P_{CUP1}, *OAZ1-if-ΔN2 (42aa from N-ter) -ha$_2$*, CEN/URA3	Current study
pPM115	P_{CUP1}, *OAZ1-if-ΔN3 (69aa from N-ter) -ha$_2$*, CEN/URA3	Current study
pPM116	P_{CUP1}, *OAZ1-if-ΔN4 (91aa from N-ter) -ha$_2$*, CEN/URA3	Current study
pPM117	P_{CUP1}, *OAZ1-if-ΔN5 (149aa from N-ter) -ha$_2$*, CEN/URA3	Current study
pPM118	P_{CUP1}, *OAZ1-if-ΔC1 (50aa from C-ter) -ha$_2$*, CEN/URA3	Current study
pPM119	P_{CUP1}, *OAZ1-if-ΔC2 (70aa from C-ter) -ha$_2$*, CEN/URA3	Current study
pPM120	P_{CUP1}, *OAZ1-if-ΔC3 (88aa from C-ter) -ha$_2$*, CEN/URA3	Current study
pPM123	*GAL4-AD- OAZ1-if-ha$_2$*, 2μ/LEU2	Current study
pPM124	*GAL4-AD- OAZ1-if-ΔN1-ha$_2$*, 2μ/LEU2	Current study
pPM125	*GAL4-AD- OAZ1-if-ΔN2 -ha$_2$*, 2μ/LEU2	Current study

pPM126	*GAL4-AD- OAZ1-if-ΔN3 -ha$_2$,* 2μ/LEU2	Current study
pPM127	*GAL4-AD- OAZ1-if-ΔN4 -ha$_2$,* 2μ/LEU2	Current study
pPM128	*GAL4-AD- OAZ1-if-ΔN5 -ha$_2$,* 2μ/LEU2	Current study
pPM129	*GAL4-AD- OAZ1-if-ΔC1 -ha$_2$,* 2μ/LEU2	Current study
pPM130	*GAL4-AD- OAZ1-if-ΔC2 -ha$_2$,* 2μ/LEU2	Current study
pPM131	*GAL4-AD- OAZ1-if-ΔC3 -ha$_2$,* 2μ/LEU2	Current study
pPM132	*GAL4-BD- OAZ1-if-ha$_2$,* 2μ/TRP1	Current study
pPM133	*GAL4-BD- OAZ1-if-ΔN1 -ha$_2$,* 2μ/TRP1	Current study
pPM134	*GAL4-BD- OAZ1-if-ΔN2 -ha$_2$,* 2μ/TRP1	Current study
pPM135	*GAL4-BD- OAZ1-if-ΔN3 -ha$_2$,* 2μ/TRP1	Current study
pPM136	*GAL4-BD- OAZ1-if-ΔN4 -ha$_2$,* 2μ/TRP1	Current study
pPM137	*GAL4-BD- OAZ1-if-ΔN5 -ha$_2$,* 2μ/TRP1	Current study
pPM138	*GAL4-BD- OAZ1-if-ΔC1 -ha$_2$,* 2μ/TRP1	Current study
pPM139	*GAL4-BD- OAZ1-if-ΔC2 -ha$_2$,* 2μ/TRP1	Current study
pPM140	*GAL4-BD- OAZ1-if-ΔC3 -ha$_2$,* 2μ/TRP1	Current study
pPM141	*GAL4-AD- ODC-ha$_2$,* 2μ/LEU2	Current study
pPM142	*GAL4-AD- ODC-ΔN1 -ha$_2$,* 2μ/LEU2	Current study
pPM143	*GAL4-AD- ODC-ΔN2 -ha$_2$,* 2μ/LEU2	Current study
pPM144	*GAL4-AD- ODC-ΔC1 -ha$_2$,* 2μ/LEU2	Current study
pPM145	*GAL4-AD- ODC-ΔC2 -ha$_2$,* 2μ/LEU2	Current study
pPM146	*GAL4-AD- ODC-ΔC3 -ha$_2$,* 2μ/LEU2	Current study
pPM147	*GAL4-AD- ODC-ΔC4 -ha$_2$,* 2μ/LEU2	Current study

pPM148	*GAL4-AD- ODC-ΔC5 -ha$_2$*, 2μ/LEU2	Current study
pPM149	*GAL4-BD- ODC-ha$_2$*, 2μ/TRP1	Current study
pPM150	*GAL4-BD- ODC-ΔN1 -ha$_2$*, 2μ/TRP1	Current study
pPM151	*GAL4-BD- ODC-ΔN2 -ha$_2$*, 2μ/TRP1	Current study
pPM152	*GAL4-BD- ODC-ΔC1 -ha$_2$*, 2μ/TRP1	Current study
pPM153	*GAL4-BD- ODC-ΔC2 -ha$_2$*, 2μ/TRP1	Current study
pPM154	*GAL4-BD- ODC-ΔC3 -ha$_2$*, 2μ/TRP1	Current study
pPM155	*GAL4-BD- ODC-ΔC4 -ha$_2$*, 2μ/TRP1	Current study
pPM156	*GAL4-BD- ODC-ΔC5 -ha$_2$*, 2μ/TRP1	Current study
pPM157	*P$_{CUP1}$, ODC-ΔN1C1-ha$_2$*, CEN/LEU2	Current study
pPM158	*P$_{CUP1}$, myc$_2$-OAZ1-ΔN1 -ha$_2$*, CEN/URA3	Current study
pPM159	*P$_{CUP1}$, myc$_2$-OAZ1-ΔN2 -ha$_2$*, CEN/URA3	Current study
pPM160	*P$_{CUP1}$, myc$_2$-OAZ1-ΔC1 -ha$_2$*, CEN/URA3	Current study
pPM161	*P$_{CUP1}$, myc$_2$-OAZ1-ΔC2 -ha$_2$*, CEN/URA3	Current study
pPM162	*P$_{CUP1}$, myc$_2$-OAZ1-ΔC3 -ha$_2$*, CEN/URA3	Current study
pPM163	*P$_{CUP1}$, myc$_2$-OAZ1-ΔN2C3 -ha$_2$*, CEN/URA3	Current study
pPM166	*P$_{CUP1}$, ODS-N1-e^K-ha$_2$-URA3*, CEN/LEU2	Current study
pPM167	*P$_{CUP1}$, ODS-N2-e^K-ha$_2$-URA3*, CEN/LEU2	Current study
pPM175 (BD-ODS-N1)	*GAL4-BD- ODS-N1-ha$_2$*, 2μ/TRP1	Current study
pPM176	*GAL4-BD- ODS-N2-ha$_2$*, 2μ/TRP1	Current study

4.1.4 Oligonuceliotides

Name/Sequence	Purpose
PM1081 TTTGAGCAGACTGCGGATATAGTATACATAGACTCTGAA CTCGATCGTACGCTGCAGGTCGAC	Forward oligo for tagging ODC (S3) (Knop et al., 1999)
PM1082 CACCCCCTCCGTCTCTCTTGCGAAAGTCGTGGTTAAATA TATCCTATCGATGAATTCGAGCTCG	Reverse oligo for tagging ODC (S2)(Knop et al., 1999)
PM1121 CATTTATTAGGTGATGAAAACTTTGTTATTTTAGAGTTTG AATGCCGTACGCTGCAGGTCGAC	Forward oligo for tagging Oaz1 (S3) (Knop et al., 1999)
PM1122 ACTTATTTAATGGTGGGATATATGCTTCTAACTGAATAT AACTGCATCGATGAATTCGAGCTCG	Reverse oligo for tagging Oaz1 (S2) (Knop et al., 1999)
PM1083 GCCGAATTCATGTCTAGTACTCAAGTAGGAAATG	EcoR1-5'ODC-forward
PM1244 CGCGGTACCCATCGAGTTCAGAGTCTATGTATACT	Kpn1-nostop-3'ODC-reverse
PM1297 GCGGGCATGCGAGCTCTACCGTTGCTTATTTTGTAATTA C	Sph1-Sac1- 5'SPE1 (ODC) promoter forward
PM1298 CGCGGTACCCCAGACATGAATTCAGTAAGTTTGAAATTC AAAGGTT	EcoR1-Kpn1-3'SPE1 (ODC) promoter reverse
PM1555 GCGCGAATTCATGAACCAAGATTTGGAACTTTTACC	EcoR1-DN1-ODC-forward
PM1556 GCGCGAATTCATGTTTCAAGCGCTCAAGGCTCGTATTG	EcoR1-DN2-ODC-forward
PM1557 CCGCGGTACCCAGTCTGCTCAAAGCCGTTGAATTG	Kpn1-nostop-DC1-ODC-reverse
PM1558 CCGCGGTACCCAATACAATCCAAACCATCACATG	Kpn1-nostop-DC2-reverse
PM1559 CCGCGGTACCCATGATCGAATAAAATACAATTCA	Kpn1-nostop-DC3-reverse
PM1560 CCGCGGTACCCCAGTTTTCTCTTCGCAATCACATG	Kpn1-nostop-DC4-reverse
PM1561 CCGCGGTACCCTTCAAATTGAAATCCACCACCTAC	Kpn1-nostop-DC5-reverse
PM1119 GACGAATTCATGTATGAAGTAATACAGAAAAGGAAAAC	EcoR1-5'OAZ1-forward
PM1131 GAACGTCTAGAGGGATGTCCGCGCACCAATCCTTAAATC	For deletion nt-206 forward
PM1132 GATTTAAGGATTGGTGCGCGGACATCCCTCTAGACGTTC	For deletion nt-206 reverse

PM1125 GACGAATTCATGGAATCTCAATTCATATTAGATTACAATG	EcoR1-5'YPL052W-forward (also used for N4 deletion of OAZ1)
PM1150 CCGCGGTACCCGCATTCAAACTCTAAAATAAC	Kpn1-nostop-OAZ1-reverse
PM1548 CGCGGAATTCATGAACGTTTTACAGAGTCCTGAACTC	EcoR1-DN1-OAZ1-forward
PM1549 CGCGGAATTCATGCTAAAAAGTAATAAGTGCACACC	EcoR1-DN2-OAZ1-forward
PM1550 GCGCGAATTCATGGACATCCCTCTAGACGTTCCACC	EcoR1-DN3-OAZ1-forward
PM1551 GCGCGAATTCATGGGTTACAATTGGAGAAAACTAGG	EcoR1-DN5-OAZ1-forward
PM1552 CCGCGGTACCCACCATTATTAATTAAATCATCTC	Kpn1-nostop-DC1-OAZ1-reverse
PM1553 CCGCGGTACCCGAAGTTTTGGTTCAGGTTGGAAG	Kpn1-nostop-DC2-OAZ1-reverse
PM1554 CCGCGGTACCCATTTATATAGGTACTGTGGTTATC	Kpn1-nostop-DC3-OAZ1-reverse
PM1432 GATCTATGGAGCAAAAGCTCATTTCTGAAGAGGACTTGAATGGAGAACAGAAATTGATCAGTGAGGAAGACCTCGGTG	BglII-2x-myc-EcoR1 (1)
PM1433 AATTCACCGAGGTCTTCCTCACTGATCAATTTCTGTTCTCCATTCAAGTCCTCTTCAGAAATGAGCTTTTGCTCCATA	BglII-2x-myc-EcoR1 (2)
ML422 GCGGAGCTCCATTACCGACATTTGGGCG	Sac1-5'CUP1 promoter-forward
PM1227 CGCGCTGCAGGCAAATTAAAGCCTTCGAGC	Pst1-3'CYC1 terminator-reverse

4.1.5 Enzymes and antibodies

Name	Source
RedTaq PCR mix (2x)	Sigma, USA
Expand High fidelity PCR System	Roche, Mannheim
Klenow Polymerase	Roche, Mannheim
Restriction endo-nuclease	New England Biolabs
T4 DNA Ligase	New England Biolabs
T4 DNA Polymerase	New England Biolabs
16B12, Anti-Ha antibody, Mouse, monoclonal	Covance
3F10, Anti-Ha antibody, Rat, monoclonal	Boehringer, Mannheim
9B11, Anti-Myc antibody, Mouse, monoclonal	Cell signaling Technology
EZview™ Red ANTI-FLAG® M2 Affinity Gel	Sigma, USA
Anti-Ha affinity Matrix	Roche, Mannheim
Anti-cdc11, rabbit, polyclonal	Santa Cruz Biotechnology
Anti-rat IgG + peroxidase	Boehringer, Mannheim
Anti-mouse IgG + peroxidase	Boehringer, Mannheim
Anti- rabbit IgG + near-infrared fluorophore (800)	Rockland
Anti-mouse IgG + near-infrared fluorophore (680, 800)	Rockland
Anti-rat IgG + near-infrared fluorophore (680, 800)	Rockland
Anti-thioredoxin, rabbit, polyclonal	Sigma, USA

4.1.6 Chemicals

Acetone

BSA (bovine serum albumin)

Chloroform

Acrylamide

Agarose (electrophoresis grade)

Avidin blocking

Biotin blocking

Calcium chloride

Coomassie-brilliant-blue R 250

DMF (dimethylformamide)

DMSO (dimethyl sulfoxide)

DTT (1,4-dithiothreitol)

EDTA ([ethylenedinitrilo]tetraacetic acid)

EGTA (ethylene-bis(oxyethylenenitrilo)tetraacetic acid)

Ethanol

Ethidium bromide

Formamide

Formaldehyde

Glycine

Isopropanol

β-mercaptoethanol

Methanol

MOPS ([morpholino]propanesulfonic acid)

Paraformaldehyde

RNase A

SDS (sodium dodecylsulfate)

Sodium azide

TEMED (tetramethylethylenediamine)

Tris (hydroxymethyl)aminomethane

Triton X-100 (t-octylphenoxypolyethoxyethanol)

Reagents listed above were purchased from Fluka, Merck, Roth, Serva, Sigma, Promega and Riedel-de-Haen.

4.1.7 Instruments

Name	Source
Curix 60-System developer machine	Agfa, München
Gel electrophoresis poIr supply and protein transfer	Amersham Biosciences, Freiburg
Centrifuge Avanti J-20 XP; Rotors, Centrifugation tubes, Scintwellation counter LS5000 TD	Beckman Coulter, München
PAGE-System MiniProtean3; Photometer (Smart Spec)	Biorad, München
Programmable Thermostate for PCR-reactions (Thermocycler T3);	Biometra, Göttingen
Table-top centrifuge 5417C, Thermostat (Thermomixer comfort)	Eppendorf, Hamburg
Phospho-Imager BAS-1500; X-ray films Super RX	Fuji, Düsseldorf
Microliter pipets	Gilson, Middelton, USA
pH-Meter;	Janna Instruments
Water bath	Eppendorf
Incubators	New Brunswick, USA
MwelliQ-water distweller	Mwellipore, Bedford, USA
Sterilization filters	Roth, Karlsruhe
Nitrocellulose membrane BA83 (0,2 µm);	Schleicher & Schüll, Dassel
PVDF	Sigma, USA
Odyssey Infrared imaging system	LI-COR biosciences, USA

4.2 Methods

4.2.1 Yeast and E.coli growth media

LB-Medium	1% -Bacto-Trypton 0.5% -Bacto-Yeast extract 1% -NaCl pH - 7.5 (adjusted with KOH) 2% -Bactoagar (LB-agar) Stock: Ampicillin was prepared separately and added to sterile LB medium (50mg/l).
YP-Medium	1%- Bacto-Yeast extract 2%- Bacto-Pepton 2%- Glucose for YPD (or) 2%- Galactose for YPGal pH - 5.5 (adjusted with HCl) 2%- Bacto-Agar (YP-Agar) Stock: 50% Glucose (prepared separately) 30% Galactose (prepared separately)
SD-Medium	6.7g/l-Yeast nitrogen base without amino acids 2%-Glucose Amino acid stock : 20mg/l Arginine, 10mg/l Histidine, 60mg/l Isoleucine, 60mg/l Leucine, 40mg/l Lysine, 10mg/l Methionine, 60mg/l Phenylalanine, 50mg/l Threonine, 40mg/l Tryptophane, 40mg/l Uracil, 20mg/l Adenine SG-Medium: 2%-Galactose instead of glucose SD or SG-Agar: 2%- Bacto-agar

4.2.2 Molecular biology and genetic methods

4.2.2.1 Isolation of plasmid DNA from *E. coli*

E. coli cells were cultivated for at least 12 hours in 3 ml LB-Medium plus 50 μg/ml ampicillin at 37°C with constant shaking at 200 rpm. After collecting the cells, they were subjected to alkaline lysis and the plasmid DNA was isolated.

4.2.2.2 Plasmid isolation with QIAprep Spin Miniprep Kit (QIAGEN)

Transformed *E. coli* cells were grown at least for 12 hours in LB media with ampicillin at 37^0C. Cells were collected and plasmid DNA was isolated according to the instructions provided by the manufacturer.

4.2.2.3 Estimation of DNA concentration

For estimating the concentration of DNA, the extinction of a DNA suspension was measured at 260 and 280 nm in several dilutions. The extinction of DNA at 260 nm is directly related to its concentration, assuming that $E_{260} = 1$ corresponds to 50 μg/ml double-stranded DNA.

4.2.2.4 Isolation of genomic DNA from yeast

Yeast cells derived from a single colony was grown in 5 ml of the appropriate medium until stationary phase (usually over night). Cells were collected by centrifugation at 4000 rpm for 5 min, washed with 1.2 M sorbitol and resuspended in 10 ml Buffer-A ,then 0.5 ml 2-mercaptoethanol was added to the suspension followed by incubation for 15 minutes at room temperature. Cells were pelleted, washed with Buffer-A and re-suspended in the same buffer supplemented with 2 % glucoronidase or zymolyase, then incubated for 30 min at 30°C which yielded spheroplasted cells. The spheroplasts were collected (4000 rpm, 5min) and resuspended in 0.5ml Buffer-B. The suspension was heated for 15 minutes at 70°C and 50 μl of 5 M KAc were added before cooling on ice for 30 min or longer. Precipitates were sedimented in a table top centrifuge for 15 minutes at 12,500 rpm. To ensure that all SDS is removed from the sample, another

50 µl of 5 M KAc was added followed by incubation on ice and centrifugation. Cleared supernatant was transferred to a new tube and DNA was precipitated by addition of 1ml, 95 % ice cold ethanol and centrifugation for 30 minutes at 12,500 rpm in 4°C. Then sediment was dried and resuspended in 250 µl TE plus 1 µl RNAse A (10 mg/ml, boiled). The suspension was incubated for 30 minutes at 37°C. 20 µl 3M NaAc and 220 µl cold (-20°C) isopropanol were added. After mixing by inversion, centrifugation for 2 minutes at 12,500 rpm in 4°C yielded precipitated DNA. After drying, DNA was resuspended in 20 µl of 0.1 M Tris, pH8 and 0.5-1 µl were run on analytical agarose gel to check for presence of RNA and DNA integrity. Concentration and purity were measured by using a spectrophotometer. DNA prepared with this method is suitable for PCR.

Buffer-A: 1.2 M sorbitol

       10 mM EDTA, pH 8.0

       100 mM SodiumCitrate

Buffer-B: 50 mM EDTA, pH 8.5

       0.2 % SDS

4.2.2.5 PCR amplification (Mullis et al., 1986)

Polymerase chain reaction (PCR) was performed in order to amplify double standard DNA *in vitro.*

PCR reaction mix: 1 µl Plasmid DNA (50ng)

       (*Yeast* or *E. coli* cells as template DNA)

       1 µl Oligonucleotide 1 (100pmol/µl)

       1 µl Oligonucleotide 2 (100pmol/µl)

       10 µl buffer 2 (10x)

       4 µl $MgCl_2$ (25 mM)

       3.5 µl Deoxynucleotide mix (10 mM)

       1 µl Polymerase mix (*Taq-* and *pfu*-DNA-polymerase Mix)

       79.5 µl H_2O

       ----

       100 µl- Total

Materials and methods

Amplification of DNA fragments for cloning was done by using the "Expand High fidelity PCR System" (Roche) according to the above mentioned protocol.

PCR reaction:

    1. Denaturation 5 min 94°C (for colony PCR 10 min instead of 5 min)

    2. Denaturation 40 sec 94°C

    3. Hybridisation 45 sec 55°C

    4. Elongation   (1 min/1Kb fragment) 72°C

    5. Repeat step 2- 4 for 32 times

    6. Extension   5 min 72°C

    7. Pause   4°C

Non high fidelity PCR reactions were performed by using the "RedTaq PCR mix" from Sigma according to the following protocol

PCR reaction mix: 0.2 µl Plasmid DNA (50 ng)

    (*Yeast* or *E. coli* cells as template DNA)

    0.2 µl Oligonucleotide 1 (100 pmol/µl)

    0.2 µl Oligonucleotide 2 (100 pmol/µl)

    2 µl RedTaq PCR mix (2x)

    17.4 µl H_2O

    ----

    20 µl- Total

PCR reaction:

    1. Denaturation 5 min 94°C (for colony PCR 10 min instead of 5 min)

    2. Denaturation 40 sec 94°C

    3. Hybridisation 45 sec 55°C

    4. Elongation   (30 sec/1Kb fragment) 72°C

    5. Repeat step 2- 4 for 32 times

    6. Extension   5 min 72°C

    7. Pause   4°C

Purification of amplified DNA was done by using the QIAGEN PCR purification kit by following the instructions provided by the manufacturer.

4.2.2.6 Agarose gel electrophoresis

Agarose gel electrophoresis was performed to analyze DNA sample. DNA fragments of different molecular weight show different electrophoretic mobility in an agarose gel matrix. Optimal separation results were obtained using 0.5-1 % (w/v) agarose gels in TAE buffer. Horizontal gel electrophoresis boxes of different sizes were used. Before loading the gel, the DNA sample was mixed with 1/6 volume of the 6x DNA-loading buffer. For examination of the DNA fragments under UV-light, agarose gels were stained with 0.1 μg/ml ethidiumbromide. In order to define the size of the DNA fragments, DNA molecular standard markers were also loaded on the gel.

TAE-Buffer: 40 mM Tris/HCl, pH 7.4

                     20 mM sodium acetate

                     1 mM EDTA

DNA-Loading dye: 2 mM EDTA, pH 8.0

                     4 % (w/v) Sucrose

                     0.025 % (w/v) Bromophenolblue

4.2.2.7 Extraction of DNA from agarose gel

Elution of DNA fragments from agarose gels was performed after cutting out the band of interest from the agarose gel and using the QIAGEN gel extraction spin kit according to the instruction manual supplied by the manufacturer. Eluted DNA was dissolved in appropriate volume of 10 mM Tris-HCl, pH 8.5.

4.2.2.8 Restriction digestion of DNA

Plasmid DNA and DNA fragments were digested with sequence-specific endo-nucleases. In order to digest 2 μg circular plasmid or linear DNA fragments, 20 units restriction enzyme (NEB) were used. The reaction was performed in the presence of enzyme specific buffer (NEB) or the double digestion buffer for approximately 180 min

at the recommended temperature. After the digestion, DNA fragments were purified if necessary.

4.2.2.9 Endfilling of digested DNA

Templates for endfilling reactions were produced by restriction digestion. The restriction enzyme was heat-inactivated according to the instruction of the producer (NEB). To the digested DNA, dNTPs were added to a 100 µM final concentration. Later Klenow fragment (1 unit/1 µg DNA) was added and incubated at room temperature for 15 min. The reaction was stopped by heating for 10 min at 75°C.

4.2.2.10 Ligation of DNA fragments

Ligation of DNA fragments after the restriction digestion was performed according to the following protocol

Ligation mix: 2 µl 10x-Ligase buffer (NEB)

~40 ng vector DNA

~30 ng insert DNA (vector: insert = 1: 3 molar)

Made up to 19 µl with deionised water

1 µl T4-DNA-Ligase (NEB)

Ligation mixes were incubated at 22°C for 1 hour or overnight. Later, 4 µl of the ligation mixes were used to transform chemical or electro competent *E. coli* cells.

4.2.2.11 Preparation of chemically competent E.coli cells

A culture of 5ml liquid LB medium was inocculated with cells of single colony of *E. coli* (DH5α or MC1061) grown on LB-agar plate and incubated overnight at 37°C. 1 % of the overnight grown culture was re-inocculated into 80 ml pre-warmed LB containing 20 mM $MgCl_2$. Cells were grown at 37°C until the OD_{600} reached 0.6. Then the culture was kept on ice for 5 min and the cells were pelleted down by spinning at 4000 rpm for 15 min at 4°C. The supernatant was discarded and the pellet was re-suspended in 32 ml of TFB1 and kept on ice for 5 min. Later the cells were pelleted down and the supernatant was discarded. The pellet was resuspended in 3.2 ml of TFB2 and kept on ice for 15 min. Then the suspension was aliquoted in desired amounts in pre-cooled eppendorf tubes and frozen in liquid nitrogen and stored at -80°C.

TFB1:   100 mM RbCl

                50 mM $MnCl_2$

                30 mM potassium acetate

                10 mM $CaCl_2$

                15 % (w/v) glycerol

                pH was adjusted to 5.8 with HCl.

                The solution was filter-sterilized.

TFB2:   10 mM MOPS

                10 mM RbCl

                75 mM $CaCl_2$

                15% (w/v) glycerol

                pH was adjusted to 6.8 with NaOH.

                The solution was filter-sterilized.

4.2.2.12 Transformation of chemical competent *E. coli* cells

50 μl competent *E. coli* cells were incubated with DNA for 10 min on ice. Afterwards the transformation mix was heat shocked at 42°C for 45 sec and kept on ice for 5 min. Later it was resuspended in 950 μl LB media <u>without</u> antibiotic, and incubated at 37°C with shaking for at least 45 min. Cells were collected by centrifugation in a table-top centrifuge at 11,000 g for 10 sec and plated on LB-agar plates supplemented with appropriate antibiotics. The plates were incubated at 37°C overnight.

4.2.2.13 Preparation of electro-competent *E. coli* cells

Overnight grown *E. coli* cultures were inocculated into pre-warmed LB to an OD_{600} 0.1. Cells were grown at 37°C to an OD_{600} 0.6. Then the culture was immediately cooled in ice and the cells were pelleted down at 4000g for 15 min in 4°C. The pellet was re-suspended in 1 L sterile cold water and the cells were pelleted down. The cells were again washed in 0.5 L of sterile ice cold water and subsequently in 20 ml of 10%

glycerol. Finally the cell pellet was resuspended in 3 ml of 10 % glycerol and then aliquoted in desired volume (40μl), then frozen in liquid nitrogen and stored at -80°C.

4.2.2.14 Transformation of electro-competent E.coli cells

The frozen cells were kept on ice for thawing. The DNA was added to the cells and incubated in ice for 10 min. The mix was later transferred to a cold 0.2 cm electroporation cuvette. The pulse was set according to the manufacturer's instruction. After the pulse, 1 ml of SOC or LB was added to the cells which were then incubated at 37°C for 1 hour before plating.

4.2.2.15 Cultivation of Yeast

Cells were streaked out on appropriate (YP or Minimal) media plate and grown at the appropriate temperature. Single colonies were inocculated in liquid YPD, YPGal selective synthetic media and incubated with shaking (160 rpm) at 30°C or 24°C for temperature sensitive strains. Unless required otherwise, cultures were usually held in exponential phase (OD_{600} 0.8 to 1) by diluting the culture in the same media.

4.2.2.16 High efficiency yeast transformation (Gietz and Woods, 2002)

The Li-Acetate method was used for yeast transformation with plasmid DNA or for gene disruption or manipulation via homologous recombination (Knop et al., 1999). Cells were inocculated to OD_{600} of 0.2 in either selective, YPD or YPGal media and grown to OD_{600} of 0.7-0.8. Then cells from 5 ml culture were collected by spinning at 4000g for 5 min. Later the pellet was suspended in 500 μl sterile water and transferred to fresh eppendorf tube. Cells were pelleted by spinning for 5 sec in table top centrifuge. Cells were washed in 250 μl of 0.1 M Li-Acetate and pelleted again. This cell pellet was supplemented with transformation mix as shown bellow. After addition of DNA to the transformation reaction, samples were mixed well by vortexing for at least 1 min and incubated at 30°C for 30 min. This was followed by incubation at 42°C for 15 min.

After cooling to room temperature, cells were collected and washed with sterile distilled water. When a vector was transformed, the cells were plated directly on selective media. In the case of gene disruption or manipulation (for G-418 resistance), cells were incubated for 1 hour in liquid non selective media, to allow for expression of the selective marker, and plated on solid selective media.

Transformation mix (1 transformation):   240 µl 50 % (w/v) PEG-3350

                                        36 µl 1 M LiAcetate

                                        50 µl boiled SS-DNA (2 mg/ml)

                                        X µl DNA

                                        34 – X µl sterile water

                                        ----

                                        360 µl- Total

4.2.2.17 Rescue of plasmids from yeast (Robzyk and Kassir, 1992)

2.0 ml yeast cultures were grown overnight in appropriate selective media. Cells were harvested by spinning at 13,000 g for 1 min. The pellet was resuspended in 100 µl of STET and ¾ volumes of 0.45 mm glass beads were added. Then the suspension was shaken in a vibrax for 5 min (max speed) for lysis. Another 100 µl of STET was added to the lysate, and after mixing on a vortex the sample was kept at 95°C for 5 min. Next, the sample was cooled briefly on ice and centrifuged at 13,000 g for 10 min in 4°C. The supernatant was collected and transferred to a fresh tube containing 75 µl of 7.5 M ammonium acetate and incubated at -20°C for 1 hour. Then, the sample was centrifuged at 13,000 g for 10 min at 4°C. 200 µl of the supernatant was added to 400 µl of ice-cold ethanol and kept at -20°C for 20 min. Then the DNA was recovered by centrifuging at 13,000 g for 20 min in 4°C. The pellet was washed with 70% ethanol. Later the pellet was air dried and resuspended in 20 µl of 10 mM Tris-HCl (pH 8.0). 5 µl of the solution was used for transformation into electro-competent *E. coli* cells.

STET: 8 % Sucrose

                  50 mM Tris/HCl, pH 8.0

                  50 mM EDTA

                  5 % Triton-X-100

                  (Autoclaved before use)

4.2.3 Biochemical and immunological methods

4.2.3.1 Yeast cell lysis by glass beads (Dohmen et al., 1995)

The yeast cells were pelleted, washed in water, and then resuspend in cold lysis buffer with protease inhibitor (cells from 10 ml culture is suspended in 500 µl lysis buffer). In equal volume of 0.45 mm glass beads was added to the cell suspension followed by lysis on a Vortex for 5 min with 1 min incubation on ice after every 1 min of vortexing. Then the lysate was centrifuged at 13,000 g for 15 min in 4°C. The supernatant was collected in an separate tube and centrifuged again for 15 min. Then the lysate was used for different purposes including protein measurement, immuno-precipitation of specific proteins and analysis of proteins by poly-acryl amide-SDS gel electrophoresis.

Lysis Buffer: 150 mM NaCl

                      5 mM EDTA

                      50 mM HEPES, pH 7.5

                      1% Trition-X-100

(Protease inhibitor [Roche, Mannheim] was added when necessary)

4.2.3.2 Yeast cell lysis by boiling

Yeast cells were pelleted and suspended in 1x LLB with or without 1% β-ME and boiled at 100°C for 5 min. Then the samples were cooled down to room temperature before further use.

LLB (Laemmli Loading Buffer):	62.5 mM Tris-HCl, pH 6.8
	2 % SDS
	10 % Glycerol
	0.002 % bromophenol blue

(DTT or β-ME was added before use when necessary)

4.2.3.3 Estimation of protein concentration

Protein concentration was estimated spectrophotometricaly by using the "BICINCHONINIC ACID PROTEIN ASSAY KIT" from Sigma and following supplier's protocol. BSA was used as a standard. The A_{562} of protein sample was correlated to the data for the standards and the protein concentration was recorded as mg/ml.

4.2.3.4 TCA precipitation of proteins

Proteins were precipitated in TCA (Trichloroacetic acid) when by incubation at a final concentration of 12% TCA for at least 60 minutes on ice. The samples were centrifuged at 4°C, 14,000 g for 20 min followed by two washing (4°C, 14,000 g for 10 min) steps with ice cold acetone (100%). Pellets were dried at 30°C for 30 minutes and resuspended in suitable reagents.

4.2.3.5 SDS-polyacrylamide gelelectrophoresis (SDS-PAGE) (Laemmli, 1970)

Proteins extracts were analysed by SDS-PAGE when required. The gel was prepared by following the standard protocol listed bellow. The electrophoretic system used was either from Hoefer scientific or BioRad.

Reagents:	1 M Tris, pH 6.8
	1.5M Tris, pH 8.8
	30 % (w/v) Acrylamide / 0.7 % Bisacrylamide

Materials and methods

----

	10 % (w/v) APS
	10 % (w/v) SDS
	TEMED
Laemmli running buffer (LRB):	25 mM Tris, pH 8.3
	192 mM Glycerol
	0.1 % (w/v) SDS

Resolving gel mix (15ml):

Final AA %	8	10	12	15
Water(ml)	7.1	6.1	5.1	3.6
1.5M Tris, pH8.8 (ml)	3.75	3.75	3.75	3.75
AA-mix (ml)	4	5	6	7.5
10% SDS (μl)	150	150	150	150
10% APS (μl)	50	50	50	50
TEMED (μl)	10	10	10	10

Stacking gel mix (5ml):

Final AA %	4
Water(ml)	3.66
1.0M Tris, pH 6.8 (ml)	0.625
AA-mix (ml)	0.650
10% SDS (μl)	50
10% APS (μl)	25
TEMED (μl)	5

Total protein derived from 0.5 OD_{600} cells per sample were loaded on the gel in case of boiled cell extract or 20-40 μg protein in case of glass bead lysis method. After electrophoresis, gels were used to transfer proteins to membranes for western blot analysis. The gels with radiolabelled proteins were dried by using a BioRad gel dryer and exposed to X-ray films or Phospho-imager plates.

4.2.3.6 Detection of proteins by western blotting

 Western blotting was used to detect proteins by using specific antibodies to a particular protein or to a tag attached to a particular protein after the separation in SDS-PAGE. The proteins were first transferred from the gel to either Nitrocellulose or PVDF membranes by using the "Semi-Dry protein transfer System" from Amersham Biosciences and transfer buffer by following the instructions of the manufacturer. 0.8 mA/cm^2 current for 60min was used for efficient transfer of proteins. After transfer, the membrane was kept in boiling water for 30 min before blocking with 3 % dry milk in PBS for 1 hour. Then the membrane was incubated with specific antibodies in appropriate dilutions in blocking solution for 1 hour. After the incubation with primary antibody the membrane was washed 30 min (5 min each, 1x PBST) before the addition of secondary antibody either coupled with HRP (peroxidase) or fluorophore 800, 680 from Rockland, USA for 45 min in blocking solution. Later the membrane was washed 45 min with 1x PBST (5 min each). The membrane probed with HRP conjugated secondary antibody was incubated with Lumi-light Plus reagent (Roche) for 30 sec before exposing to light sensitive X-ray film. In case of membrane probed with fluorophore-coupled secondary antibody, the signal was detected by using the "Odyssey Infrared imaging system" (LI-COR biosciences, USA). The signal was visualised and quantified by using the software "Odyssey v1.2".

Materials: Whatman filter paper

                                   Ponsue

                                   Nitrocellulose membrane

                                   PVDF membrane

                                   Non-fat dry milk powder

The PVDF membranes were kept in 100 % methanol for 10 min before the transfer to blotting buffer.

Transfer buffer (Blotting buffer):	25 mM Tris
	190 mM Glycine
	20 % (v/v) Methanol
	0.2 % (w/v) SDS

PBS:	137 mM NaCl
	2.7 mM KCl
	8.1 mM Na_2HPO_4
	1.5 mM KH_2PO_4
	pH 7.4
PBST:	PBS with 0.1 % Tween-20

HSWB:	1 M NaCl
	10 mM Na_2HPO_4
	0.5 % Tween-20
	(High salt wash buffer was used only when required)

Removing antibodies:

Membranes were incubated in fresh 0.2 N NaOH for 5 min. After several changes, membranes were washed thoroughly with water before reprobing.

4.2.3.7 Immunoprecipitation

Cells were lysed with glass beads as described in 3.2.3.1. 100 μg protein extract was incubated with 0.5 μg of specific antibody for a minimum of 2 hours to overnight. After 40 μl of protein A Sepharose was added and kept at 4°C with rotation. Then antibody-antigen-protein A Sepharose complexs were pelleted by spinning for 2 sec. The complex was washed several times with 800 μl lysis buffer with 0.1 % SDS. Immunoprecipitation of Flag-tagged protein were performed by using 30 μl "EZview™ Red ANTI-FLAG® M2 Affinity Gel". Ha-tagged proteins were immunoprecipitated with "Anti-Ha affinity Matrix". After the immunoprecipitation the sample was either

boiled directly in 2x LLB or after elution with antigen specific peptides against specific antibody (Flag-peptide from Sigma and Ha-peptide from Roche).

4.2.3.8 Measuring protein stability by *in vivo* pulse-chase analysis (Ramos et al., 1998)

Protein stability was determined by using pulse-chase analysis. Yeast cells were grown until mid-log phase (OD_{600} = 0.8-1.0) and 25 ml of culture was centrifuged at 3000 g for 5 min. The cell pellet was washed once with 800 μl pulse solution and the cells were resuspended in 600 μl pulse solution. 200 μCi of [S^{35}]-methionine was added to pulse label proteins for 5 min with mild shaking in a thermostat at 30°C. The cells were pelleted in a microcentrifuge and the supernatant was discarded. The cell pellet was resuspended in 400 μl of chase solution and kept at 30°C with mild shaking. Immediately for " 0 min ", 100 μl of cell suspension was transferred to a tube containing 500 μl lysis buffer. Later cells were collected in the same manner at respective time points. The samples were either frozen in liquid nitrogen and stored at -80°C or processed directly for cell lysis. Extract with equal amount of total protein were taken for immunoprecipitation of radio labelled proteins. Protein was then analyzed by SDS-PAGE and autoradiography. The signal was quantified by using the software "AIDA".

Reagents: [S^{35}]-Methionine or mixture of methionine and cysteine

Pulse solution: 3x-SD containing 4 % glucose without methionine

Chase solution: 3x-SD containing 4 % glucose with 10 mM methionine
              with 0.1 mg/ml cycloheximide.

Lysis buffer

Glass beads (acid washed)

Filter paper discs (9 mm)

Trichloroacetic acid (TCA)

50 % Protein A-Sepharose in water or affinity matrix with cross linked antibody

4.2.3.9 Yeast Two-Hybrid assay for detecting protein-protein interaction *in vivo* (James et al., 1996)

Protein-protein interactions were detected by using the yeast two-hybrid assay as described (James et al., 1996). The plasmids expressing the bait or prey were respectively transformed into the host cell. Protein interaction was detected by following the expression of reporter genes (*HIS3* or *ADE2*) that allow cells to grow in media without histidine or adenine.

A bait construct expressed a fusion of Gal4 DNA binding domain to a protein of interest. A prey construct expressed a fusion of the Gal4 activation domain to another protein of interest. The reporter genes were under the control of hybrid promoter containing Gal4 binding site (UAS).

5 Results

5.1 Identification of ornithine decarboxylase antizyme (Oaz1) in *S. cerevisiae*

The family of obvious antizyme orthologues detectable in the databases currently comprises more than 40 members. An inspection of their alignment revealed a conserved architecture with two homologous regions that are separated from each other by divergent linker sequences of variable length (shown in Figure 13 for selected antizyme orthologues). A conserved N-terminal sequence (D1) is centred at the +1 frameshifting site present in all antizymes (Figure 13). The larger C-terminal region D2 has been linked to ODC binding and degradation (Chen et al., 2002) (Ichiba et al., 1994).

In order to identify a sequence encoding a presumptive ODC antizyme in *S. cerevisiae*, the genome was searched with generalized profiles that were based upon a multiple alignment of antizyme sequences derived from various fungal species constructed by our collaborators Hartmut Scheel and Kay Hofmann (Memorec Biotech, Cologne, Germany). The generalized profile method constitutes a sensitive means to identify distant homologues based on family-wide conserved sequence features (Bucher et al., 1996). After a few iterations of profile construction the previously uncharacterised *S. cerevisiae* ORF "YPL052w" was identified to encode a polypeptide related to C-terminal parts of antizymes in other species. Obvious orthologues of "YPL052w" are also present in the genome of other closely related Hemiascomycetes. Upon close inspection, the genomic locus of "YPL052w" and its upstream sequences exhibits several features that are strikingly similar to those found in known antizyme genes (Figure 11). A putative ATG start codon is located 274 base pairs upstream of the annotated start codon of ORF "YPL052w". The upstream ATG represents the translational start site of a short ORF that ends with a TGA Stop codon after 207 bases. This ORF, referred to as "ORF1", is too short to be annotated in the Saccharomyces genome database.

```
ATGTATGAAGTAATACAGAAAAGGAAATAACAAAAACAAGTTTTACAGAGTCCTGAACTCATGAGGCTCATAGAGGACCCATCAAATCTGGGTATT   99  ORF1
 M  Y  E  V  I  Q  K  R  K  T  K  I  I  N  V  L  Q  S  P  E  L  M  R  L  I  E  D  P  S  N  L  G  I    33

TCTTTACATTTCCAGTAAGTTCACTGCTAAAAAGTAATAAGTGCACACCACCAAATCTTCTACTATAGTTTGGCTAGTGGGGGATTTAAGGAT     198
 S  L  H  F  P  V  S  S  L  L  K  S  N  K  C  T  P  M  P  K  L  S  T  Y  S  L  A  S  G  G  F  K  D   66

TGGTGCGCGTGACATCCCCTCTAGACGTTCCACCAGAGATTGATATCATCGATTTTTACTGGGATGTTATTTTATGCATGGAATCTCAATTCATTATTAGA   297  ORF2
 W  C  A  *      D  I  P  L  D  V  P  P  E  I  D  I  I  D  F  Y  W  D  V  I  L  C  M  E  S  Q  F  I  L  D   99

TTACAATGTTCCGTCAAAAAAATAAGGGGAACAATCAGAGAGTCTGTTGCTAAGCTGTTGAAAAAATAAGCTTGTAAACGATATGAAAACTACGTTAAAAAG   396
 Y  N  V  P  S  K  N  K  G  N  N  Q  K  S  V  A  K  L  L  K  N  K  L  V  N  D  M  K  T  T  L  K  R    132

ACTAATTTATAATGAAAATACCAAGCAATATAAAAATAATAAATAGCCACGATGGTTACACAGGCTCGCAGTATTTCATACTGTATCT           495
 L  I  Y  N  E  N  T  K  Q  Y  K  N  N  N  S  H  D  G  Y  N  W  R  K  L  G  S  Q  Y  F  I  L  Y  L    165

TCCCCTATTTACGCCAGGAACTGATTTGGTGTAAACTTAATGAAAACTATTTCCATGTTGTATTACCATCTTCTTACTGAATAGTAGGAACGTTCATGATAA   594
 P  L  F  T  Q  E  L  I  I  W  C  K  L  N  E  N  Y  F  H  V  V  L  P  S  L  L  N  S  R  N  V  H  D  N    198

CCACAGTACCTATATAAAGATTGGTTACTTGCCCTTTAGAGTTAATAAATGGTTAATAATGATTAATTCAAAATTCAAATTCGAATACATGAAATTGAGATT   693
 H  S  T  Y  I  N  K  D  W  L  A  L  L  E  L  T  S  N  L  N  Q  N  F  K  F  E  Y  M  K  L  R  L    231

GTATATTTTAAGAGATGATGATTAATAATAATGGTTTGGATCTCTTTGAAAAATCTTAACTGGGTCGGTGGGAAAACTGATTAAAAATGAAGAGATAGAGAAGT   792
 Y  I  L  R  D  D  L  I  N  N  G  L  D  L  L  K  N  L  N  W  V  G  G  K  L  I  K  N  E  D  R  E  V    264

CTTGTGAACTCGACCGATTTAGCTACGGATTCTATTTCTCATTTATTAGGTGATGAAAACTTTGTTATTTTAGAGTTTGAATGCTAA           880
 N  L  S  T  D  L  A  T  D  S  I  S  H  L  L  G  D  E  N  F  V  I  L  E  F  E  C  *    292
```

Fig. 11. Coding sequence of the *OAZ1* (ODC Antizyme) genomic locus together with the encoded polypeptides

The ORF1 including a TGA stop codon (shown in bold) encompasses the sequence until position 210. Upon a predicted ribosomal frameshifting resulting from skipping the first nucleotide in this stop codon (marked by an asterisk), translation continues in the +1 frame (ORF2). The ATG codon of the annotated ORF "YPL052w" is shown in bold.

Results

The stop codon of ORF1 is embedded in a sequence stretch of ~20 nucleotides, which is well conserved around the established ribosomal frameshifting site in mammalian antizyme mRNAs (Figure 12). If an analogous +1 ribosomal frameshifting that results in the omission of the U in the UGA stop codon in the mRNA is assumed in *S. cerevisiae,* translation would shift to a second reading frame (ORF2) to produce a putative 292 residue polypeptide. The C-terminal 202 amino acids of this protein are encoded by the annotated ORF "YPL052w".

```
                                                  ▼
Saccharomyces cerevisiae  AGTTTGGCTAGTGGGGGATTTAAGGATTGGTGCGCGTGACATCCCTCTAGACGTTCCACC
Saccharomyces paradoxus   AGTTTGACTGGCGGCGGGCTTTAAGGATTGGTGCGCGTGACATCCCTCTAGACCTTCCTCC
Saccharomyces bayanus     AGTTTGACTAGTAGTGGGGTTTAAGGATTGGCGCGCGTGACGTCCCTTTAGATCTTTCTGC
Saccharomyces mikatae     AGTTTGGCTAGCTGCGGCTTTAAGGATTGGCGCGCGTGACATCCCTTTGAATATTCCTCT
Saccharomyces castellii   TCTTTAACGAGCAGTGGATTTAAGGATTGGTATGCGTGACATCGGAGACGGGATCATCTT
Saccharomyces kluyverii   TACACTTTGAAAGATGGCACCTACCAGTGGTCTCCGTGACATGAGAGCCACTTTTATGCC
Kluyveromyces waltii      TACACTGTGCGGGATGGGTGTGAGGAGTGGTGCCCGTGACACCGGACCTTGGATTGACTA
Ashbya gossypii           TGCTCCTCGAGGACCGGGTACGCGGAATGGTTGGCGTGACAGGGGGGCGGGGGGCGCAGTC

S. pombe                  GGCTCTACGCCCGGCAGGGGGCGCGGAATGGTGCTCCTGAGCGCGCTTGAGCGCTCAAGACC  AF217277
Neurospora crassa        TCCACTACACCGGCGTCACAGGGGCCGAGTGGTATTCCTGAGGTCCCTTCGACGGGACTTCC  BX294028
C. elegans               TGCTCGACACCAGCCCGGCCGACGTCGGATGGTGTTTTTGACGCCCCCATGGCGTGCTCAC  AF217278
D. melanogaster          CCCATCTCTCTCGGCCTAGGGCCTCTGTGGTGGTCCTGATGTCCCTGTCCACCACAGAAC  U29529
Homo sapiens AZ1         TGTAGTAACCCGGCTCCGGGGCCTCGGTGGTGCTCCTGATGCCCCTCACCCACCCGTGAA  U09202
Homo sapiens AZ2         TGCAGGCACATTGTTCCAGGGCCTCTGTGGTGCTCCTGATGCCCCTCACCCACTGTCGAA  AF057297
Homo sapiens AZ3         TTGACACTCCAGCCCCGGTTCCTGCCTCCAGTGCTCCTGAGTCCCTATTACCTTTACTGTT  AF175296
Homo sapiens AZ4         TGTCGTCACCCGGGTCCGGGGCCTCGGTGGTGCTCCTGATGTCCCTCACCCACCCGTGAA  AF293339
```

Fig. 12. Sequence alignment of +1 frameshifting site in various antizyme genes

Alignment of genomic or cDNA sequences encompassing the frameshifting sites in established antizyme genes. Conserved positions are printed on black background. A triangle indicates the position of the frameshifting site.

In support of the inferred frameshifting site, the resulting protein sequence that is encoded by sequence encompassing this site exhibits a striking similarity to the D1 motif in known antizymes (Figure 13). The presumed antizymes of *S. cerevisiae* and its relatives moreover display homology to the D2 domain of established antizyme orthologues from other eukaryotes, which is likely to have an αβα fold (Figure 13). Taken together, these data suggested that *S. cerevisiae* ODC antizyme is encoded by a locus, termed *OAZ1* for <u>O</u>DC <u>a</u>nti<u>z</u>yme, which extends from the beginning of ORF1 to the end of "YPL052w" on chromosome XVI. According to this hypothesis, and similar to its counterparts in other eukaryotes, synthesis of Oaz1 in *S. cerevisiae* would also involve a ribosomal frameshifting event.
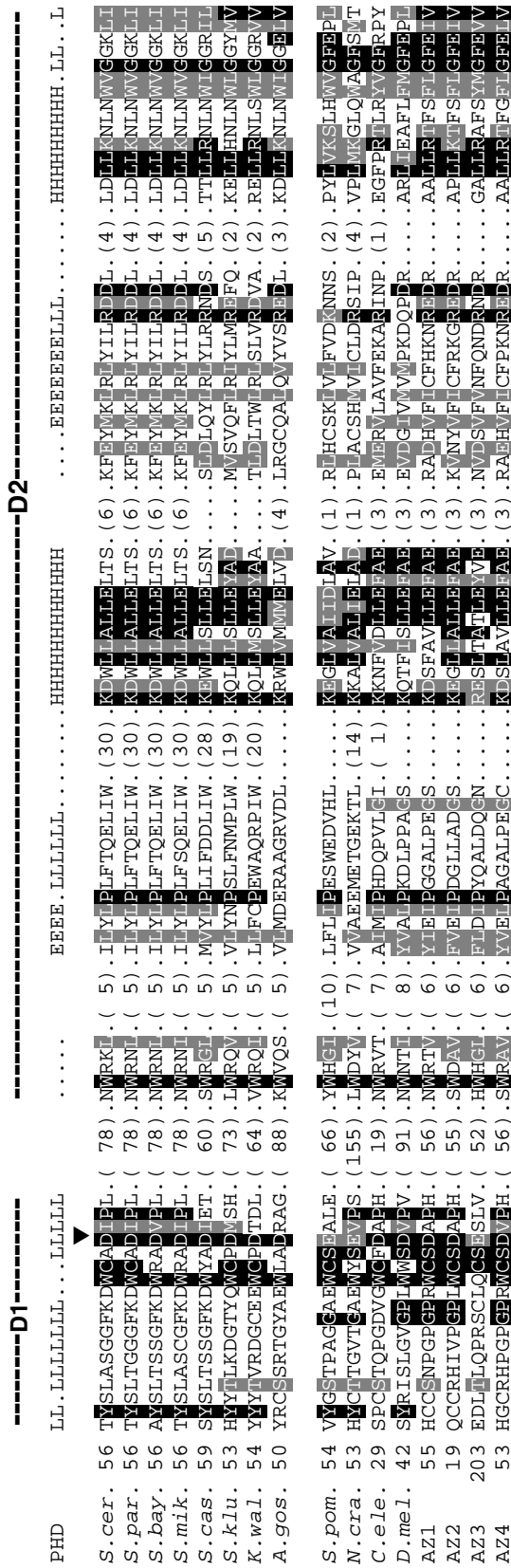
```
               ------D1------              ------------------------D2------------------------
PHD            LL.LLLLLL...LLLLL    ....    EEEE.LLLLLL.....HHHHHHHHHH    HHHHHHHHHH  ....EEEEEELLL.....HHHHHHHHH  HHHHHHHHH.LL..L
                                ▼

S.cer. 56  TYSLASGGFKDWCADIPL.( 78).NWRKI.( 5).IIYIPLFTQELIW.(30).KDWIIALLELTS.( 6).KFEYMKIRIYILRDDL.( 4).LDIIKNLNWVGGKLI
S.par. 56  TYSLTGGGFKDWCADIPL.( 78).NWRNI.( 5).IIYIPLFTQELIW.(30).KDWIIAILELTS.( 6).KFEYMKIRIYILRDDL.( 4).LDIIKNLNWVGGKLI
S.bay. 56  AYSLTSSGFKDWRADVPL.( 78).NWRNI.( 5).IIYIPLFTQELIW.(30).KDWIIAILELTS.( 6).KFEYMKIRIYILRDDL.( 4).LDIIKNLNWVGGKLI
S.mik. 56  TYSLASCGFKDWRADIPL.( 78).NWRNI.( 5).IIYIPLFSQELIW.(30).KDWIIALLELTS.( 6).KFEYMKIRIYILRDDL.( 4).LDIIKNLNWVGGKLI
S.cas. 59  SYGLTSSGFKDWYADIET.( 60).SWRGI.( 5).MYYLPLIFDDLIW.(28).KEWILSLLELSN......SLDLQYLRIYLRRNDS.( 5).TTLLRNLNWIGGRIL
S.klu. 53  HYYILKDGTYQWCPDWSH.( 73).LWRQV.( 5).VLYNPSLFNMPLW.(19).KQLLISLLEYAD.....MVSVQFIRIYLMREFQ.( 2).KEILHNLNWLGGYMV
K.wal. 54  YYYIVRDGCEEWCPDTDL.( 64).VWRQI.( 5).LLFCPEWAQRPIW.(20).KQLIMSLLEYAA.....TLDLTWIRLSLVRDVA.( 2).RELLRNLSWLGGRVV
A.gos. 50  YRCSRTGYAEWLADRAG.( 88).KWVQS.( 5).VLMDERAAGRVDL.....KRWLVMMMELVD.( 4).LRGCQAIQVYVSREDL.( 3).KDLIKNLNWIGGELV

S.pom. 54  VYGSTPAGCAEWCSEALE.( 66).YWHGI.(10).LFLIPESWEDVHL.....KEGIVAIIDIAV.( 1).RIHCSKIVIFVDKNNS.( 2).PYIVKSLHWVGFEPL
N.cra. 53  HYCTTGVTCAEWYSEVPS.(155).LWDYV.( 7).VVAEEMETGEKTL.(14).KKALVAIIELAD.( 1).PLACSHMVICLDRSIP.( 4).VPLMKGLQWAGFSMT
C.ele. 29  SPCSTQPGDVGWCFDAPH.( 19).NWRVT.( 7).AIMIPHDQPVLGI.( 1).KKNFVDLLEFAE.( 3).EMERVLAVFEKARINP.( 1).EGFPRTLRYVGFRPY
D.mel. 42  SYRISLGVGPIWWSDVPV.( 91).NWNTI.( 8).YVALPKDLPPAGS.....KQTFISLLEFAE.( 3).EVDGIVMVMPKDQPDR.....ARLIEAFLFMGFEPL
AZ1    55  HCCSNPGPGPRMCSDAPH.( 56).NWRTV.( 6).YIEIPGGALPEGS.....KDSFAVLLEFAE.( 3).RADHVFICFHKNREDR.....AALLRTFSFLGFEIV
AZ2    19  QCCRHIVPGPIWCSDAPH.( 55).SWDAV.( 6).FVEIPDGLLADGS.....KEGLLALLEFAE.( 3).KVNYVFICFRKGREDR.....APLLKTFSFLGFEIV
AZ3   203  EDLILQPRSCIQCSESIV.( 52).HWHGI.( 6).FIDIPYQALDQGN.....RESITATLEYVE.( 3).NVDSVFVNFQNDRNDR.....GALLRAFSYMGFEVV
AZ4    53  HGCRHPGPGPRMCSDVPH.( 56).SWRAV.( 6).YVELPAGALPEGC.....KDSIAVLLEFAE.( 3).RAEHVFICFPKNREDR.....AALLRTFGFLGFEIV
```

Fig. 13. Alignment of antizyme orthologues from selected species

A triangle indicates the position of the frameshifting site. Conserved residues are printed on black background, and positions assigned to amino acids with similar physicochemical properties are shaded in grey if supported by at least 50% of a total of 40 antizyme family members that were compared in this analysis (only 8 are shown). The sequences of a region termed D1 were aligned such that the frameshifting sites occupy equivalent positions. In the top row the secondary structure as calculated via PHD (Rost, 1996) is presented. Only positions with an expected average accuracy > 82 % were considered. The abbreviations denote the following secondary structure types: e, extended (beta-sheet), a, alpha-helix and l, loop.

5.2 Oaz1 mediates degradation of ornithine decarboxylase by the proteasome

To test the hypothesis that *S. cerevisiae OAZ1* encodes a putative ODC antizyme experimentally, I first asked whether this gene, as some of its counterparts in other eukaryotes including mammals (see Introduction), is indeed required for the regulated turnover of ODC. To address this question, genomic tags leading to an expression of ODC marked with 3 copies of the ha epitope at the C terminus were generated. These tags were introduced into a wild-type strain and a congenic strain deleted for sequences encompassing the annotated ORF "YPL052w", which encodes about two thirds of the presumptive Oaz1. The steady state levels of ODC in these two strains grown with and without treatment of the polyamine spermidine (100 μM) for 3 hours were determined by anti-ha western blot analysis (Figure 14A). Quantification of the signals revealed that the wild-type (wt) contained only ~50% of the ODC as compared to the *oaz1-Δ* strain (Figure 14B, grey bars). The presence of 100 μM spermidine in the culture medium resulted in a further reduction of Oaz1 levels in wt to ~12%, whereas no changes were observed in *oaz1-Δ* (Figure 14B, black bars).
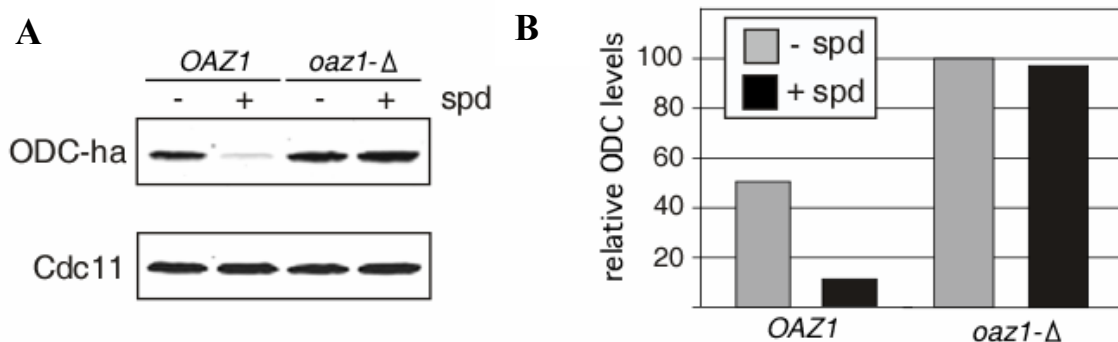
Fig. 14. Analysis of ODC levels in *oaz1-Δ*

(**A**) Steady state levels of ODC-ha in strains PMY1 (wt) and PMY2 (*oaz1-Δ*) grown for 3 hours in the absence (- spd) or presence of 100 μM spermidine (+ spd) were analyzed by anti-ha western blotting. The blot was simultaneously probed with anti-Cdc11 antibodies to control for differences in protein loading.
(**B**) Quantitation of fluorescence signals shown in (A). Values were normalised using the data obtained for Cdc11 and are given in % of the signal detected for *oaz1-Δ* grown in the absence of spermidine, which was set to 100 %.

Results

Next the kinetics of ODC disappearance was studied after addition of 100 μM spermidine to cultures of wild-type and *oaz1-Δ* mutant cells. Samples were collected at various time points and ODC protein levels were analyzed by anti-ha western blotting. In wild-type cells, ODC levels dropped rapidly to an extent that they were below detection already 60 min after spermidine addition (Figure 15). In the *oaz1-Δ* mutant, in contrast, ODC levels were not affected by spermidine. This data indicated that the presence of Oaz1 is required for controlling the levels of ODC in response to changes in polyamine concentrations, consistent with its presumed function of an ODC antizyme and a role in ODC turnover.
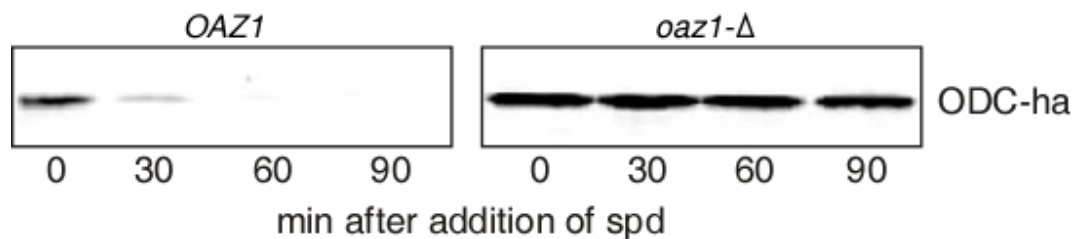
Fig. 15. Spermidine chase of ODC-ha in wild-type and *oaz1-Δ* cells
ODC-ha in cell extracts was detected in wild-type and *oaz1-Δ* at the indicated time points after adding spermidine to a concentration of 100 μM to the media. Samples were analyzed by using anti-ha western blotting.

To verify that the observed down-regulation of ODC upon addition of spermidine in wild-type cells reflects differences of ODC half-life, pulse chase analyses were performed to determine ODC turnover rates wild-type and *oaz1-Δ* cells. As shown in Figure 16A and quantified in Figure 16B, addition of 100 μM spermidine to the culture of the wild-type strain resulted in the induction of a rapid turnover of ODC ($t_{1/2}$~9 min) when compared to ODC turnover rates in wild-type cells without additional spermidine. Deletion of *OAZ1* resulted in a drastic stabilization of ODC, with spermidine having no effect on its stability.
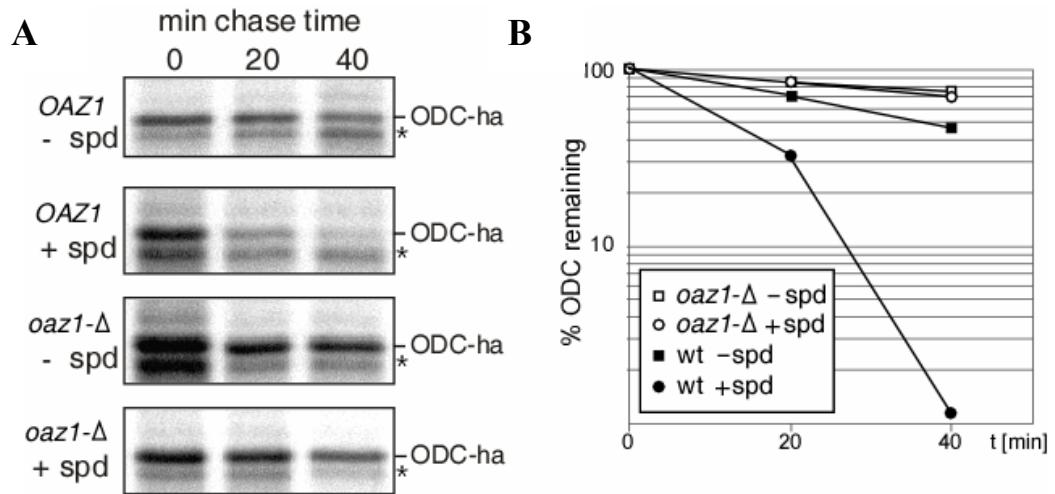
Fig. 16. Pulsechase analysis of ODC turnover

(**A**) Wild-type and *oaz1*-Δ cells were grown for 3 hours in the absence or presence of 100 µM spermidine before labelling. An asterisk marks the position of a non-specific band.
(**B**) Quantitation of radioactive ODC-ha signals shown in (A), which were normalised using data for non-speficic background bands.

The observation that spermidine-induced degradation of ODC required the presence of the *OAZ1* gene suggested that levels of Oaz1 are controlled by polyamines. Addition of polyamine has been shown to result in the increase of antizyme in other species. To test for spermidine induction of Oaz1, a sequence encoding 3 copies of the myc epitope was fused in frame to the 3' end of ORF2 on chromosome XVI. When extracts of the so marked strain were assayed by anti-myc western blotting, a protein with an apparent molecular weight of ~40 kDa was detected (Figure 17). The size is consistent with the calculated molecular weight of the predicted Oaz1-myc$_3$ polypeptide encoded from the inferred ATG start codon of ORF1 to the end of ORF2 (34 kDa) plus the C-terminal myc tag (~6 kDa). The level of Oaz1-myc$_3$ increased when spermidine was added to the culture media. The effect was even more striking when the *spe1*-Δ mutant lacking ODC was used in the experiment. In the absence of supplemented spermidine, this strain, which is unable to synthesize spermidine, did not contain detectable amounts of Oaz1 (Figure 17). Addition of high amounts of spermidine, however, also resulted in a strong induction of Oaz1 in this mutant. Together these results demonstrated that a regulation of Oaz1 levels is underlying the observed effects of spermidine on ODC stability.
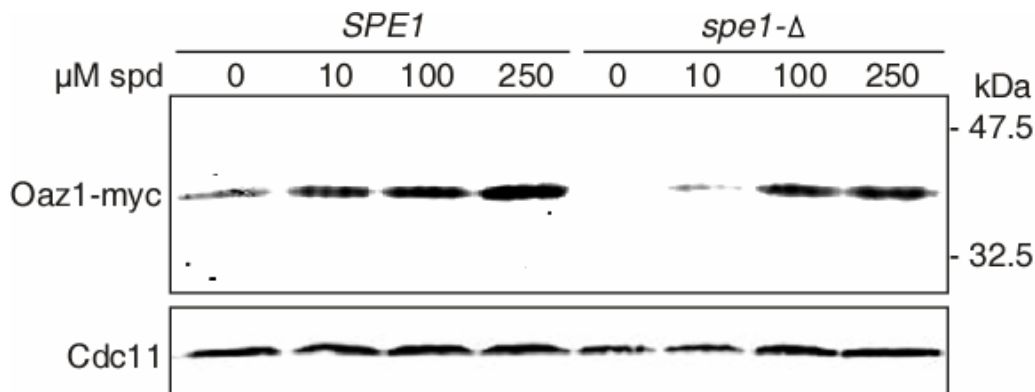
Fig. 17. Spermidine-induction of Oaz1-myc
Extracts from chromosomally tagged wt or *spe1*-Δ (=*odc*-Δ) strains were analysed by anti-myc western blotting. Both strains were incubated in the presence of the indicated concentrations of spermidine in the media. The lower panel shows the Cdc11 loading control.

5.3 ODC degradation requires a functional proteasome

Previous reports indicated that an intact proteasome is required for spermidine-induced degradation of ODC (Elias et al., 1995) (Gandre and Kahana, 2002) (Hoyt et al., 2003). In strains carrying either the *cim3-1/rpt6* mutation affecting an essential ATPase subunit (Rpt6) of the 19S activator complex of the 26S proteasome, or in *pre1-1* and *pre2-1* mutants, in which the β4 or β5 subunits of the 20S proteasome core are mutated, were transformed with a plasmid expressing ODC-ha from the native *SPE1* (=ODC) promoter. ODC-ha levels in those strains were analyzed by anti-ha western blot. As shown in Figure 18 spermidine-induced degradation of ODC was severely impaired in the strains with defective proteasomes. Together these data showed that Oaz1 is required for spermidine-induced degradation of ODC by the proteasome establishing its role as an ODC antizyme in *S. cerevisiae*. Degradation of ODC in mammals has been the paradigm of ubiquitin-independent degradation by the proteasome. It has been reported recently that degradation of ODC by the proteasome in *S. cerevisiae* does not require ubiquitin either (Gandre and Kahana, 2002) (Hoyt et al., 2003). Together these

data indicated that regulated antizyme-mediated and ubiquitin-independent degradation of ODC is conserved from *S. cerevisiae* to humans.
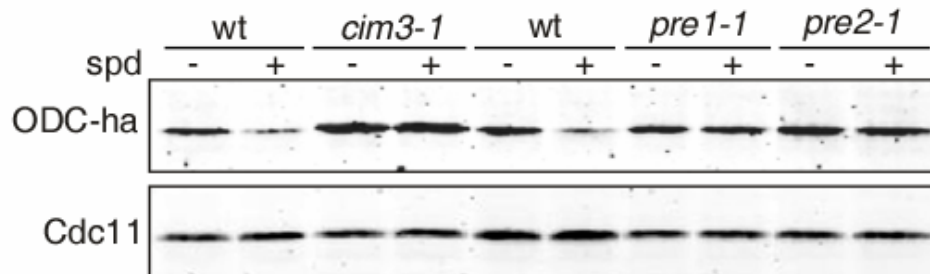
Fig. 18. ODC degradation is proteasome dependent
Steady state levels of ODC-ha expressed from P_{ODC} in the centromeric plasmid pPM67 in wt or proteasome mutants grown for 3 hours in the absence (- spd) or presence of 100 μM spermidine (+ spd) were analyzed by anti-ha western blotting. Lower part, anti-Cdc11 loading control.

5.4 Oaz1 physically interacts with ODC

Having established that Oaz1 is required for regulated proteolysis of ODC in *S. cerevisiae*, I next asked whether its mode of action is similar to that of its counterpart AZ1 in mammals (see Introduction). Therefore interaction of *S. cerevisiae* ODC and Oaz1 was tested *in vivo*. Using the two-hybrid assay, a strong interaction of ODC with Oaz1, as well as of ODC with itself was detected (Figure 19A). The latter result demonstrated that dimerisation of yeast ODC could be detected with this procedure. The former result was consistent with a model, in which, in analogy to mammalian systems, heterodimer formation underlies the targeted degradation of ODC in *S. cerevisiae*. To confirm this result biochemically, epitope-tagged versions of ODC and Oaz1 were co-expressed in yeast cells. Both proteins carried two copies of the ha epitope at their C-termini. Oaz1 was in addition tagged with a flag epitope at the N-terminus. Immunoprecipitations were carried out with anti-flag antibodies. ODC-ha was detected in precipitates from extracts of flag-Oaz1-ha co-expressing cells, but was absent from cell extracts lacking it (Figure 19B). Together these data showed that Oaz1 forms a complex with ODC in *S. cerevisiae* consistent with its function as an ODC antizyme.

A

B
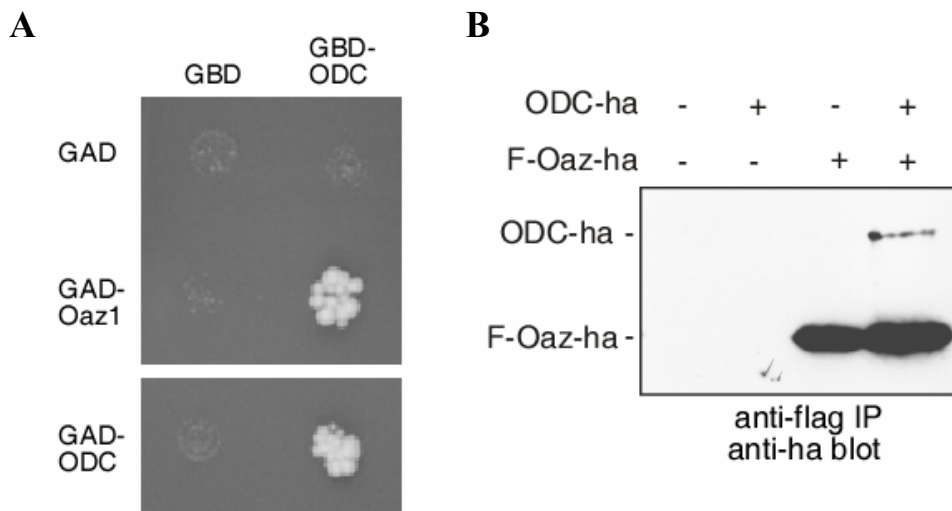
Fig. 19. Oaz1 physically interacts with ODC *in vivo*

(**A**) Two hybrid interaction of Oaz1 and ODC. Strain PJ69-4A was transformed with plasmids expressing Oaz1 or ODC as fusions to the Gal4 activating domain (GAD) or the Gal4 DNA binding domain (GBD). Plasmids expressing just GAD or GBD were used as controls. Interaction was assayed on SD media lacking histidine to monitor expression of a *HIS3* reporter gene that is under the control of P_{GAL}. Colony growth indicates interaction.
(**B**) ODC co-immunoprecipitates with Oaz1. Extracts from strain YHI29/1 (*pre1-1*) expressing either ODC-ha, flag (F)-Oaz1-ha or both were subjected to immunoprecipitation with anti-flag resin. Immunprecipitated proteins were analyzed by SDS-PAGE and anti-ha western blotting.

5.5 Yeast ODC N-terminus contains the degradation signal

In mouse, ODC degradation is achieved by exposure of its C-terminal degradation signal upon antizyme binding. Fusion of the mouse C-terminal ODC-degradation signal to a stable reporter protein resulted in ubiquitin-<u>in</u>dependent degradation of the reporter by the proteasome (Zhang et al., 2003). Since as shown above, Oaz1 strongly interacts with ODC, hypothesized that yeast ODC contains a degradation signal that functions similarly as the mouse ODC degradation signal. In order to identify the assumed degradation signal, the N- and C-termini of yeast ODC were systematically truncated as shown in Figure 20A.

A

B
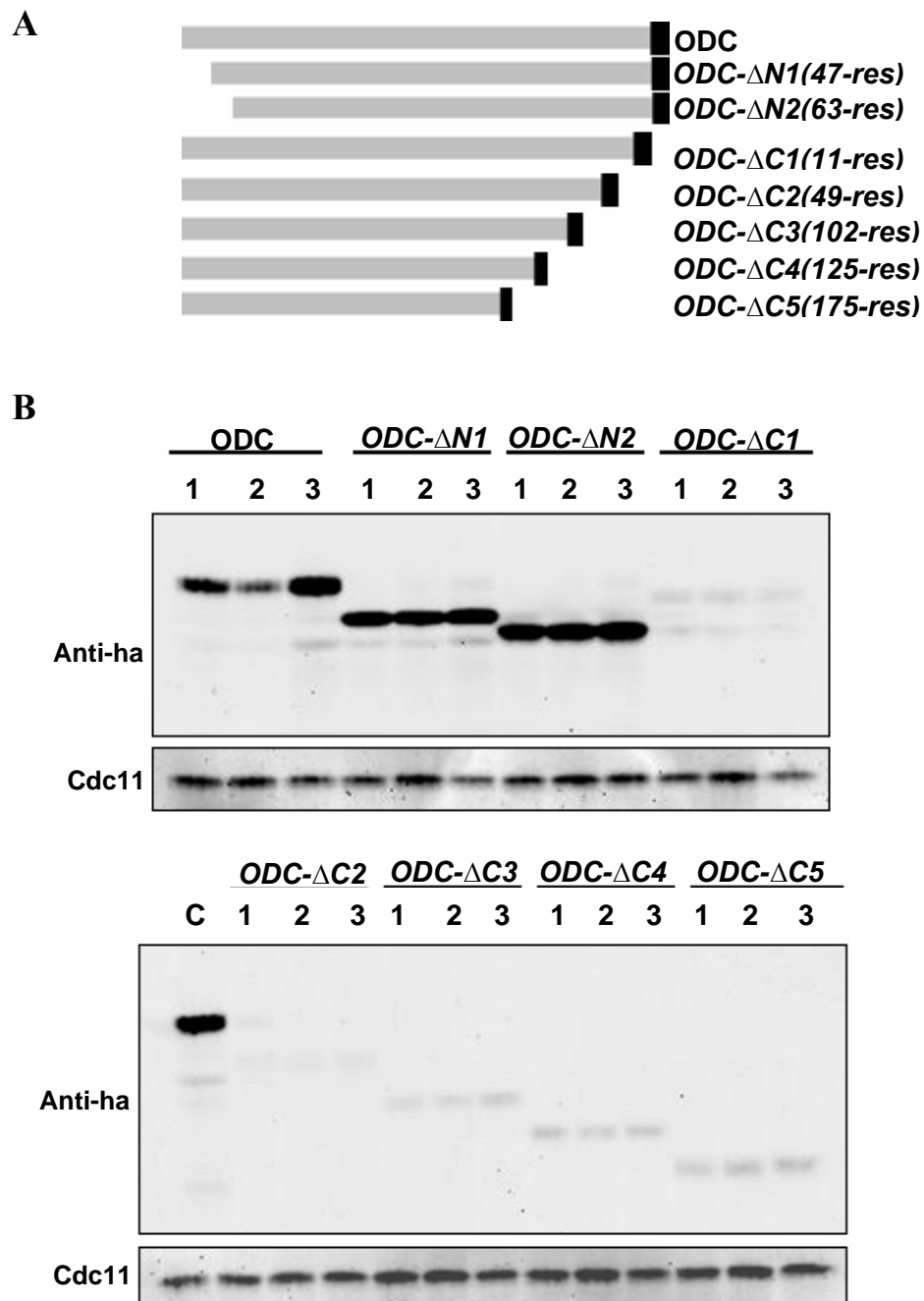
Fig. 20. ODC N-terminus is essential for its Oaz1 dependent degradation
(**A**). Schematic representation (not to scale) of the deletions in the N- or C-terminus of yeast ODC.
(█ indicates Ha tag). Numbers in parentheses indicate number of deleted residues.
(**B**). Anti-ha western blot showing the steady state levels of full length and ODC deletion mutants
in 1.) wild-type cells grown without 100 μM spermidine, 2.) wild-type cells grown with 100 μM
spermidine for 3 hours, 3.) *oaz1-Δ* cells without spermidine. C.) control *oaz1-Δ* strain expressing
full length ODC without spermidine. Lower panels show Cdc11 loading controls.

Results

Full length ODC and the truncation mutants carrying the ha tag at the C-terminus were expressed from the copper-inducible P*CUP1* promoter in a centromeric plasmid (Figure 20A). Wild-type and *oaz1-Δ* strains were transformed with plasmids carrying full length ODC or its truncated derivatives. Cells were grown in medium containing 100 μM CuSO$_4$ in order to induce expression. The transformants of the wild-type strain were grown in the absence or presence of 100 μM spermidine in order to test for Oaz1-mediated degradation. Since *oaz1-Δ* cells were unable to perform polyamine-induced ODC degradation (Figure 16), transformants of the *oaz1-Δ* strain were grown in medium without spermidine. Proteins were detected on the western blot by using anti ha antibody.

As shown in Figure 20B, the ODC level was low in wild-type cells grown in the presence of spermidine, which is consistent with the notion that spermidine induces Oaz1-dependent degradation of ODC (Figure 14 and 16). In *oaz1-Δ* cells, in contrast, the ODC level was higher confirming that Oaz1 is required for ODC degradation. Truncation of 47 residues at the N-terminus of ODC (*ODC-ΔN1*), however, led to an accumulation of this protein in wild-type cells grown either in the presence or absence of 100 μM spermidine. The *ODC-ΔN1* protein also accumulated in *oaz1-Δ* cells grown in the absence of spermidine (Figure 20B).
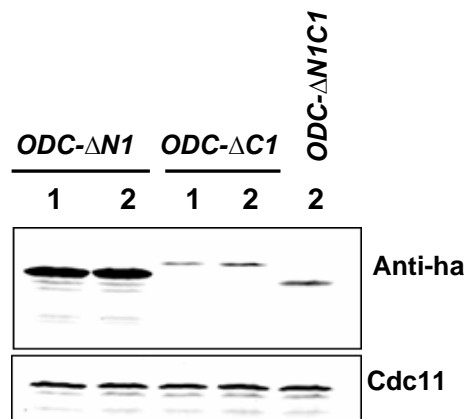
Fig. 21. Analysis of truncated ODC levels
Anti-ha western blot showing the steady state levels of ODC truncations Δ*N1,* Δ*C1and* Δ*N1C1* in, 1.) wild-type strain grown in the presence of 100 μM spermidine for 3 hours, 2.) *oaz1-Δ* strains. Lower panel is the Cdc11 internal loading control.

Results

This result showed that N-terminal truncation of ODC prevents Oaz1-dependent proteasomal degradation. Further truncation at the ODC N-terminus (*ODC-ΔN2*) also resulted in protection against Oaz1-mediated degradation (Figure 20B).

All the C-terminal deletions of ODC, in contrast, yielded low amounts of these proteins in wild-type as well as in *oaz1-Δ* cells (Figure 20B). When N- and C-termini of ODC (*ODC-ΔN1C1*) were deleted together, low amounts of this truncated protein was present in *oaz1-Δ* cells (Figure 21). Taken together these results suggested that C-terminal truncations of ODC resulted in inherently unstable proteins and their degradation was independent of Oaz1.
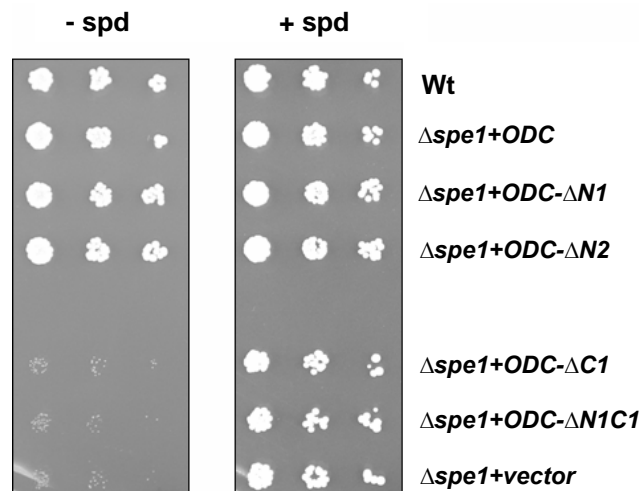
Fig.22. ODC N-terminal deletion mutants are functional
spe1-Δ strain transformed with plasmids expressing either full length or deletion mutants *(ΔN1, ΔN2, ΔC1 and ΔN1C1)* of ODC were spotted on minimal media plates without (-spd) or with 100 μM spermidine (+spd) and grown for 3days at 30°C. Wild-type (Wt) and *spe1-Δ* strains with empty vector were used as control.

From the results described above (Figure 19) it is clear that the functional ODC enzyme is a homodimer. Antizyme, however, appears to have affinity towards ODC and therefore it is able to disrupt the homodimer and to form ODC/Oaz1 heterodimers. I decided to measure the effect of ODC truncations on its ability to form homodimers by using the yeast two-hybrid interaction assay. The ODC truncation mutants after their fusion to Gal4 DNA-binding domain, however, resulted in the activation of reporter gene (*HIS3* and *ADE2*) expression independent of the presence of a Gal4 activation

domain (data not shown). Therefore I decided to use a *spe1-Δ (=odc Δ)* strain that cannot perform *de novo* polyamine synthesis in order to address the question as to whether the truncated ODC variants are capable of forming functional dimers. The *spe1-Δ* strain has severe growth defects when grown in minimal media without polyamines. These growth defects can be reversed either by transforming a wild-type copy of *SPE1* (ODC) gene or by adding polyamines to the growth media.

Full length and ODC truncation constructs was transformed with the *spe1-Δ* strain and grown on minimal media in the absence or presence of 100 μM spermidine. As shown in the Figure 22, the *spe1-Δ* strain expressing ODC, *ODC-ΔN1* or *ODC-ΔN2* were able to grow on media without additional spermidine. The *spe1-Δ* strain expressing *ODC-ΔC1, ODC-ΔN1C1* or a vector control in contrast, were not able to grow on media lacking spermidine. The growth of all these transformants was restored by the addition of 100 μM spermidine to the media. These results (Figure 22, right panel) indicate that the N1 and N2 truncations of ODC had no negative effect on the homodimer formation because *ODC-ΔN1*and *ODC-ΔN2* were functional and able to complement the growth defect of the *spe1-Δ* strain. In contrast, *ODC-ΔC1* and *ODC-ΔN1C1* were not able to complement the growth defect and were also present in low amounts when tested by western blotting (Figure 20 and 21). These data suggested that the C-terminally truncated ODC variants were not functional. This may either be due the negative effect of C-terminal deletions of ODC on their homodimer formation or due to a low abundance of these variants in the cell.

Based on these results (Figure 20, 21 and 22) I hypothesised that the N-terminal 47 residue motif contains the yeast <u>O</u>DC <u>d</u>egradation <u>s</u>ignal (hereafter referred to as **ODS**) that targets ODC for Oaz1-mediated ubiquitin-independent proteasomal degradation. It was not clear, however, from these results whether the ODC N-terminal degradation signal itself is sufficient for targeting ODC to the proteasome. In order to test this assumption experimentally, a construct expressing ODS-ha-Ura3 fusion protein was generated. Wild-type, *doa4-Δ, rpn10-Δ, rad23-Δ, fes1-Δ, hsc82-Δ, oaz1-Δ* and *pre1-1* strains were transformed with the plasmid expressing ODS-ha-Ura3. Steady state levels of the fusion protein were determined by western blotting using anti-ha antibody.

Results

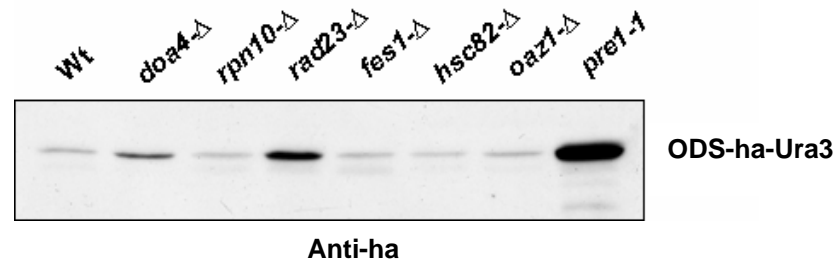

Fig. 23. Proteasomal targeting of Ura3 by ODS (yeast ODC degradation signal)
Anti ha western blot showing ODS-Ura3 protein levels in wild-type, *doa4-Δ, rpn10-Δ, rad23-Δ, fes1-Δ, hsc82-Δ, oaz1-Δ* and *pre1-1* strains. Cells were grown in media containing 100 μM CuSO$_4$ in order to induce the gene expression from P$_{CUP1}$ promoter.

Figure 23 shows that levels of the ODS-ha-Ura3 fusion were low in wild-type cells when compared to the proteasome-defective *pre1-1* cells. This suggested that ODS-ha-Ura3 fusion protein is efficiently degraded in the wild-type cells and that the degradation requires a functional proteasome. Then I asked if the proteasomal degradation of ODS-ha-Ura3 fusion protein requires a functional Oaz1. Figure 23 shows that the fusion protein levels were similar in the wild-type and *oaz1-Δ* cells. This result suggested that ODS-ha-Ura3 protein was efficiently degraded in the *oaz1-Δ* cells leading to the conclusion that Oaz1 is not required for the degradation of the ODS-ha-Ura3 fusion protein.

Having established that ODS-ha-Ura3 fusion protein degradation is Oaz1-independent, I then asked whether it is ubiquitin-dependent. In order to test that, the levels of fusion protein were assayed in *doa4-Δ* cells. Doa4 is a ubiquitin de-conjugating enzyme that is involved in recycling of ubiquitin in the cell. Deletion of *DOA4* results in the reduction of free ubiquitin levels in the cell, thereby leading to an impairment of ubiquitin-dependent proteasomal protein degradation (Gandre et al, 2002). Figure 23 shows that the levels of ODS-ha-Ura3 fusion protein in *doa4-Δ* cells were similar to its levels in wild-type cells. These results suggested that the ODS-ha-Ura3 fusion protein was efficiently degraded in *doa4-Δ* cells and that its degradation is ubiquitin-independent.

Often the fusion of an unstructured domain to a reporter results in the generation of misfolded proteins that are degraded by the cellular quality control system. In order

to test if the fusion of ODS to ha-Ura3 resulted in the formation of a misfolded protein, the steady state levels of ODS-ha-Ura3 fusion protein were analysed in the *fes1-Δ* and *hsc82-Δ* strains. Fes1 is a nucleotide exchange factor for the Hsp70 family chaperone Ssa1. Fes1 has been shown to be involved in degradation of misfolded protein (Marcel Fröhlich, personal communication). Hsc82 is one of the Hsp90 family chaperones and together with Hsp82 is shown to be involved in the degradation of misfolded proteins (Marcel Fröhlich, personal communication). ODS-ha-Ura3 fusion protein levels (Figure 23) in *fes1-Δ* cells were similar to those in the wild-type cells. Similarly the ODS-ha-Ura3 fusion protein levels in *hsc82-Δ* cells were comparable to those in wild-type cells. However in the latter case, it is worth noting that the loss of *HSC82* can be compensated by the gene product of the *HSP82* gene. The low steady state levels of ODS-ha-Ura3 in the *fes1-Δ* cells, however, suggested that ODS fusion to ha-Ura3 did not result in the formation of a misfolded protein.

Degradation of mouse ODC has been suggested to involve binding to a ubiquitin receptor site in the proteasome (Zhang et al., 2003). In order to test if the proteasome-associated proteins Rpn10 and Rad23 (See Introduction) that are involved in targeting ubiquitylated proteins to the proteasome are required for ODS-ha-Ura3 fusion protein degradation, its steady state levels were analyzed in *rpn10-Δ* and *rad23-Δ* strains. ODS-ha-Ura3 fusion proteins appeared to be degraded normally in *rpn10-Δ* cells as the steady state levels of this fusion protein were similar to its levels in wild-type cells (Figure 23) *rad23-Δ* cells, in contrast, showed significantly higher levels of ODS-ha-Ura3 when compared to the wild-type cells (Figure 23). This result suggested that Rad23 is required for efficient degradation of ODS-ha-Ura3 fusion protein. Rad23 is an Uba/Ubl domain containing protein (see Introduction) and it acts as an adaptor for delivering ubiquitylated proteins to the proteasome. It is worth noting that the loss of Rad23 function can be partially compensated by other adaptor proteins like Dsk2 and Did1 (see Introduction). The marginal accumulation of ODS-ha-Ura3 fusion protein suggested that ODS-ha-Ura3 protein degradation may involve components of the targeting machinery that are also required for delivery of ubiquitylated proteins to the proteasome.

Taken together the results shown in Figure 20, 21 and 23 indicated that ODS represents the degradation signal that targets ODC for ubiquitin-<u>in</u>dependent proteasomal degradation upon binding to Oaz1. These data suggested that Oaz1 does not directly mediate binding of the ODC/Oaz1 heterodimer to the proteasome. Oaz1 rather appears to be necessary to expose ODS, which in turn mediates targeting to the proteasome. The adaptor protein Rad23 may contribute to this targeting of ODC.

5.6 The ODC N-terminus interacts with 19S lid components of the proteasome

The results described in the previous section showed that ODS can target a reporter protein to the proteasome for ubiquitin-<u>in</u>dependent degradation. Although it is known for many years that ODC is an ubiquitin-<u>in</u>dependent substrate of the proteasome, the mechanism of targeting ODC to the proteasome via its degradation signal is still unidentified. It has been suggested that multi-ubiquitin chains attached to substrates mediate their targeting by binding to ubiquitin receptors (Rpn10 and Rpt5) in the proteasome (see introduction). As ODC lacks the multi-ubiquitin chain, its targeting is still unclear. One possibility is that the ODC degradation signal can bind to the known ubiquitin receptors in the proteasome or it may bind to yet unknown binding sites in the proteasome. In order to test this, the binding of ODS to subunits of the 19S cap of the proteasome was assayed via the yeast two-hybrid interaction system. As shown in Figure 24, ODS fused to the Gal4-binding domain strongly interacted with all the 19S lid components fused to the Gal4-activation domain. However, there was no measurable interaction detected between ODS and the 19S base components including Rpn10 and Rpt5. This result indicates that binding of ODC degradation signal to proteasomal lid components may underlie the ubiquitin-<u>in</u>dependent targeting of ODC.

A	**B**	**A**		**B**	

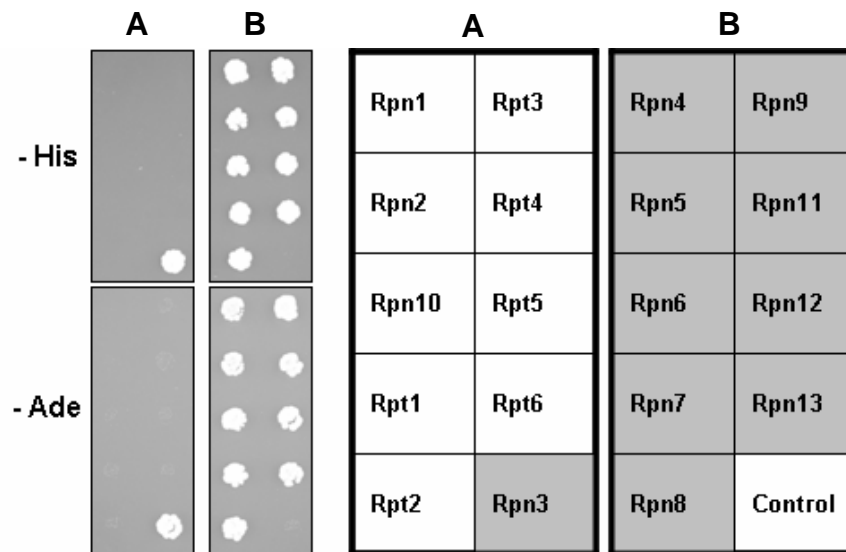| A		B	
Rpn1	Rpt3	Rpn4	Rpn9
Rpn2	Rpt4	Rpn5	Rpn11
Rpn10	Rpt5	Rpn6	Rpn12
Rpt1	Rpt6	Rpn7	Rpn13
Rpt2	Rpn3	Rpn8	Control

Fig. 24. ODS interacts with 19S lid components of the proteasome
The two hybrid reporter strain PJ69-4A was transformed with plasmids expressing Gal4-binding domain(GBD)-ODS and Gal4-activation domain (GAD) fused to individual 19S cap subunits. Cells carrying both plasmids were spotted on several SD media plates. Growth on the plate lacking histidine and the plate without adenine indicates expression of reporter genes (*HIS3* or *ADE2*) due to interaction of the fusion proteins. Cells expressing GBD-ODS and GAD alone were used as a control. The table to the right lists the corresponding subunits. The grey shade marks subunits that interact with ODS.

5.7 Polyamines induce ribosomal frameshifting during translation of *OAZ1 mRNA*

As outlined in chapter 4.1, the complex genomic structure of the *OAZ1* gene suggested that synthesis of Oaz1 protein involves a ribosomal frameshifting event. For ODC antizyme in mammals, it has been demonstrated that translational frameshifting is induced by polyamines (see Introduction). The observed spermidine-inducibility of Oaz1 suggested that a similar mechanism may operate in *S. cerevisiae* as well. To investigate the mechanism underlying the inducible synthesis of Oaz1, fusions of a sequence encoding 2 copies of the myc epitope with the 5' end of ORF1 and of a sequence encoding 2 copies of the ha epitope with the 3' end of ORF2 were generated. Two otherwise identical constructs were generated that carried both tags but that were distinguished either by the presence (*OAZ1*) or the absence of the frameshifting site (*OAZ1-if*; "if" denotes an in-frame fusion of ORF1 and ORF2).

A

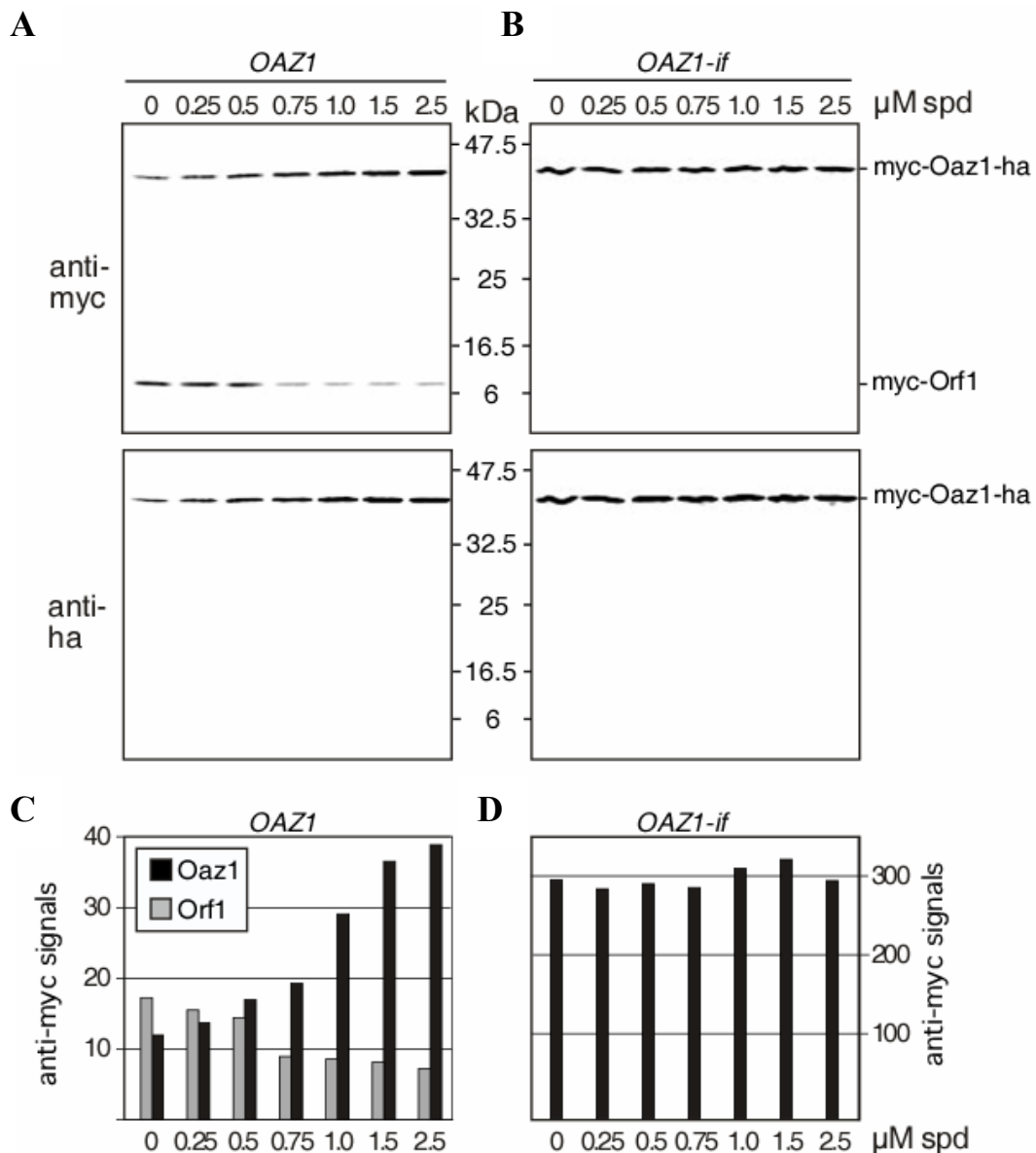

B

C

D

Fig. 25. Synthesis of Oaz1 involves spermidine-inducible frameshifting

(**A, B**) Western blot analysis of *pre1-1* mutant strain YHI29/1 transformed with centromeric plasmids expressing, from P$_{CUPI}$, either (**A**) *OAZ1* including the frameshift site or (**B**) *OAZ1-if*, an in-frame fusion of ORF1 and ORF2 that was generated by deleting the T nucleotide marked with an asterisk in Fig. 11. Both constructs were fused at their 5' ends to a sequence encoding 2 copies of the myc tag and at their 3' ends to a sequence encoding two copies of the ha tag. Cells were grown in presence of the indicated concentrations of spermidine and 100 µM CuSO$_4$ to induce expression from P$_{CUPI}$. Extracts were analysed simultaneously for myc and ha tagged proteins by immunoblotting.
(**C, D**) Quantitation of fluorescence signals shown in A and B, respectively.

Results

To generate the latter construct, the T nucleotide within the TGA stop codon of ORF1 was deleted. Both constructs were expressed from the unrelated P_{CUP1} promoter to exclude any putative effects of polyamines on transcriptional regulation.

In addition I chose the proteasome deficient *pre1-1* mutant (Heinemeyer et al., 1991) as a host strain because it turned out that Oaz1 is degraded by the proteasome and that this process is influenced by polyamines (described in a later section). The effects of spermidine on ribosomal frameshifting were therefore studied in *pre1-1* cells, which were transformed with centromeric plasmids carrying the constructs described above.

The presence of tagged polypeptides in cell extracts was analysed by western blotting (Figure 25A and B). Cells expressing the construct containing the frameshift site showed increasing myc-Oaz1-ha signals with rising spermidine concentration in the growth media. The strain expressing the in-frame fusion, in contrast, yielded myc-Oaz1-ha signals that did not respond to changes of the spermidine concentration in the media (Figure 25B). Note that the levels of tagged Oaz1 in the latter strain were ~10-fold higher than those obtained with the strain requiring induced frameshifting to synthesize Oaz1. In both strains these signals were detectable with anti-myc as well as with anti-ha antibodies supporting the notion that spermidine-induced ribosomal frameshifting had taken place during expression from the *OAZ1* construct. This conclusion was supported further by the detection of the faster migrating myc-Orf1 polypeptide, in this case only with the anti-myc antibody, in the extracts of the strain expressing *OAZ1* bearing the frameshifting site. The intracellular concentration of this polypeptide declined with increasing spermidine concentration in the growth media (Figure 25A and C).

Together the data described above proved the prediction that Oaz1 is expressed from ORF1 and ORF2 as a result of a spermidine-induced ribosomal frameshifting. This notion is supported by the ability of an *OAZ1-if* construct expressed from P_{CUP1} to complement the defect of the *oaz1-Δ* mutant in the degradation of ODC (Figure 26). An otherwise identical construct bearing the authentic frameshifting site also resulted in efficient complementation of *oaz1-Δ* even without supplemented spermidine. This result indicated that P_{CUP1} provided an expression level of *OAZ1* sufficient for efficient targeting of ODC without additional polyamines in the media for the induction of ribosomal frameshifting.

 A construct expressing only the annotated ORF "YPL052w", in contrast, showed no complementation of *oaz1-Δ* supporting the notion that this ORF does not encode a functional antizyme.
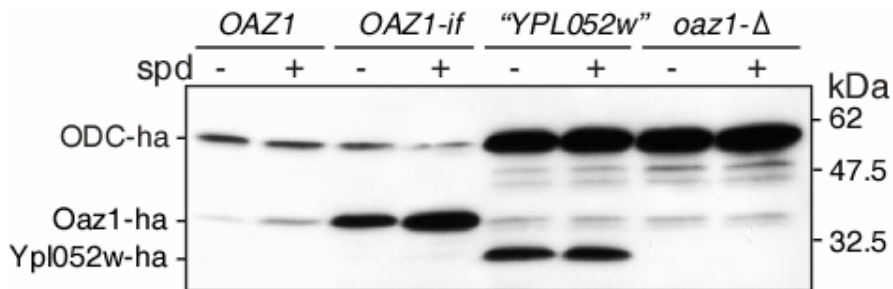

Fig. 26. *OAZ1-if* complements *oaz1-Δ* defect in the ODC degradation
An *OAZ1* gene lacking the frameshift mediates ODC degradation. Strain PMY2 (*oaz1-Δ ODC-ha*) was transformed with an empty vector or with plasmids expressing, from P_{CUP1}, either *OAZ1, OAZ1-if* or ORF "YPL052w". All 3 constructs were fused at their 5' ends to a sequence encoding an flag-6His tag and at their 3' ends to a sequence encoding two copies of the ha tag. Transformants were grown in the presence of 100 μM $CuSO_4$ and either in the absence or presence of 100 μM spermidine as indicated. Yeast cell extracts were analysed by anti-ha immunoblotting.

The results shown in Figure 26 also indicated that relatively low amounts of antizyme are sufficient to mediate degradation of the bulk of ODC. The residual ODC appears to be fairly resistant to Oaz1-induced degradation. The constructs used in Figure 26 carried N-terminal flag-His_6 tags. Similar results were obtained with N-terminal myc_2, although this tag appeared to reduce the efficiency of Oaz1 in ODC targeting (data not shown).

5.8 *Cis* regulatory elements associated with +1 ribosomal frameshifting during decoding of yeast *OAZ1 mRNA*

Decoding of *OAZ1 mRNA* involves programmed polyamine-induced +1 ribosomal frameshifting as was shown in Figure 25. The mechanism of polyamine-induced frameshifting during the decoding of antizyme *mRNA* is conserved in other species as well. *Cis* elements that are important for +1 ribosomal frameshifting have been mapped in mammalian antizyme *mRNA* (see Introduction). However the mechanisms that govern polyamine induction of +1 ribosomal frameshifting are still unknown. This is mainly due to the fact that the element(s) responsible for polyamine induction of +1 ribosomal frameshifting so far has not been identified.

Therefore, I decided to identify the element(s) important for ribosomal frameshifting during decoding of antizyme mRNA. In order to achieve this, I took the MYC$_2$-OAZ1-HA$_2$ construct that was generated for the previous experiments (Results 4.7) and introduced several deletions into the 5' as well as 3' end of *OAZ1* (Figure 27A). The proteasome defective *pre1-1* strain was again chosen as a host for expression of full length as well as the truncated *OAZ1* for reasons described in the previous section (Results 4.7). The *pre1-1* transformants were grown in minimal media in the absence or presence of 10 μM spermidine. Cells were harvested when the cultures had reached the exponential phase. Oaz1 protein levels were analysed by using anti-ha western blotting. Cdc11 served as an internal loading control.

Levels of the proteins encoded by different *OAZ1* variants provided a measure of +1 frameshifting efficiency during the decoding of *OAZ1 mRNA,* because transcription and protein degradation is not influenced by polyamines as P$_{CUP1}$-driven constructs were used in *pre1-1* cells (Figure 27). The differences in the protein steady state levels could clearly be attributed to different frameshifting rates as otherwise identical constructs lacking the frameshifting site gave equal protein amounts for all the deletion constructs as well as the full length *OAZ1* (data not shown).
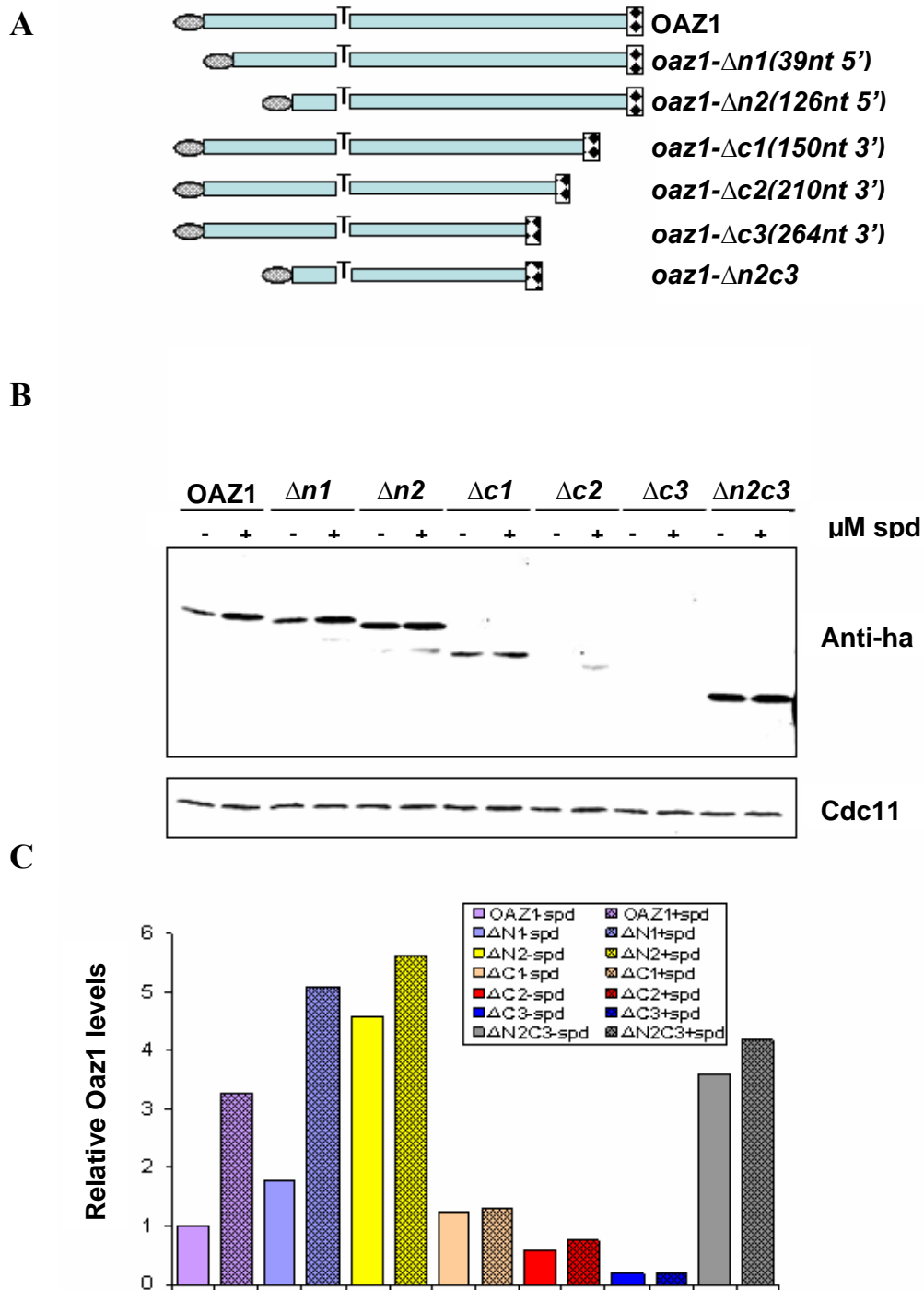
A

B

C

Fig. 27. *OAZ1mRNA* **5' and 3' elements regulates +1 ribosomal frameshifting**
(A) Schematic representation of deletion constructs derived from *OAZ1* (not to scale). Sequences
ecoding Myc and Ha tags were fused to 5' and 3' ends, respectively. The frameshifting site (T) is
indicated.
(B) Anti-ha western blot showing the protein levels of different *OAZ1* variants in *pre1-1*.
 (-, +) indicates the absence or presence of 10 μM spermidine in the media. Cells were grown in
media with 100 μM CuSO$_4$. Cdc11 was used as a loading control.
(C) Quantitation of signals shown in (B)

Results

The cells that carried full length *OAZ1* accumulated ~3 fold more protein when grown in the presence of 10 μM spermidine compared to cells grown without additional spermidine consistent with polyamine induction of +1 ribosomal frameshifting (Figure 27B). Levels of Oaz1-Δn1 proteins were ~1.5 fold higher than those of wild-type Oaz1 both when cells were grown in the presence or absence of spermidine (Figure 27B). This result indicated that deletion of 39 nucleotides at the 5' end of *OAZ1* led to an increase in the polyamine-induced +1 ribosomal frameshifting.

This result suggested that an element at the 5' end of *OAZ1 mRNA* negatively regulates +1 ribosomal frameshifting. Cells expressing *oaz1-Δn2*, in contrast, accumulated similarly high amounts of the Oaz1-n2 protein also when grown in the absence of spermidine (~4.5 fold higher than wild-type Oaz1; Figure 27). Addition of spermidine, however, did not lead to a strong increase in Oaz1-n2 protein levels as compared to the cells grown in the absence of spermidine. This result suggested that the first 126 nucleotide of *OAZ1 mRNA* contains an element that negatively regulated +1 ribosomal frameshifting in the absence of polyamines.

As also shown in Figure 27, 3' truncations of *OAZ1 mRNA (oaz1-Δc1, oaz1-Δc2 and oaz1-Δc3)* abolished polyamine induction of +1 ribosomal frameshifting. Deletion of 150 nucleotides of the 3' end of *OAZ1 (oaz1-Δc1)* resulted in protein levels that were similar to those observed for wild-type Oaz1 in cells grown in the absence of additional polyamine. More extensive deletions into the 3' end of *OAZ1 mRNA (oaz1-Δc2, oaz1-Δc3)* resulted in protein levels significantly below those detected for wild-type Oaz1. These results suggested that sequences within the 3' end of *OAZ1 mRNA* mediate polyamine-induced +1 ribosomal frameshifting.

If 5' (126 nt) and 3' (264 nt) deletions were introduced into the same *OAZ1 mRNA* gene (*oaz1-n2c3*) this lead to an accumulation of the truncated protein even in the absence of spermidine in the growth media (Figure 27). This result suggested that the 5' negative element of +1 ribosomal frameshifting present in the *OAZ1 mRNA* is regulated in a polyamine-dependent manner by the positive element at its 3' end. A model for polyamine-regulated ribosomal frameshifting during the decoding of *OAZ1 mRNA* that integrates all these findings is presented in the Discussion.

5.9 Control of Oaz1 levels involves its ubiquitin-mediated degradation by the proteasome

While I was studying the effects of mutations affecting proteasome function on ODC levels, I observed that Oaz1 levels were also increased. As shown in Figure 28 for the *pre1-1* mutant, Oaz1 accumulated to much higher levels in such strains. I next asked whether degradation of Oaz1 by the proteasome was ubiquitin-dependent. To test this, I expressed Oaz1-ha as an in-frame fusion of ORF1 and ORF2 (Oaz1-if, see chapter 4.7) results) in a mutant with a temperature-sensitive ubiquitin-activating enzyme (*uba1*) and in mutants lacking various ubiquitin-conjugating enzymes (*ubc*) (Jentsch, 1992). Increased levels of Oaz1 were detected in the *uba1* mutant (grown at the semi-permissive temperature of 30°C) and in a strain lacking *UBC4* and *UBC5* (McGrath et al., 1991; Seufert and Jentsch, 1990) (Figure 28). Mutants lacking other Ubc-encoding genes such as *ubc1, ubc2, ubc6 ubc7, ubc8, ubc10,* and *ubc13* had Oaz1 levels comparable to the wild type (data not shown).
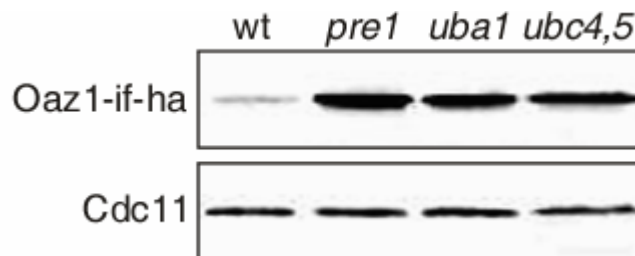
Fig. 28. Oaz1 accumulates in cells with defects in the ubiquitin proteasome system

Oaz1-ha steady state levels detected by anti-ha western blotting in the strains indicated. *OAZ1-if-ha* was expressed from P$_{CUP1}$ in plasmid pPM58. Lower part, anti-Cdc11 loading control.

Having shown that Oaz1 accumulates in cells that are defective in the ubiquitin/proteasome system (Figure 28), I then asked if the accumulation is due the reduced Oaz1 turnover in those cells. In order to test that, pulse chase experiments were performed and turnover rates of Oaz1 in *pre1-1*, *uba1,* and *ubc4 ubc5* mutants were assayed (Figure 29A and B). Oaz1 was rapidly degraded in wild-type cells, but its degradation was impaired in the proteasome-defective *pre1-1* cells suggesting that Oaz1 is degraded by the proteasome.

Oaz1 turnover was moreover impaired in the *uba1-ts and ubc4, ubc5-Δ* cells suggested that Oaz1 degradation requires ubiquitylation and its levels are directly controlled by Ubc4/Ubc5-mediated ubiquitin-dependent proteolysis by the proteasome.
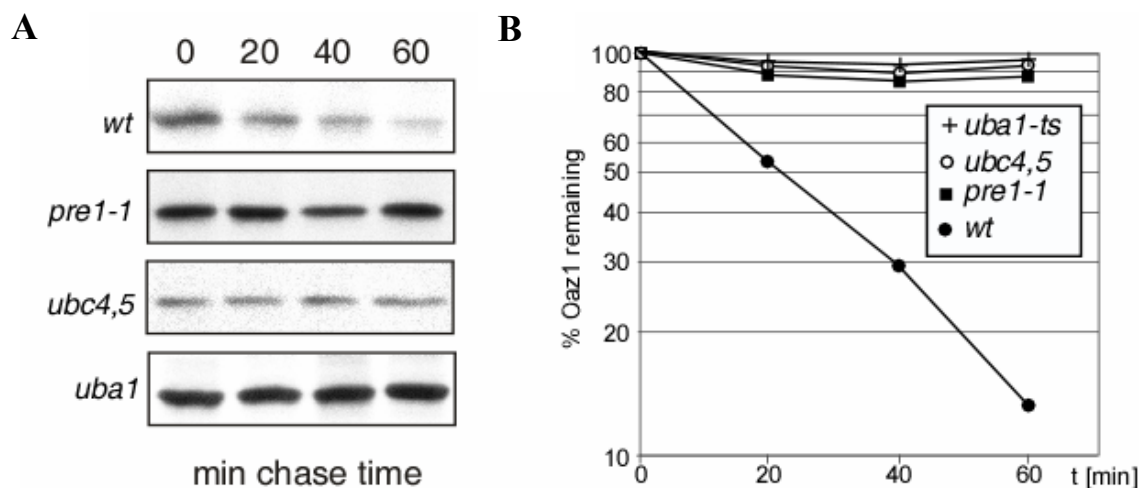
Fig. 29. Oaz1 degradation is ubiquitin and proteasome-dependent

(**A**) Pulse chase analysis of Oaz1 turnover in JD47-13C, *pre1-1, ubc4-5,* and *uba1* cells.
(**B**) Quantitation of data shown in (A).

A prediction of the results described above is that Oaz1 should be ubiquitylated prior to degradation. To verify this, Oaz1-ha was co-expressed with myc-tagged ubiquitin (myc-Ub) and anti-ha immunoprecipitations were performed in wild-type cells. Myc-Ub-Oaz1-ha conjugates were precipitated from cells co-expressing these two tagged proteins but were absent from control strains expressing either of the two proteins alone (Figure 30). The more abundant of these conjugates were also detectable with anti-ha antibody, but only after overexposing the western blot (data not shown). Since the extracts were boiled in the presence of 2 % SDS prior to immunoprecipitation, I conclude that myc-Ub was covalently attached to Oaz1.
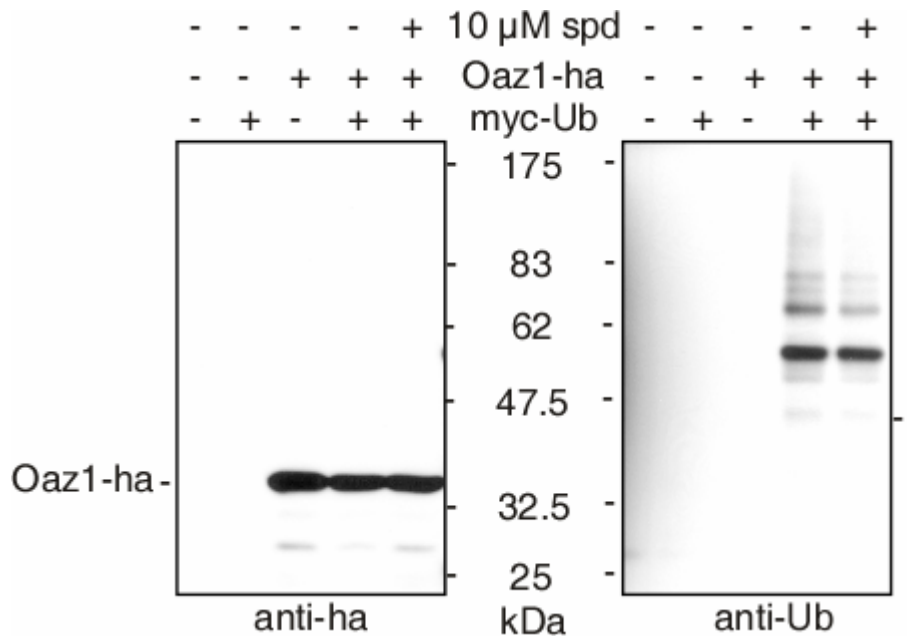
Fig. 30. Oaz1 is ubiquitylated in vivo
JD47-13C(Wt) transformants expressing either *OAZ1-if-ha*, myc-Ub, or both were grown in the presence of 100 μM CuSO$_4$. Where indicated, spermidine (10 μM) was added to the media 1 hour before extraction. After immunoprecipitation with anti-ha antibodies, precipitates were analyzed by anti-myc and anti-ha western blotting. Ubiquitylated forms of Oaz1-ha are indicated by an open-ended bracket.

5.10 Polyamines block degradation of Oaz1

While studying ribosomal frameshifting during the synthesis of Oaz1, I observed that spermidine addition to the growth media increased Oaz1 levels even when it was expressed from the control construct (*OAZ1-if*) that lacked the frameshift (Figure 25). This effect of spermidine on Oaz1 levels, however, was not detected in the proteasome-deficient *pre1-1* mutant (Figure 25B). Since expression of *OAZ1-if* was driven from P_{CUP1}, an effect of spermidine on the transcriptional regulation of this construct appeared unlikely. These observations suggested that ubiquitin-mediated degradation of Oaz1 by the proteasome is influenced by polyamine levels. To follow up on this initial finding, I applied spermidine in concentrations ranging from 0 to 10 μM to a culture wild-type cells expressing *OAZ1-if* from P_{CUP1}. As a result, I observed a dose-dependent increase (up to ~4 fold) in Oaz1 signal (Figure 31A and B).
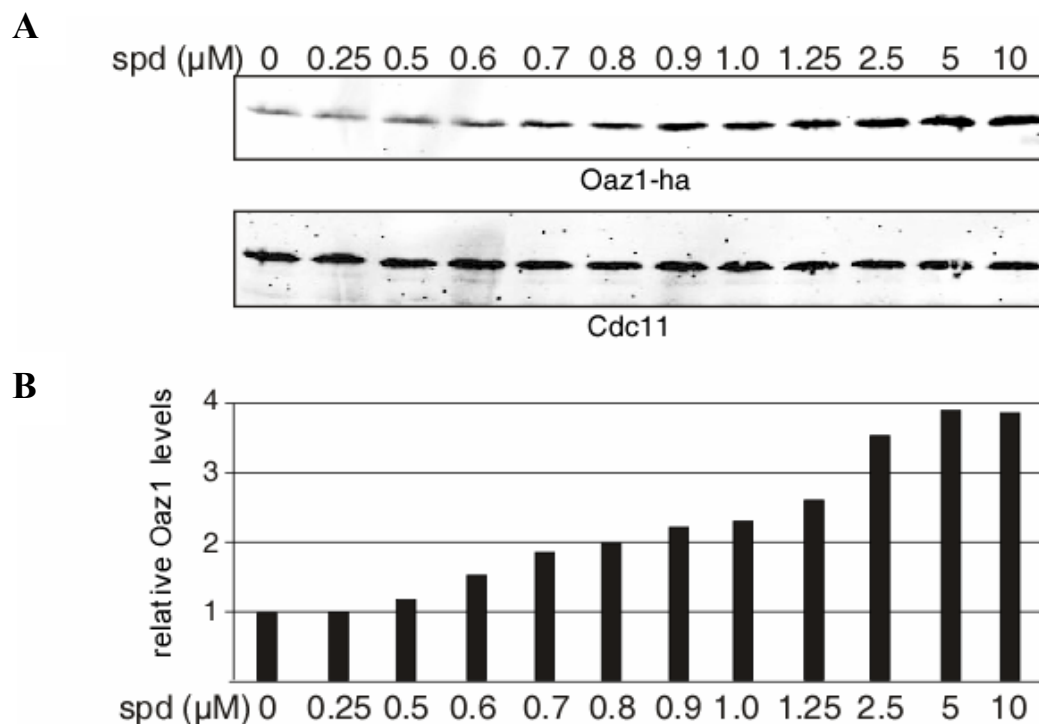
A

B

Fig. 31. Polyamine dependent increase of Oaz1 level
(**A**) Analysis of the effects of spermidine on Oaz1 levels in the absence of ribosomal frameshifting. Wild-type train JD47-13C transformed with pPM58 expressing *OAZ1-if-ha* was grown for 1 hour in the presence of spermidine at the indicated concentrations. Extracts were analysed by anti-ha western blotting. Cdc11 was detected simultaneoulsy as a loading control.
(**B**) Quantitation of data shown in (A).

Results

In order to test whether the dose-dependent increase of Oaz1 levels was due to an inhibition of its degradation, Oaz1 turnover was measured by pulse chase analysis with varying spermidine concentration as indicated in Figure 32A. Quantitation of radioactive signals clearly showed that spermidine, when present, reduced Oaz1 turnover in a dose-dependent manner (Figure 32B). This result suggested that spermidine inhibition of Oaz1 degradation led to the dose-dependent increase of Oaz1 steady state levels as shown in Figure 32.
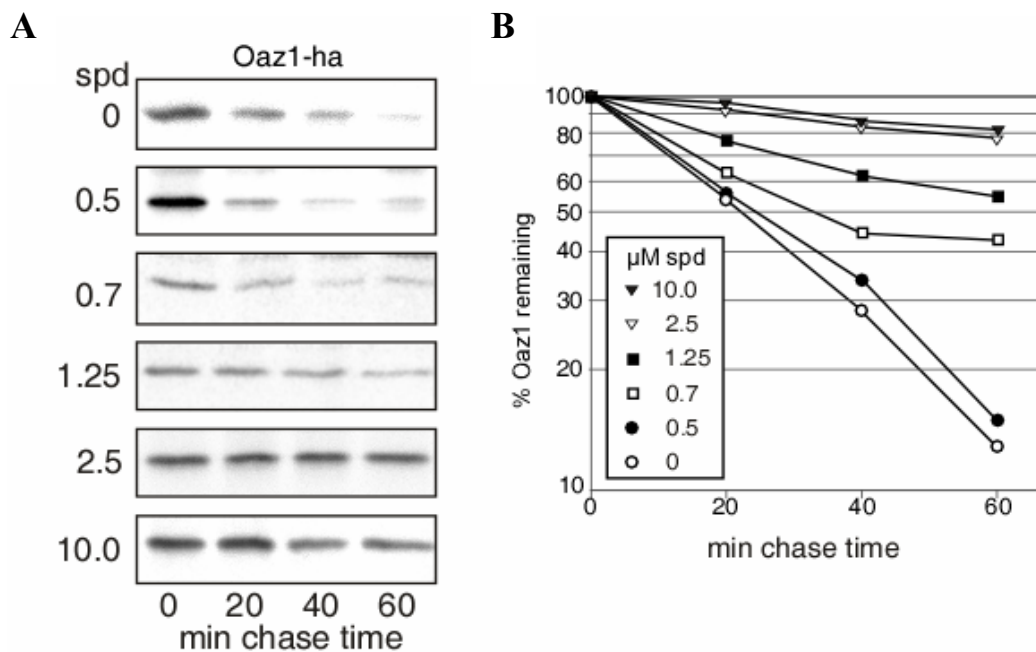
Fig. 32. Spermidine inhibits degradation of Oaz1
(**A**) Pulse chase detection of concentration dependent inhibition of Oaz1 degradation by polyamines in wt cells (JD47-13C). Spermidine at the indicated concentrations was added 1 hour before pulse labelling.
(**B**) Quantitation of data shown in (A).

Results

In order to test whether the observed inhibitory effect of spermidine was specific for Oaz1 degradation or whether this polyamine acted as a general inhibitor of proteolysis, I used established test substrates of ubiquitin-mediated proteolysis. R-β-galactosidase (R-βgal) is degraded by the N-end rule pathway, whereas Ub-P-βgal is degraded by the ubiquitin-fusion degradation (UFD) pathway (Johnson et al., 1995; Varshavsky, 1996). M-βgal served as a stable control protein. In marked contrast to the effect on Oaz1, spermidine addition to the growth media of cells expressing the βgal test proteins had no effects on their steady state levels (Figure 33A and B) or their turnover rates (Figure 33C and D).
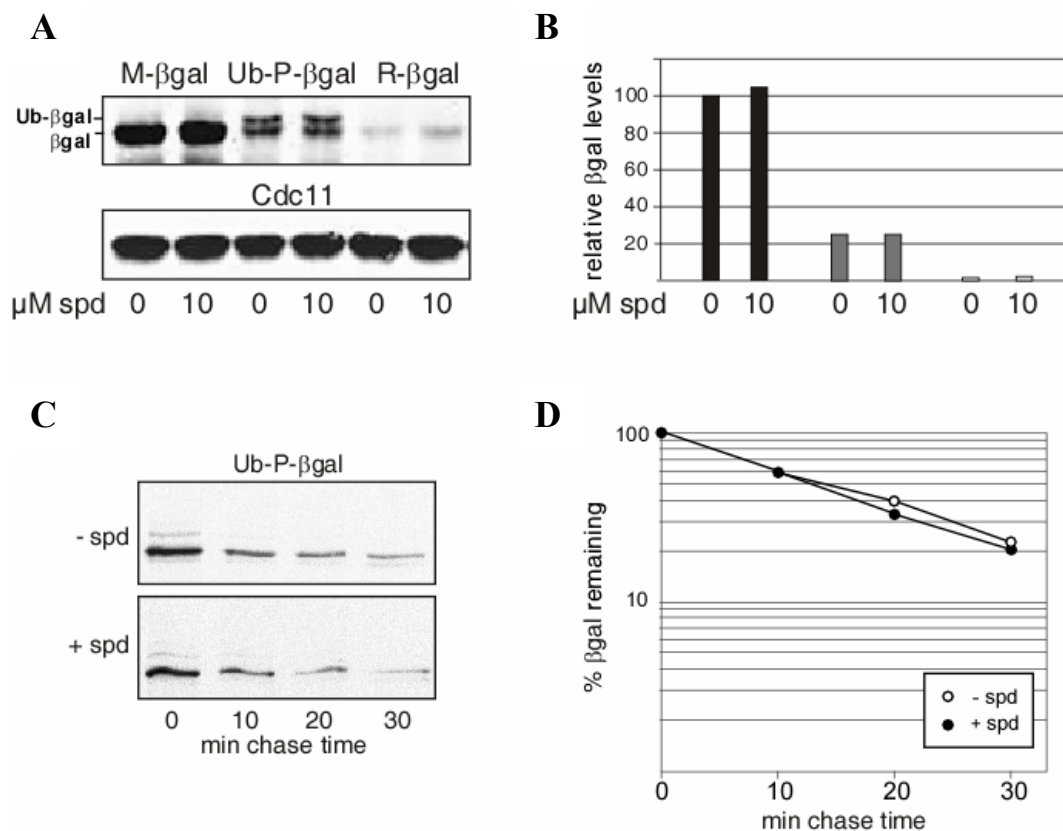

Fig. 33. Spermidine has no general effect on turnover rates of proteolytic substrates
(**A**) Steady state levels of proteolytic test substrate detected by anti-ha western blotting (upper part). Anti-Cdc11 loading control (lower part). β-galactosidase (βgal) variants were expressed as ubiquitin fusions (Ub-X-βgal).
(**B**) Quantitation of data in (A).
(**C**) Pulse chase detection of Ub-P-βgal turnover rates.
(**D**) Quantitation of data in (C).

Since, as described above, Oaz1 degradation is ubiquitin-dependent, I asked whether spermidine inhibited ubiquitylation of Oaz1 or whether the turnover of ubiquitylated Oaz1 is blocked. To address this question, I again co-expressed myc-Ub with Oaz1-ha, this time in the presence of spermidine in the medium. Addition of the polyamine resulted in a reduction of detectable ubiquitylated forms of Oaz1-ha as shown above in Figure 30. These data indicated that spermidine interferes with degradation of Oaz1 by inhibiting its ubiquitylation.

5.11 Isolation of Peptide aptamers inhibiting ubiquitin dependent protein degradation in *S. cerevisiae*

Peptide aptamers are novel tools that have been used in several recent molecular studies. Peptide aptamers that specifically inhibit activity of cdk2 have been isolated (Colas et al., 1996). This suggested that aptamers can be applied as inhibitors of specific protein activities. In order to isolate peptide aptamers that inhibit ubiquitin-dependent protein degradation in *S. cerevisiae,* a genetic screen was established that is illustrated schematically in Figure 33. Wild-type cells expressing N-end rule (R-Ura3) or UFD (Ub-V-Ura3) test substrates (see previous chapter) were transformed with libraries (pJM2 and pJM3) that express thioredoxin based peptide aptamers (Colas et al., 1996).
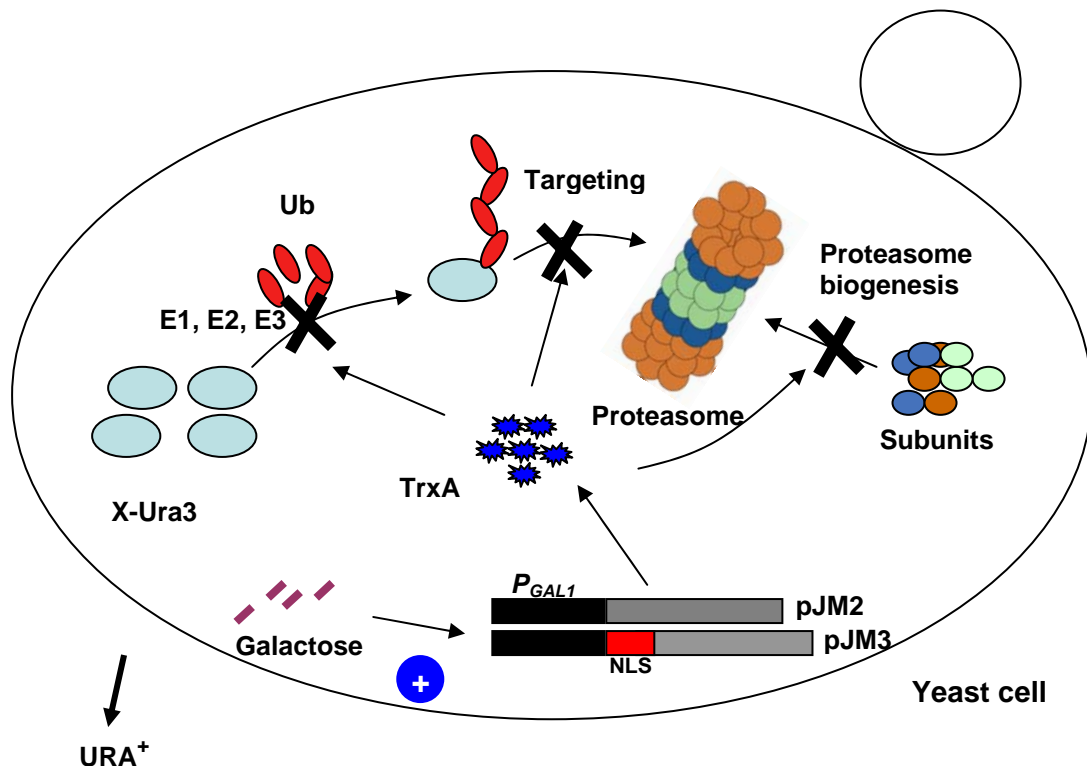

Fig. 34. Schematic representation of genetic screen to isolate peptide aptamers blocking protein degradation in *S. cerevisiae*
A schematically depicted wild-type yeast cell is transformed with plasmid library expressing thioredoxin-based peptide aptamers (pJM2 or pJM3). The cell, in addition, expresses either R-Ura3 or Ub-V-Ura3. pJM2-expressed peptide aptamers should be localized to the cytosol where as pJM3 expressed aptamers are localized to the nucleus because they contain a nuclear localization signal. Transformants are plated onto galactose-containing media in order to induce aptamer expression from the P_{GAL1} promoter. The aptamer clones that protected the Ura3-based test substrate from proteasomal degradation were selected as "Ura$^+$" by growing the cells on medium without uracil.

Cells expressing peptide aptamers that inhibit the degradation of the test substrates were able to form colonies detectable after incubation for 4 days on galactose media (SG) without uracil. Cells from those colonies were transferred to fresh selective SD (glucose) or SG (galactose) media both lacking uracil for confirmation of the phenotype. Only those clones that grow well on SG medium lacking uracil but not on the corresponding SD media were chosen for further analysis. Then the plasmids expressing the selected aptamers were rescued from *S. cerevisiae* cells. These plasmids were then introduced again into wild-type cells that expressed the test substrate and the growth assay was repeated. The screen for stabilization of the UFD substrate Ub-V-Ura3 yielded 5 aptamer clones that reproducibly produced Ura$^+$ phenotype (Figure 35A). The screen for aptamers that stabilized the N-end rule substrate R-Ura3 yielded 11 clones (Figure 35B).

A   **B**

WCGPCKM	WT
WCGPreqtslnrsmgwrmeismwiGPCK	V21
WCGPepgapflcwiwyncmsegglGPCK	V22
WCGPylrnrldfkwtlglkmwiwnGPCK	V23
WCGPekarararlwrcadrlwllfGPCK	V31
WCGPkgermtgsrfmmwlwvkdgqGPCK	V32

WCGPCKM	WT
WCGPrtypywvGPCKM	N21
WCGPlvngeffahrrsmgwtgcwcGPCKM	N22
WCGPntrpyggffishveGPCKM	N23
WCGPspgsdcwmkdpvsrvypwffGPCKM	N24
WCGPkgwrdvldefvgalaqtserGPCKM	N25
WCGPwmeaqdhfggasysnyprilGPCKM	N26
WCGPvtgrdslyrflsgsdlaretGPCKM	N27
WCGPreediarvssvfggfsvrleGPCKM	N28
WCGPrargvayvlrskfpdrlwtvGPCKM	N29
WCGPypkhgrlerrlydwwlvmfgGPCKM	N31
WCGPevgwairrdwhkrfvcfvgtGPCKM	N32

Fig. 35. Peptide aptamers inhibiting protein degradation in *S. cerevisiae*
(**A**). List of peptide aptamers that inhibit Ub-V-Ura3 test substrate degradation. The peptide sequences that are in marked in black and small letters are random peptides inserted into the active site of *E. coli* thioredoxin protein (shown in pink). Clone names in blue indicate that the aptamers carry a nuclear localization signal. Red lines highlight putative motifs present in several of the aptamers.
(**B**). List of peptide aptamers that inhibit R-Ura3 test substrate degradation. Colors are used as in (A).

Results

In order to confirm the cellular expression of the selected peptide aptamers, they were detected by western blotting using anti-thioredoxin antibody. Wild-type cells were transformed with plasmids expressing the selected aptamers (stabilising R-Ura3) and grown in media containing 2 % of galactose. Cells were harvested when they had reached mid-log growth phase and equal amount of cell lysates were taken for western blot analysis. Figure 36 shows that all the selected aptamers are well expressed in cells grown in galactose media. No significant expression, in contrast, was to be detected when the same clones were grown in glucose-containing media (data not shown).
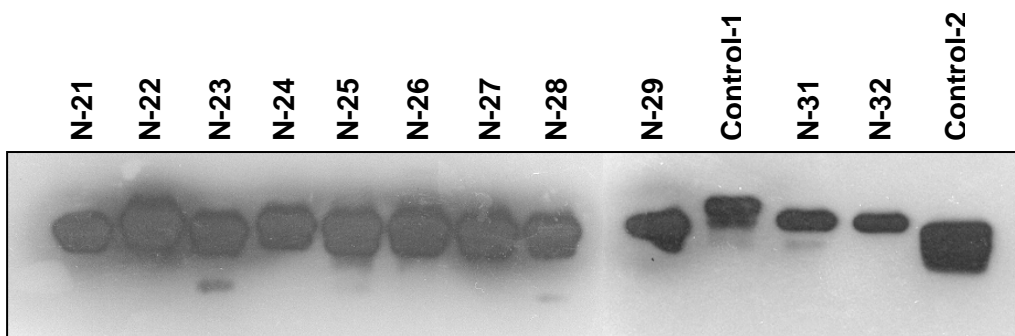

Fig. 36. Expression of peptide aptamers
Anti-thioredoxin western blot. Aptamers stabilizing the R-Ura3 test substrate were detected by anti-thioredoxin western blotting. The plasmids carrying the selected clones were introduced into wild-type cells which were grown in media containing 2 % galactose. Two randomly picked aptamer clones were used as controls.

Cells that carry mutations in the ubiquitin/proteasome system usually show growth defect when grown in media containing the arginine analogue canavanine (Ramos et al., 1998). Canavanine, when inserted into polypeptide chains generates misfolded proteins that are degraded by the proteasome in an ubiquitin-dependent manner.

In order to test the effects of the selected aptamers expression on cell growth, wild-type cells carrying these aptamers were spotted onto SD and SG plates containing 0.8 µg/ml canavanin and incubated at 30°C for 3 days. As shown in Figure 37A and B the cells expressing the aptamers clones N31 and N32 showed significant growth defects on the galactose plate containing canavanine. In contrast, these cells showed normal growth on the corresponding glucose plates. Cells expressing other aptamer

----

clones also showed reduced growth on galactose plates with canavanine when compared to wild-type. The *ump1-Δ* mutant that is impaired in proteasome function served as a canavanine-hypersensitive control (Ramos et al., 1998). These results suggested that most of the selected aptamers, upon induction, appear to target components of the ubiquitin/proteasome system that are not only required for the degradation of the Ura3-based test substrates but also for the turnover of misfolded protein.
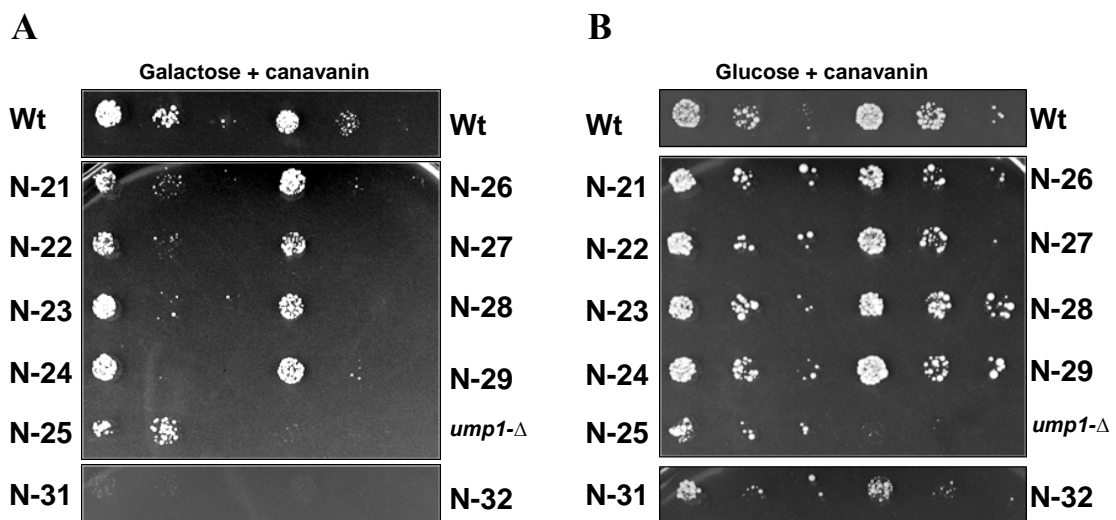
Fig. 37. Effect of aptamer expression on cell growth
(A) Wild-type strain JD47-13C transformed with selected aptamers (Figure 36) as indicated were spotted on an SG plate containing 0.8 µg/ml canavanin and grown at 30°C for 4 days. The *ump1-Δ* strain containing an empty vector was used as a canavanine-hypersensitive control.
(B) Same as (A) except the cells were grown SD media.

Proteasome biogenesis is a complex multistep process (see introduction). In order to identify aptamers that inhibit proteasome activity or proteasome biogenesis, they were introduced into a strain that carried epitope-tagged variants of the proteasomal β2/Pup1 subunit and the proteasomal maturation factor Ump1 (JD131). Cells were grown in selective media containing 2 % galactose and harvested when they reached mid-log phase. The harvested cells were then lysed and subjected to immunoprecipitation with anti-thioredoxin antibody. The samples were later analysed by anti-ha western blotting (Figure 38).

| CL | N24 | N31 | N32 | Control |

Pro-Pup1-ha —
Pup1-ha —
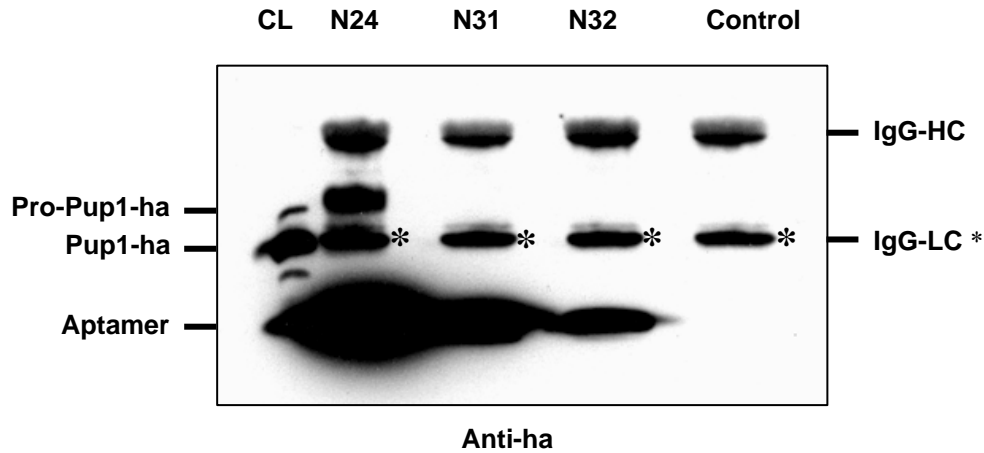Aptamer —

IgG-HC
IgG-LC *

Anti-ha

Fig. 38. Aptamer associates with proteasome component in the cell
Strain JD131 carrying chromosomally ha tagged Pup1and Ump1was transformed with the aptamer clones N24, N31 and N32. Transformants were grown in selective media containing 2 % galactose. Cell extracts were subjected to immunoprecipitation with anti-thioredoxin antibody. Samples were then analyzed by anti-ha western blot. CL indicates the whole cell lysate from untransformed JD131. The JD131 strain with empty plasmid was used as control. The position of the chains of IgG antibody used in the immunoprecipitation are indicated. Note that the light chain (*LC) co-migrates with mature Pup1-ha. The thioredoxin co-migrates with Ump1-ha.

Aptamer N24 precipitated together with a complex containing the proteasomal subunit Pup1/β2. The clones N31 and N32 as well as all the other aptamers studied (Figure 35A) did not bind to either of the tagged proteins (Figure 38, and data not shown). These results suggested that aptamer N24 may stabilize the test substrate by directly inhibiting proteasome activity or its assembly and maturation in the cell. The observation that N24 co-precipitated the propeptide-bearing precursor form of Pup1/β2 is consistent with the possibility that it interacts specifically with proteasomal precursor complexes. Alternative explanations that would be consistent with the data, however, include that N24 interacted with unassembled Pro-Pup1, or that it binds mature proteasome as well as its precursor complexes. Mature Pup1 could not be clearly detected in the experiment shown in Figure 38 because it co-migrated with the lighter chain of the antibody used for immunoprecipitation.

Taken together the data shown in above proved that a genetic screen has been established that allows to an isolation of aptamers that inhibit the ubiquitin/proteasome system in *S. cerevisiae*.

Sequence analysis detected a few similarities between some of the aptamers (underlined in Figure 35). Particularly striking is the presence of a (M)WI/L(W) motif found in four out of five aptamers that stabilised UFD substrates. Another putative example is a four residue TXPY motif found in aptamer N21, which only contains a seven residue random peptide due to the generation of an additional restriction site within the inserted random DNA sequence. The same motif is present in an identical position within aptamer N23. A functional significance of these putative motifs, however, was not yet addressed experimentally.

6 Discussion

In the current study I have identified the orthologue of human *AZ1* in the yeast *S. cerevisiae* which is termed *OAZ1* (ODC antizyme 1). Antizyme was first identified in mammals. The presence of an antizyme-like protein in *S. cerevisiae* has been controversial because it was reported that the degradation of ODC in the yeast does not require antizyme-like protein (Gandre and Kahana, 2002). Previous biochemical approaches (Toth and Coffino, 1999) as well as bioinformatic analyses (Zhu et al., 2000) moreover failed to identify antizyme in the yeast *S. cerevisiae*. Our identification of *OAZ1*, however, is consistent with another study that showed that the degradation of ODC in *S. cerevisiae,* upon addition of polyamine, indeed requires synthesis of new protein (Gupta et al., 2001). In addition, we detected closely related genes in the genomes of other Hemiascomycetes as well, thereby extending the antizyme family by a set of fungal sequences, whose existence has been postulated. The sequence similarity, the conservation of the domain structure and the presence of a putative frameshifting site all point to a common evolutionary origin of *S. cerevisiae OAZ1* and ODC antizyme genes in other eukaryotes. Moreover the identification of *S. cerevisiae OAZ1* therefore established a evolutionary conservation of a regulatory mechanism governing the polyamine synthesis in eukaryotes. The analysis of *S. cerevisiae* Oaz1, in addition revealed a novel mechanism regulating antizyme levels that involves its ubiquitin-dependent degradation. In the following chapters I will therefore discuss the findings obtained in this study and how they contribute to the current understanding of the mechanisms that regulate polyamine biosynthesis in eukaryotes. In this context, I will discuss new findings that will help to understand ODC targeting to the proteasome and polyamine-regulated decoding of *OAZ1 mRNA*.

6.1 Conservation of ODC antizyme function and the regulation of polyamine biosynthesis

6.1.1 ODC is the target for regulating polyamine biosynthesis

Synthesis of polyamines in prokaryotes as well as in eukaryotes involves conversion of arginine to ornithine which is catalysed by the enzyme ornithine decarboxylase (ODC). Bacteria and plants have an additional pathway for synthesis of polyamines. In eukaryotes like yeast and animals, in contrast, ODC and SamDC are the two rate limiting enzymes in the polyamine biosynthesis (Coffino, 2001b). Naturally ODC and SamDC are the main targets in the regulation of polyamine biosynthesis. ODC however is more important than SamDC because it synthesizes the diamine putrescine whereas SamDC is required exclusively for synthesis of higher polyamine such as spermidine and spermine. Feedback regulation of polyamine synthesis appears to be mainly achieved by regulating ODC levels. In bacteria, polyamines were shown to regulate ODC levels by controlling its gene expression (Cohen, 1998). In eukaryotes, however, regulation of ODC levels by polyamines occurs mainly posttranslationally (Li and Coffino, 1992) (Gupta et al., 2001).

6.1.2 Oaz1 is the *S. cerevisiae* orthologue of mammalian antizyme

The regulation of metabolic pathways often involves allosteric inhibition of key enzyme activity by their metabolic product. Enzyme levels are also often controlled by regulation of their gene expression at the level of transcription or translation. Regulation of ODC levels by polyamine in yeast and mammals, however, is not mediated by allosteric inhibition. ODC levels also do not appear to be at the transcriptional or translational stages in those organisms (van Daalen Wetters et al., 1989) (Fonzi, 1989). An exception seems to be the fungus *Neurospora crassa,* in wich polyamines control ODC levels by regulating its gene transcription (Hoyt et al., 2000). Posttranslational regulation of ODC level in mammals is achieved by antizyme-mediated ubiquitin-independent degradation of ODC by the proteasome (Heller et al., 1976) (Murakami and Hayashi, 1985) (Murakami et al., 1992). In the yeast *S. cerevisiae,* ODC degradation has been shown to require the proteasome and to be ubiquitin-independent as well

(Mamroud-Kidron et al., 1994) (Mamroud-Kidron and Kahana, 1994) (Gandre and Kahana, 2002). These reports suggested that ODC regulation is conserved between *S. cerevisiae* and mammals. It was reported that polyamine-induced degradation of ODC is inhibited by blocking protein synthesis in *S. cerevisiae* suggesting that *de novo* synthesis of protein is required for degradation of ODC (Gupta et al., 2001). These authors speculated about the expression of an antizyme which would act similar to the antizyme in mammals. Consistent with this assumption, the result shown in Figure 11, 12 and 13 demonstrated that *S. cerevisiae* possesses an orthologue of mammalian antizyme.

Although the overall sequence similarity between *OAZ1* and its mammalian orthologue *AZ1* is only ~6%, they share significant sequence identity in the D1 and D2 regions as shown in Figure 13. More striking is the decoding of antizyme from two ORFs as shown in Figure 11 and the conservation of +1 ribosomal frameshifting site as shown in Figure 12. The experimental data presented in Figure 14 showed that in, wild-type cells, ODC levels are reduced drastically when spermidine is added to the growth media. In *oaz1-Δ* cells, in contrast, the ODC levels remained unchanged upon addition of spermidine. These data clearly showed that in *S. cerevisiae* regulation of ODC levels by polyamines is dependent on *OAZ1*. This argument is supported by the kinetic data shown in Figure 15, where ODC levels dropped rapidly in wild-type cells and remained unchanged in *oaz1-Δ* cells even after longer incubation with spermidine. Altogether the evidence is in line with the assumption that *OAZ1* is indeed the missing antizyme orthologue in *S. cerevisiae*, whose function I have discussed in more detail in the following chapters.

6.1.2.1 Oaz1 mediates ODC degradation

In mammals, antizyme is known to have at least four isoforms namely *AZ1, AZ2, AZ3* and *AZ4* (Heller et al., 1976) (Ivanov et al., 1998) (Ivanov et al., 2000b) (Coffino, 2001b). All of them have approximately the same sequence similarity with *OAZ1* as seen in Figure 13. Among the four known isoforms, *AZ1* has been studied most extensively. Az1 inhibits ODC enzymatic activity by disrupting ODC homodimers and forming ODC/Az1 heterodimers (Li and Coffino, 1992) (Mitchell and Chen, 1990). In

addition Az1 mediates the ubiquitin-independent degradation of ODC by the proteasome (Murakami and Hayashi, 1985) (Murakami et al., 1992). Similar to its mammalian orthologues, *S. cerevisiae* Oaz1 mediates ubiquitin-independent degradation of ODC by the proteasome. The data presented in Figure 14 showed that *OAZ1* is essential for the regulation of ODC level. Importantly, as revealed by the pulse chase analysis, ODC is indeed degraded upon addition of polyamine to wild-type cells and it is drastically stabilized in *oaz1-Δ* cells (Figure 16). The data in Figure 17 depicts that addition of polyamine to the media resulted in an increases of Oaz1 levels in a dose-dependent manner. As in mammals, the addition of polyamines induces a raise of Oaz1 levels and in turn rapid turnover of ODC in *S. cerevisiae*. The possible molecular function of ODC antizyme therefore appears to be conserved from yeast to mammals.

6.1.2.2 ODC degradation is proteasome -dependent

Proteasomal protein degradation is mainly ubiquitin-dependent (Hershko and Ciechanover, 1998). However Az1-mediated ODC degradation is one of a few example of ubiquitin-independent proteasomal degradation in mammals (Murakami et al., 1992). In *S. cerevisiae,* ODC degradation has been shown to be proteasome-dependent as well as ubiquitin-independent (Mamroud-Kidron and Kahana, 1994; Mamroud-Kidron et al., 1994) (Gandre and Kahana, 2002). However those reports have not convincingly shown that polyamine-induced ODC degradation is proteasome-dependent in *S. cerevisiae*. The data shown in Figure 18 clarifies that the polyamine-induced ODC degradation in the yeast *S. cerevisiae* is also proteasome-dependent as ODC is not degraded in the *pre1-1, pre2-1* and *cim3-1* cells that are defective in proteasome function.

6.1.2.3 Oaz1 interaction with ODC underlies its mechanism of action

In mammals, antizyme interaction with ODC exposes a degradation signal that is recognised by the proteasome. For mouse ODC the C-terminal 37-residues were shown to contain the degradation signal that targets ODC upon antizyme binding (Zhang et al., 2003). It has been shown that the N-terminus of mouse ODC along with C-terminus of antizyme is required for ODC/Az1 heterodimer formation (Li and Coffino, 1994).

However the N-terminus of Az1 has also been shown to be important for the degradation of ODC even though it is not necessary for its binding. The data shown in Figure 19A confirmed that in *S. cerevisiae* ODC forms homodimers. However, when Oaz1 is present, it forms a heterodimer with ODC. These data proved that the molecular mechanism involved in targeting ODC to the proteasome by Oaz1 in *S. cerevisiae* is similar to the mammalian system. I therefore hypothesized that Oaz1 binding may expose a degradation signal recognized by the proteasome (see below).

6.1.2.4 ODC N-terminus mediates the ubiquitin independent proteasomal targeting

Substrates that are degraded by the proteasome are commonly ubiquitylated with few exceptions such as ODC, Rpn4 and p53 (Murakami et al., 1992) (Xie and Varshavsky, 2001) (Asher et al., 2005). The poly ubiquitin chain (minimum four ubiquitins) on the substrate serves as a signal that binds to the proteasomal subunits Rpn10 and Rpt5 thereby allowing the proteasome to identify the substrate (Pickart and Cohen, 2004). In addition, shuttling factors such as Rad23, Dsk2 and Ddi1 that contain both Uba (Ubiquitin associated) and Ubl (Ubiquitin like) domains may contribute to proteasomal targeting (Madura, 2004) (Elsasser et al., 2004) (Verma et al., 2004) (Kim et al., 2004). They are known to bind to the polyubiquitin chain via their Uba domain and to the proteasome via their Ubl domain thereby mediating substrate delivery to the proteasome. A recent report suggested that the targeting of ubiquitylated proteins to the proteasome is achieved by several partially redundant mechanisms (Verma et al., 2004).

Interestingly, aside of the ubiquitin-dependent mechanisms, the proteasome is able to degrade ubiquitin-independent substrates such as ODC. An *in vitro* study showed that degradation of ODC can be inhibited by the addition of tetra-ubiquitin chains suggesting that ODC may be targeted to the same binding site as ubiquitylated proteins (Zhang et al., 2003). From this study, however, it is not clear whether ODC degradation occurs via the known ubiquitin receptors or alternative binding sites. It is worth noting that the mechanisms that targets substrates to the proteasome are still poorly understood. A feasible hypothesis that explains ubiquitin-independent targeting of ODC is that its degradation signal may share structural similarities with a motif

presented by ubiquitin chain. Although the crystal structure of mouse ODC is known, the structure of the ODC degradation signal is not resolved due its high flexibility (Kern et al., 1999).

In *S. cerevisiae* a deletion of 47 residues from the ODC N-terminus led to accumulation of the protein in wild-type cells to levels similar to those in *oaz1-Δ* cells (Figure 20B). This deletion, however, did not interfere with ODC homodimer formation or its activity. From these data it is not clear whether Oaz1 can still interact with N-terminally truncated ODC. Binding of mammalian Az1 to ODC, however, has been mapped to the same domains that are involved in ODC homodimer formation (Li and Coffino, 1994). It is therefore likely that yeast Oaz1 can still interact with N-terminally truncated ODC. This conclusion argues against the possibility that the stabilization of N-terminally truncated ODC is due to its inability to interact with Oaz1. Taken together the most appealing explanation therefore is that the N-terminus of yeast ODC contains a degradation signal that targets it for ubiquitin-independent proteasomal degradation upon binding to Oaz1. In contrast, deletions into the C-terminus of ODC resulted in unstable probably misfolded versions of ODC.

For a long time it was believed that antizyme and ODC, when bound to each other, constitute a degradation signal that is identified by the proteasome. The signal in mouse ODC that is responsible for its degradation, however, if fused to a stable reporter protein, can target it for proteasomal degradation *in vitro* (Zhang et al., 2003). This signal which is located at the C-terminus of mouse ODC therefore appears to constitute an autonomous degradation signal that can function in the absence of Az1. Other experiments indicated that the binding of mammalian antizyme to ODC helps to expose this degradation signal (Zhang et al., 2003). Yeast ODC lacks the C-terminal extension similar to its mammalian counterparts. Instead it carries an N-terminal extension that is missing from mammalian ODC. As this extension is required for yeast ODC degradation, I tested whether it results in an unstable protein when fused to a stable reporter. As shown in Figure 23 this appears to be the case. Moreover the degradation of the fusion protein is proteasome-dependent as it accumulated in the *pre1-1* strain. It was also possible, however, that the fusion of ODC N-terminus to the reporter may have resulted in the formation of a misfolded protein that would be recognized by the quality

control system and eventually be degraded by the proteasome. But the data in Figure 23 ruled out such a scenario. The degradation of the fusion protein was neither affected by *fes1-Δ* nor by *doa4-Δ*. Fes1 is a nucleotide exchange factor for Hsp70 chaperones required for degradation of misfolded proteins (Marcel Fröhlich, personal communication). Doa4 is a deubiquitylating enzyme required for recycling of ubiquitin. Mutants lacking Doa4 are impaired in ubiquitin-mediated proteolysis (Gandre et al., 2002). The lack of an effect of *doa4-Δ* on levels of the fusion protein carrying the ODC N-terminus indicated that its degradation is ubiquitin-independent. I conclude that the N-terminal 47 residues constitute a transplantable degradation signal termed **ODS** (ODC degradation signal).

Interestingly, the ODS fusion protein level is significantly elevated in *rad23-Δ* cells. As described above, Rad23 has been implicated in the transfer of ubiquitylated proteins to the proteasome. The data in Figure 23 suggested that Rad23 may also be involved in ubiquitin-independent targeting of ODC to the proteasome. Deletion of the proteasomal ubiquitin receptor Rpn10, in contrast, had no effect on ODS fusion protein levels. A possible explanation for the above observation is that Rad23 recognizes a feature of ODS that may mimic a motif of a ubiquitin chain.

The two-hybrid interaction assay detected strong binding of ODS to all 10 tested subunits of the 19S lid sub-complex (Figure 24). There was, however, no detectable interaction with any subunit of the 19S base sub-complex, which includes the known ubiquitin receptors Rpn10 and Rpt5. These data suggested that ODS targets ODC to the proteasome by binding to novel receptor sites in the 19S lid. The data suggests further that multiple such binding sites are present in the lid. An alternative explanation would be that the two-hybrid assay also detected indirect interactions of ODS due to complex formation of the lid subunits. This appears unlikely, however, as there are only few interactions between the lid subunits detected in this system by using the same constructs (data not shown) (Cagney et al., 2001). These data suggested that ODC may not be targeted to the proteasome by binding to the known ubiquitin receptors, instead its interaction with the 19S lid may underlie the mechanism that targets ODC. This argument is supported by a report showing that recruitment of substrates to the proteasome 19S cap is sufficient for its degradation (Janse et al., 2004).

Discussion

To summarise, in *S. cerevisiae* ODS targets ODC for ubiquitin-independent degradation. The targeting of ODC may be facilitated by the adapter protein Rad23 and may in addition involve direct binding to 19S lid subunits (figure 38). These observations are novel but need further biochemical validation.
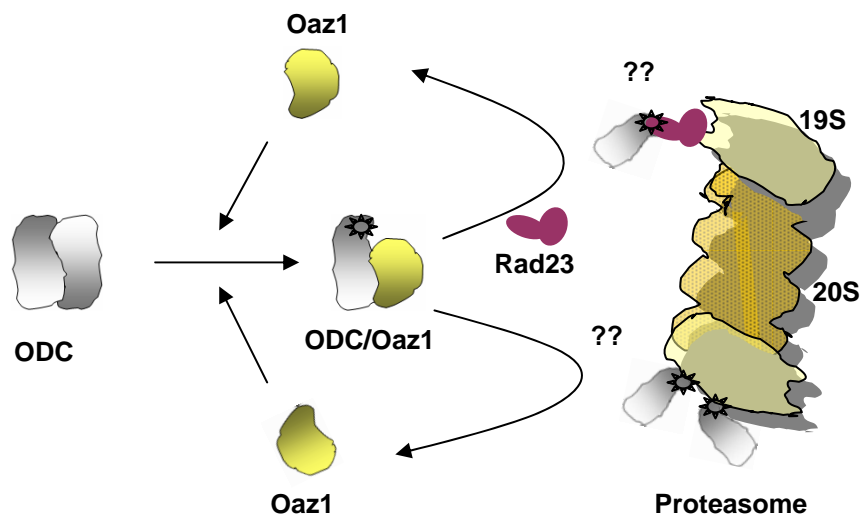

Fig. 38. Model for ODC targeting to proteasome in *S. cerevisiae*
Oaz1 binds to ODC and forms a ODC/Oaz1 heterodimer. The exposed N-terminal degradation signal (ODS) either binds to the Rad23 adaptor protein or directly to the 19S cap of the proteasome thereby targeting ODC without ubiquitylation.

6.1.3 Regulation of polyamine biosynthesis and +1ribosomal frameshifting

Synthesis of Oaz1 from two open reading frames is controlled by polyamine-regulated programmed ribosomal frameshifting (Figure 25). Disruption of ORF2 resulted in abrogation of ODC degradation. Ectopic expression of the annotated ORF "YPL052w" did not restore degradation. An in-frame fusion of ORF1 and ORF2, in contrast, resulted in a complementation of this defect in ODC degradation. These and related results established that ribosomal frameshifting is essential for synthesis of a functional Oaz1 in *S. cerevisiae*. Whereas many viruses utilize programmed frameshifting (commonly -1) to decode their RNAs, there are only few examples for an employment of such

mechanisms in the synthesis of cellular proteins. In *S. cerevisiae*, aside of the retrotransposon Ty, two genes have been proposed to utilize a programmed +1 ribosomal frameshifting in their decoding. *EST3* encodes a protein required for telomer replication (Morris and Lundblad, 1997). *ABP140* encodes an actin filament-binding protein (Asakura et al., 1998).

In all these cases, a tRNA slippage at a CUU Leu codon in a sequence (CUU AGG/A), in which it is followed by a slowly recognised codon appears to underly the frameshifting event (Sundararajan et al., 1999). A similar sequence element is absent from the frameshifting sites in antizyme genes from yeast and other species (Figure 12). Here an occlusion model has been proposed, in which sequences upstream of the frameshifting site and a downstream pseudoknot modify the structure in the A site of the ribosome occupied by the UGA termination codon such that an Asp or a Glu codon in the +1 frame is recognized by the respective tRNAs (Namy et al., 2004).

Despite the differences in the sequences of the frameshifting sites, +1 ribosomal frameshifting in decoding of both Ty1 and Oaz1 is induced by polyamines (Balasundaram et al., 1994) (Figure 25). Whether polyamines more generally stimulate +1 frameshifting in *S. cerevisiae*, however, is unclear as no data are available on the effects of polyamines on the rates of frameshifting in decoding of *EST3* and *ABP140*. It also remains to be investigated whether ribosomal frameshifting signals and their recognition are conserved among *mRNAs* of antizyme orthologues. It was reported that decoding of a test construct containing the rat antizyme cDNA in *S. cerevisiae* involves a -2 ribosomal frameshifting. Whether this event is stimulated by polyamines was not tested (Ivanov et al., 1998b).

The discovery of the *OAZ1* gene in *S. cerevisiae* provides an easy to manipulate *in vivo* system that will help to understand underlying mechanisms and the sequence requirements for polyamine-induced ribosomal frameshifting. Towards this end, a first mapping of *cis* elements in *OAZ1 mRNA* controlling +1 ribosomal frameshifting was carried out by introducing 5' and 3' truncations (Figure 27).

Discussion

Truncations into the 5' end of the *OAZ1 mRNA* resulted in relatively high rates of +1 ribosomal frameshifting independent of the absence or presence of polyamines in the media (Figure 27). These data suggested the presence of a sequence, termed '*OAZ1* frameshift repressive element (**OFRE**)' located close to the 5' end of the transcript (Figure 39A). Deletion of the inferred OFRE results in constitutive high rates of frameshifting.

Deletion of 3' sequences of the *OAZ1 mRNA* also abolished polyamine responsiveness of the frameshifting event. In contrast to the deletion of OFRE, however, the rate of frameshifting during decoding of 3' truncated *OAZ1 mRNA* was relatively low and similar to those found for wild-type *OAZ1* in the absence of polyamines. These data suggested the presence of a sequence, termed '*OAZ1* polyamine responsive element (**OPRE**)', which stimulates frameshifting in the presence of polyamines. Interestingly, a combination of 5' and 3' truncations into *OAZ1* (*oaz1-Δn2c3* in Figure 27) yielded relatively high frameshifting rates both in the presence and absence of polyamines. Since these frameshifting rates were similarly high as those detected for an *OAZ1* construct lacking OFRE (*oaz1-Δn2* in Figure 27), these data suggested that OPRE functions by mediating a relief of inhibition of frameshifting by OFRE (Figure 39B).

As illustrated in the model shown in Figure 39C and D, the OFRE may form a tertiary structure inhibiting the +1 frameshifting. In the presence of polyamines, OPRE disrupts this structure of OFRE thereby allowing frameshifting to occur at a higher rate. According to this model, frameshifting during the decoding of *OAZ1 mRNA* is mainly controlled via negative regulation by OFRE. Consistent with this idea, frameshifting rates are higher when OFRE is deleted alone or along with OPRE than for the wild-type *OAZ1 mRNA*. In this model, the conserved core sequence surrounding the frameshifting site are sufficient to mediate frameshifting whereas the elements discussed above have a regulatory impact on its rate.
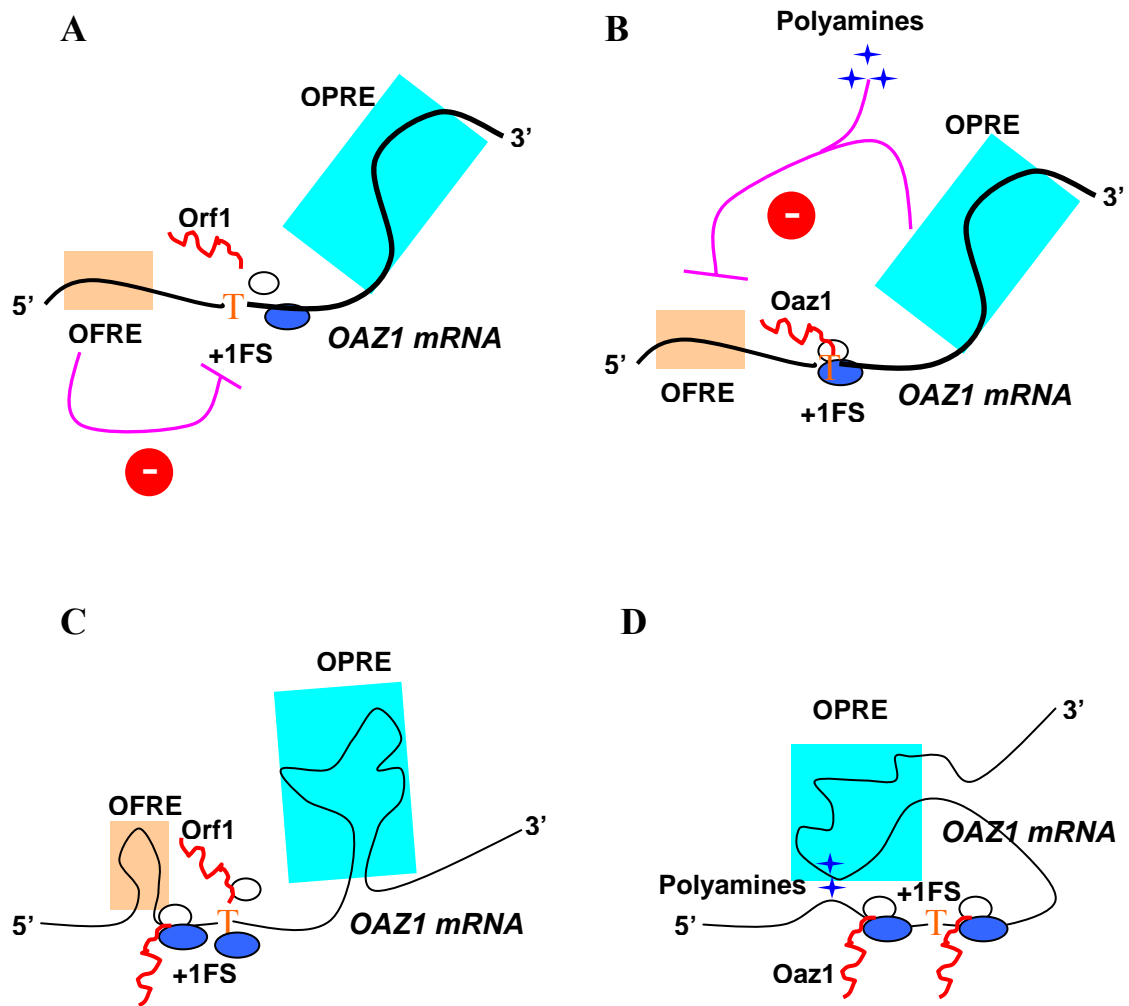

Fig. 39. Genetic and structural models depicting the regulation of polyamine-dependent +1 ribosomal frameshifting in decoding of *OAZ1 mRNA*

(A) Genetic model that shows the decoding of *OAZ1 mRNA* in the absence of polyamines. The +1 ribosomal frameshifting event is negatively regulated by OFRE (*OAZ1* frameshifting repressor element) leading to translational termination.

(B) Genetic model that shows the decoding of *OAZ1 mRNA* in the presence of polyamines. The +1 ribosomal frameshifting event is positively regulated by polyamines and OPRE (*OAZ1* polyamine responsive element), inhibit the negative regulator OFRE, thereby leading to the synthesis of Oaz1.

(C) Structural model showing a speculative *mRNA* structure corresponding to OFRE terminating the translation at the +1 ribosomal frameshifting site in the absence of polyamines.

(D) Structural model showing that the polyamines induce +1 ribosomal frameshifting event by disrupting the OFRE structure via interaction with OPRE.

6.2 Regulation of antizyme degradation by polyamines

I noticed that polyamine addition to the media resulted in increased Oaz1 protein levels even when an in-frame construct that did not require frameshifting was used (Figure 26). Further analysis revealed that Oaz1 is subject to ubiquitin-mediated proteolysis by the proteasome. The data shown in Figure 28 depicted that Oaz1 accumulates to higher levels in cells carrying mutations in the ubiquitin-activating enzyme Uba1 (E1), the ubiquitin-conjugating enzymes Ubc4 and Ubc5, or the proteasome. Figure 29 shows that degradation of Oaz1 is inhibited by these mutations. Taken together these data established that Oaz1 is degraded by the proteasome in an ubiquitin-dependent manner. Similarly, an E1 requirement was previously reported for degradation of AZ1 in mammalian cells, but ubiquitylated forms of it were not detected (Gandre et al., 2002). In yeast, I detected such forms for Oaz1 indicating that ubiquitylation is essential for its proteasomal degradation (Figure 30). Upon addition of spermidine to the growth media, I observed a dose-dependent inhibition of Oaz1 degradation (Figure 31 and 32). How may polyamines interfere with Oaz1 degradation? There are examples in the literature both for the inhibition of proteasomal degradation of a ubiquitylated substrate and for the inhibition of the ubiquitylation of a protein by small organic compounds. Degradation of a ubiquitylated dihydrofolate reductase was shown to be inhibited by the folic acid analogue methotrexate (Johnston et al., 1995). I detected a reduction rather than a stabilization of ubiquitylated forms of Oaz1 upon spermidine addition, suggesting that polyamines, in contrast, interfere with ubiquitylation of Oaz1 (Figure 30). Similar observations were made for mammalian spermidine/spermine N-acetyltransferase (SSAT), a key enzyme in polyamine catabolism. Ubiquitylation of SSAT was inhibited *in vitro* by polyamine analogues (Coleman and Pegg, 2001). It was proposed that binding of the analogue brings about a conformational change of SSAT that inhibits its ubiquitylation. A similar mechanism may underlie the inhibition of Oaz1 degradation by spermidine.

Alternatively, the enzymes that mediate ubiquitylation of Oaz1 may be inhibited by spermidine. One example of an E3 ubiquitin ligase whose activity is regulated by a small organic compound is Ubr1 in *S. cerevisiae*. This ligase indirectly regulates the uptake of dipeptides by controlling the stability of the transcriptional repressor Cup9

that blocks expression of the *PTR1* dipeptide transporter gene. Dipeptides at low concentrations act as allosteric activators of the Ubr1 ligase activity towards Cup9 and thereby induce their uptake (Turner et al., 2000). In a diversion of such a mechanism, an as yet to be identified E3 enzyme responsible for Oaz1 ubiquitylation might be inhibited by polyamines. I favour a model, in which spermidine binding to Oaz1 inhibits its ubiquitylation, based on the observation that SSATs were detected in searches that used antizyme-based profiles (Hartmut Scheel and Kay Hofmann, personal communication). In a reverse approach, profiles constructed from acetyl transferases alignments moreover retrieved several antizymes. In both cases the sequence similarity, however, was below the threshold that would establish a clear evolutionary relationship. Secondary structure prediction for the putative homologous region in acetyl transferases and antizymes, however, indicated that they share a common αβα motif (Hartmut Scheel and Kay Hofmann, personal communication). In the crystal structure of yeast N-acetyltransferase Gna1, this αβα motif overlaps with the binding site for Acetyl-CoA and the substrate (Peneff et al., 2001). By analogy, this domain is likely to be involved in spermidine binding within SSAT enzymes. I hypothesize that the spermidine-dependent stabilization of antizyme may be due to a direct binding of spermidine to an αβα motif in the C-terminal region of antizyme.

Based on these data I propose that polyamines regulate their synthesis by controlling Oaz1 levels via two separate mechanisms. The first mechanism is the induction of ribosomal frameshifting in decoding of *OAZ1* mRNA by a mechanism that is poorly understood (see previous chapter). The second mechanism is the inhibition of Oaz1 proteolysis. I propose that the latter mechanism ensures a rapid recovery from a state in which ODC is down-regulated by antizyme. In this model, a drop of polyamine levels below a critical threshold does not only prevent *de novo* synthesis of antizyme but also results in a turnover of its existing pools thereby allowing for a rapid recovery of ODC activity. Polyamines thus appear to mediate an efficient feedback control of their formation by affecting both the synthesis and turnover rates of ODC antizyme (Figure 40).
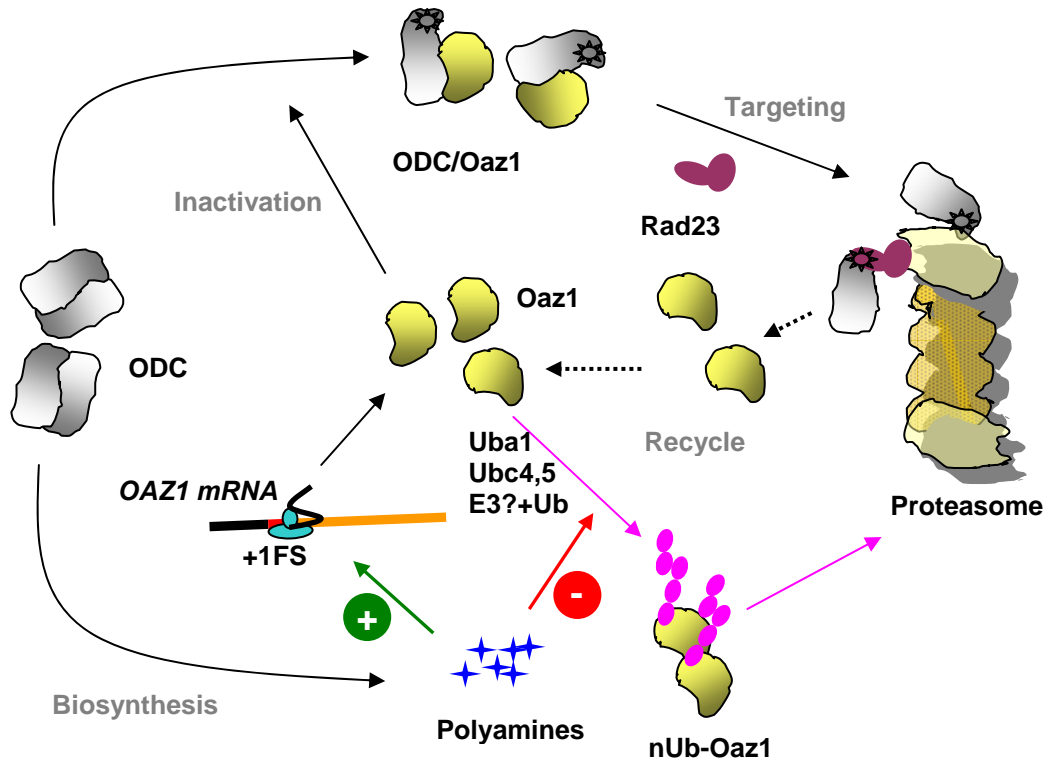
Fig. 40. Regulation of polyamine biosynthesis in S. cerevisiae
Polyamines regulate their biosynthesis by inducing ODC degradation. Free polyamines induce +1
ribosomal frameshifting during the decoding of *OAZ1 mRNA*. This in turn increases Oaz1 levels.
Later Oaz1 inactivates ODC by forming ODC/Oaz1 heterodimer. The exposed ODC degradation
signal (ODS) targets ODC for ubiquitin independent proteasomal degradation. This process may
in part be mediated by Rad23. Oaz1 is recycled after targeting ODC. However Oaz1 itself is
degraded by the proteasome. Degradation of Oaz1 is ubiquitin dependent and involves Uba1 (E1),
Ubc4, 5 (E2) and an as yet unknown E3. Free polyamines however effectively block Oaz1
degradation by inhibiting the ubiquitylation of Oaz1 by unknown mechanism.

6.3 Genetic screen to isolate peptide inhibitors of ubiquitin proteasome system

Peptide aptamers are novel genetic tools based on which I established a genetic screen
for the identification of peptide sequences that block the ubiquitin/proteasome system.
As illustrated in Figure 34, peptide aptamers that inhibit ubiquitin-dependent proteolysis
could be selected using Ura3-based proteolytic test substrates (Figure 35). Upon

induction, the isolated aptamers interestingly caused growth defects on canavanin plates (Figure 37). These data suggested that the selected aptamers inhibit the degradation of misfolded proteins that are generated as a result of canavanin incorporation. These effects of the aptamers may be due to the inhibition of either ubiquitylation, proteasome activity or its biogenesis thereby leading to accumulation of misfolded proteins. The data shown in Figure 38 supported the notion that some of the aptamers bind to the proteasome thereby inhibiting its activity or biogenesis. The exact targets of the selected aptamers are yet to be determined. Moreover, the specificity of this screen can now be improved to isolate more peptide aptamers that directly interfere with proteasome by using the ODS-ha-Ura3 substrate developed in this study, because of its ubiquitin-independent mode of degradation. Isolation of a larger number of such proteasome-specific aptamers may help to identify motifs that inhibit proteasome function or assembly.

Some of the first thioredoxin-based aptamers isolated in this study shared short motifs (Figure 36). For example a (M)WI/L(W) motif was found in four out of five aptamers stabilising UFD substrates. The functional significance of this or other motifs was not experimentally up until now. If such specific motifs could be identified, it still needs to be demonstrated that they can function without the context of thioredoxin, before they can be considered as a starting point for the development of novel proteasome-specific drugs.

7 References

Abedi, M.R., Caponigro, G. and Kamb, A. (1998) Green fluorescent protein as a scaffold for intracellular presentation of peptides. *Nucleic Acids Res*, 26, 623-630.

Adams, J. (2003) The proteasome: structure, function, and role in the cell. *Cancer Treat Rev*, 29 Suppl 1, 3-9.

Adams, J. (2004) The proteasome: a suitable antineoplastic target. *Nat Rev Cancer*, 4, 349-360.

Adams, J., Behnke, M., Chen, S., Cruickshank, A.A., Dick, L.R., Grenier, L., Klunder, J.M., Ma, Y.T., Plamondon, L. and Stein, R.L. (1998) Potent and selective inhibitors of the proteasome: dipeptidyl boronic acids. *Bioorg Med Chem Lett*, 8, 333-338.

Ahmad, N., Gilliam, A.C., Katiyar, S.K., O'Brien, T.G. and Mukhtar, H. (2001) A definitive role of ornithine decarboxylase in photocarcinogenesis. *Am J Pathol*, 159, 885-892.

Albertsen, M., Bellahn, I., Kramer, R. and Waffenschmidt, S. (2003) Localization and function of the yeast multidrug transporter Tpo1p. *J Biol Chem*, 278, 12820-12825.

Almond, J.B. and Cohen, G.M. (2002) The proteasome: a novel target for cancer chemotherapy. *Leukemia*, 16, 433-443.

Almrud, J.J., Oliveira, M.A., Kern, A.D., Grishin, N.V., Phillips, M.A. and Hackert, M.L. (2000) Crystal structure of human ornithine decarboxylase at 2.1 A resolution: structural insights to antizyme binding. *J Mol Biol*, 295, 7-16.

Aravind, L. and Koonin, E.V. (2000) The U box is a modified RING finger - a common domain in ubiquitination. *Curr Biol*, 10, R132-134.

Arendt, C.S. and Hochstrasser, M. (1997) Identification of the yeast 20S proteasome catalytic centers and subunit interactions required for active-site formation. *Proc Natl Acad Sci U S A*, 94, 7156-7161.

Asher, G., Tsvetkov, P., Kahana, C. and Shaul, Y. (2005) A mechanism of ubiquitin-independent proteasomal degradation of the tumor suppressors p53 and p73. *Genes Dev*, 19, 316-321.

References

Aviel, S., Winberg, G., Massucci, M. and Ciechanover, A. (2000) Degradation of the epstein-barr virus latent membrane protein 1 (LMP1) by the ubiquitin-proteasome pathway. Targeting via ubiquitination of the N-terminal residue. *J Biol Chem*, 275, 23491-23499.

Balasundaram, D., Dinman, J.D., Wickner, R.B., Tabor, C.W. and Tabor, H. (1994) Spermidine deficiency increases +1 ribosomal frameshifting efficiency and inhibits Ty1 retrotransposition in Saccharomyces cerevisiae. *Proc Natl Acad Sci U S A*, 91, 172-176.

Bercovich, Z. and Kahana, C. (2004) Degradation of antizyme inhibitor, an ornithine decarboxylase homologous protein, is ubiquitin-dependent and is inhibited by antizyme. *J Biol Chem*, 279, 54097-54102.

Beste, G., Schmidt, F.S., Stibora, T. and Skerra, A. (1999) Small antibody-like proteins with prescribed ligand specificities derived from the lipocalin fold. *Proc Natl Acad Sci U S A*, 96, 1898-1903.

Bochtler, M., Ditzel, L., Groll, M. and Huber, R. (1997) Crystal structure of heat shock locus V (HslV) from Escherichia coli. *Proc Natl Acad Sci U S A*, 94, 6070-6074.

Boname, J.M. and Stevenson, P.G. (2001) MHC class I ubiquitination by a viral PHD/LAP finger protein. *Immunity*, 15, 627-636.

Borden, K.L. and Freemont, P.S. (1996) The RING finger domain: a recent example of a sequence-structure family. *Curr Opin Struct Biol*, 6, 395-401.

Bucher, P., Karplus, K., Moeri, N. and Hofmann, K. (1996) A flexible motif search technique based on generalized profiles. *Comput Chem*, 20, 3-23.

Cagney, G., Uetz, P. and Fields, S. (2001) Two-hybrid analysis of the Saccharomyces cerevisiae 26S proteasome. *Physiol Genomics*, 7, 27-34.

Capili, A.D., Schultz, D.C., Rauscher, I.F. and Borden, K.L. (2001) Solution structure of the PHD domain from the KAP-1 corepressor: structural determinants for PHD, RING and LIM zinc-binding domains. *Embo J*, 20, 165-177.

Cason, A.L., Ikeguchi, Y., Skinner, C., Wood, T.C., Holden, K.R., Lubs, H.A., Martinez, F., Simensen, R.J., Stevenson, R.E., Pegg, A.E. and Schwartz, C.E. (2003) X-linked spermine synthase gene (SMS) defect: the first polyamine deficiency syndrome. *Eur J Hum Genet*, 11, 937-944.

References

Chen, H., MacDonald, A. and Coffino, P. (2002) Structural elements of antizymes 1 and 2 are required for proteasomal degradation of ornithine decarboxylase. *J Biol Chem*, 277, 45957-45961.

Cheng, J.K., Lee, S.Z., Yang, J.R., Wang, C.H., Liao, Y.Y., Chen, C.C. and Chiou, L.C. (2004) Does gabapentin act as an agonist at native GABA(B) receptors? *J Biomed Sci*, 11, 346-355.

Childs, A.C., Mehta, D.J. and Gerner, E.W. (2003) Polyamine-dependent gene expression. *Cell Mol Life Sci*, 60, 1394-1406.

Coffino, P. (2001a) Antizyme, a mediator of ubiquitin-independent proteasomal degradation. *Biochimie*, 83, 319-323.

Coffino, P. (2001b) Regulation of cellular polyamines by antizyme. *Nat Rev Mol Cell Biol*, 2, 188-194.

Cohen, S.S. (1998) A guide to the polymianes. In. oxford university press, p. 53.

Colas, P., Cohen, B., Jessen, T., Grishina, I., McCoy, J. and Brent, R. (1996) Genetic selection of peptide aptamers that recognize and inhibit cyclin-dependent kinase 2. *Nature*, 380, 548-550.

Coscoy, L. and Ganem, D. (2003) PHD domains and E3 ubiquitin ligases: viruses make the connection. *Trends Cell Biol*, 13, 7-12.

Coscoy, L., Sanchez, D.J. and Ganem, D. (2001) A novel class of herpesvirus-encoded membrane-bound E3 ubiquitin ligases regulates endocytosis of proteins involved in immune recognition. *J Cell Biol*, 155, 1265-1273.

Deveraux, Q., Ustrell, V., Pickart, C. and Rechsteiner, M. (1994) A 26 S protease subunit that binds ubiquitin conjugates. *J Biol Chem*, 269, 7059-7061.

Dohmen, R.J., Stappen, R., McGrath, J.P., Forrova, H., Kolarov, J., Goffeau, A. and Varshavsky, A. (1995) An essential yeast gene encoding a homolog of ubiquitin-activating enzyme. *J Biol Chem*, 270, 18099-18109.

Elias, S., Bercovich, B., Kahana, C., Coffino, P., Fischer, M., Hilt, W., Wolf, D.H. and Ciechanover, A. (1995) Degradation of ornithine decarboxylase by the mammalian and yeast 26S proteasome complexes requires all the components of the protease. *Eur J Biochem*, 229, 276-283.

Elliott, P.J., Zollner, T.M. and Boehncke, W.H. (2003) Proteasome inhibition: a new anti-inflammatory strategy. *J Mol Med*, 81, 235-245.

References

Ellison, M.J. and Hochstrasser, M. (1991) Epitope-tagged ubiquitin. A new probe for analyzing ubiquitin function. *J Biol Chem*, 266, 21150-21157.

Elsasser, S., Chandler-Militello, D., Muller, B., Hanna, J. and Finley, D. (2004) Rad23 and Rpn10 serve as alternative ubiquitin receptors for the proteasome. *J Biol Chem*, 279, 26817-26822.

Feith, D.J., Shantz, L.M. and Pegg, A.E. (2001) Targeted antizyme expression in the skin of transgenic mice reduces tumor promoter induction of ornithine decarboxylase and decreases sensitivity to chemical carcinogenesis. *Cancer Res*, 61, 6073-6081.

Figueiredo-Pereira, M.E., Chen, W.E., Li, J. and Johdo, O. (1996) The antitumor drug aclacinomycin A, which inhibits the degradation of ubiquitinated proteins, shows selectivity for the chymotrypsin-like activity of the bovine pituitary 20 S proteasome. *J Biol Chem*, 271, 16455-16459.

Fong, L.Y., Feith, D.J. and Pegg, A.E. (2003) Antizyme overexpression in transgenic mice reduces cell proliferation, increases apoptosis, and reduces N-nitrosomethylbenzylamine-induced forestomach carcinogenesis. *Cancer Res*, 63, 3945-3954.

Fonzi, W.A. (1989) Regulation of Saccharomyces cerevisiae ornithine decarboxylase expression in response to polyamine. *J Biol Chem*, 264, 18110-18118.

Gandre, S., Bercovich, Z. and Kahana, C. (2002) Ornithine decarboxylase-antizyme is rapidly degraded through a mechanism that requires functional ubiquitin-dependent proteolytic activity. *Eur J Biochem*, 269, 1316-1322.

Gandre, S. and Kahana, C. (2002) Degradation of ornithine decarboxylase in Saccharomyces cerevisiae is ubiquitin independent. *Biochem Biophys Res Commun*, 293, 139-144.

Ghislain, M., Udvardy, A. and Mann, C. (1993) S. cerevisiae 26S protease mutants arrest cell division in G2/metaphase. *Nature*, 366, 358-362.

Ghoda, L., van Daalen Wetters, T., Macrae, M., Ascherman, D. and Coffino, P. (1989) Prevention of rapid intracellular degradation of ODC by a carboxyl-terminal truncation. *Science*, 243, 1493-1495.

Gietz, R.D. and Sugino, A. (1988) New yeast-Escherichia coli shuttle vectors constructed with in vitro mutagenized yeast genes lacking six-base pair restriction sites. *Gene*, 74, 527-534.

References

Gietz, R.D. and Woods, R.A. (2002) Transformation of yeast by lithium acetate/single-stranded carrier DNA/polyethylene glycol method. *Methods Enzymol*, 350, 87-96.

Gimelli, G., Giglio, S., Zuffardi, O., Alhonen, L., Suppola, S., Cusano, R., Lo Nigro, C., Gatti, R., Ravazzolo, R. and Seri, M. (2002) Gene dosage of the spermidine/spermine N(1)-acetyltransferase (SSAT) gene with putrescine accumulation in a patient with a Xp21.1p22.12 duplication and keratosis follicularis spinulosa decalvans (KFSD). *Hum Genet*, 111, 235-241.

Glickman, M.H., Rubin, D.M., Coux, O., Wefes, I., Pfeifer, G., Cjeka, Z., Baumeister, W., Fried, V.A. and Finley, D. (1998) A subcomplex of the proteasome regulatory particle required for ubiquitin-conjugate degradation and related to the COP9-signalosome and eIF3. *Cell*, 94, 615-623.

Gritli-Linde, A., Nilsson, J., Bohlooly, Y.M., Heby, O. and Linde, A. (2001) Nuclear translocation of antizyme and expression of ornithine decarboxylase and antizyme are developmentally regulated. *Dev Dyn*, 220, 259-275.

Gruendler, C., Lin, Y., Farley, J. and Wang, T. (2001) Proteasomal degradation of Smad1 induced by bone morphogenetic proteins. *J Biol Chem*, 276, 46533-46543.

Gupta, R., Hamasaki-Katagiri, N., White Tabor, C. and Tabor, H. (2001) Effect of spermidine on the in vivo degradation of ornithine decarboxylase in Saccharomyces cerevisiae. *Proc Natl Acad Sci U S A*, 98, 10620-10623.

Haas, A.L. and Rose, I.A. (1982) The mechanism of ubiquitin activating enzyme. A kinetic and equilibrium analysis. *J Biol Chem*, 257, 10329-10337.

Halmekyto, M., Hyttinen, J.M., Sinervirta, R., Utriainen, M., Myohanen, S., Voipio, H.M., Wahlfors, J., Syrjanen, S., Syrjanen, K., Alhonen, L. and et al. (1991) Transgenic mice aberrantly expressing human ornithine decarboxylase gene. *J Biol Chem*, 266, 19746-19751.

Hampton, R.Y. (2002) ER-associated degradation in protein quality control and cellular regulation. *Curr Opin Cell Biol*, 14, 476-482.

Handley-Gearhart, P.M., Stephen, A.G., Trausch-Azar, J.S., Ciechanover, A. and Schwartz, A.L. (1994) Human ubiquitin-activating enzyme, E1. Indication of potential nuclear and cytoplasmic subpopulations using epitope-tagged cDNA constructs. *J Biol Chem*, 269, 33171-33178.

Hatakeyama, S., Yada, M., Matsumoto, M., Ishida, N. and Nakayama, K.I. (2001) U box proteins as a new family of ubiquitin-protein ligases. *J Biol Chem*, 276, 33111-33120.

References

Hayashi, S., Murakami, Y. and Matsufuji, S. (1996) Ornithine decarboxylase antizyme: a novel type of regulatory protein. *Trends Biochem Sci*, 21, 27-30.

Heinemeyer, W., Fischer, M., Krimmer, T., Stachon, U. and Wolf, D.H. (1997) The active sites of the eukaryotic 20 S proteasome and their involvement in subunit precursor processing. *J Biol Chem*, 272, 25200-25209.

Heinemeyer, W., Kleinschmidt, J.A., Saidowsky, J., Escher, C. and Wolf, D.H. (1991) Proteinase yscE, the yeast proteasome/multicatalytic-multifunctional proteinase: mutants unravel its function in stress induced proteolysis and uncover its necessity for cell survival. *Embo J*, 10, 555-562.

Heinemeyer, W., Ramos, P.C. and Dohmen, R.J. (2004) The ultimate nanoscale mincer: assembly, structure and active sites of the 20S proteasome core. *Cell Mol Life Sci*, 61, 1562-1578.

Heller, J.S., Fong, W.F. and Canellakis, E.S. (1976) Induction of a protein inhibitor to ornithine decarboxylase by the end products of its reaction. *Proc Natl Acad Sci U S A*, 73, 1858-1862.

Hershko, A. and Ciechanover, A. (1998) The ubiquitin system. *Annu Rev Biochem*, 67, 425-479.

Hershko, A., Heller, H., Elias, S. and Ciechanover, A. (1983) Components of ubiquitin-protein ligase system. Resolution, affinity purification, and role in protein breakdown. *J Biol Chem*, 258, 8206-8214.

Hochstrasser, M. (2000) Evolution and function of ubiquitin-like protein-conjugation systems. *Nat Cell Biol*, 2, E153-157.

Hoege, C., Pfander, B., Moldovan, G.L., Pyrowolakis, G. and Jentsch, S. (2002) RAD6-dependent DNA repair is linked to modification of PCNA by ubiquitin and SUMO. *Nature*, 419, 135-141.

Hoyt, M.A., Broun, M. and Davis, R.H. (2000) Polyamine regulation of ornithine decarboxylase synthesis in Neurospora crassa. *Mol Cell Biol*, 20, 2760-2773.

Hoyt, M.A., Zhang, M. and Coffino, P. (2003) Ubiquitin-independent mechanisms of mouse ornithine decarboxylase degradation are conserved between mammalian and fungal cells. *J Biol Chem*, 278, 12135-12143.

Huibregtse, J.M., Scheffner, M., Beaudenon, S. and Howley, P.M. (1995) A family of proteins structurally and functionally related to the E6-AP ubiquitin-protein ligase. *Proc Natl Acad Sci U S A*, 92, 2563-2567.

References

Ichiba, T., Matsufuji, S., Miyazaki, Y., Murakami, Y., Tanaka, K., Ichihara, A. and Hayashi, S. (1994) Functional regions of ornithine decarboxylase antizyme. *Biochem Biophys Res Commun*, 200, 1721-1727.

Igarashi, K. and Kashiwagi, K. (1999) Polyamine transport in bacteria and yeast. *Biochem J*, 344 Pt 3, 633-642.

Ivanov, I.P., Anderson, C.B., Gesteland, R.F. and Atkins, J.F. (2004) Identification of a new antizyme mRNA +1 frameshifting stimulatory pseudoknot in a subset of diverse invertebrates and its apparent absence in intermediate species. *J Mol Biol*, 339, 495-504.

Ivanov, I.P., Gesteland, R.F. and Atkins, J.F. (1998) A second mammalian antizyme: conservation of programmed ribosomal frameshifting. *Genomics*, 52, 119-129.

Ivanov, I.P., Matsufuji, S., Murakami, Y., Gesteland, R.F. and Atkins, J.F. (2000a) Conservation of polyamine regulation by translational frameshifting from yeast to mammals. *Embo J*, 19, 1907-1917.

Ivanov, I.P., Rohrwasser, A., Terreros, D.A., Gesteland, R.F. and Atkins, J.F. (2000b) Discovery of a spermatogenesis stage-specific ornithine decarboxylase antizyme: antizyme 3. *Proc Natl Acad Sci U S A*, 97, 4808-4813.

James, P., Halladay, J. and Craig, E.A. (1996) Genomic libraries and a host strain designed for highly efficient two-hybrid selection in yeast. *Genetics*, 144, 1425-1436.

Janne, J., Alhonen, L., Pietila, M. and Keinanen, T.A. (2004) Genetic approaches to the cellular functions of polyamines in mammals. *Eur J Biochem*, 271, 877-894.

Janse, D.M., Crosas, B., Finley, D. and Church, G.M. (2004) Localization to the proteasome is sufficient for degradation. *J Biol Chem*, 279, 21415-21420.

Jariel-Encontre, I., Pariat, M., Martin, F., Carillo, S., Salvat, C. and Piechaczyk, M. (1995) Ubiquitinylation is not an absolute requirement for degradation of c-Jun protein by the 26 S proteasome. *J Biol Chem*, 270, 11623-11627.

Jiang, J., Ballinger, C.A., Wu, Y., Dai, Q., Cyr, D.M., Hohfeld, J. and Patterson, C. (2001) CHIP is a U-box-dependent E3 ubiquitin ligase: identification of Hsc70 as a target for ubiquitylation. *J Biol Chem*, 276, 42938-42944.

Joazeiro, C.A. and Weissman, A.M. (2000) RING finger proteins: mediators of ubiquitin ligase activity. *Cell*, 102, 549-552.

References

Ju, D. and Xie, Y. (2004) Proteasomal degradation of RPN4 via two distinct mechanisms, ubiquitin-dependent and -independent. *J Biol Chem*, 279, 23851-23854.

Kamura, T., Koepp, D.M., Conrad, M.N., Skowyra, D., Moreland, R.J., Iliopoulos, O., Lane, W.S., Kaelin, W.G., Jr., Elledge, S.J., Conaway, R.C., Harper, J.W. and Conaway, J.W. (1999) Rbx1, a component of the VHL tumor suppressor complex and SCF ubiquitin ligase. *Science*, 284, 657-661.

Kern, A.D., Oliveira, M.A., Coffino, P. and Hackert, M.L. (1999) Structure of mammalian ornithine decarboxylase at 1.6 A resolution: stereochemical implications of PLP-dependent amino acid decarboxylases. *Structure Fold Des*, 7, 567-581.

Kim, I., Mi, K. and Rao, H. (2004) Multiple interactions of rad23 suggest a mechanism for ubiquitylated substrate delivery important in proteolysis. *Mol Biol Cell*, 15, 3357-3365.

Kim, K.B., Myung, J., Sin, N. and Crews, C.M. (1999) Proteasome inhibition by the natural products epoxomicin and dihydroeponemycin: insights into specificity and potency. *Bioorg Med Chem Lett*, 9, 3335-3340.

Knipfer, N. and Shrader, T.E. (1997) Inactivation of the 20S proteasome in Mycobacterium smegmatis. *Mol Microbiol*, 25, 375-383.

Knop, M., Siegers, K., Pereira, G., Zachariae, W., Winsor, B., Nasmyth, K. and Schiebel, E. (1999) Epitope tagging of yeast genes using a PCR-based strategy: more tags and improved practical routines. *Yeast*, 15, 963-972.

Koegl, M., Hoppe, T., Schlenker, S., Ulrich, H.D., Mayer, T.U. and Jentsch, S. (1999) A novel ubiquitination factor, E4, is involved in multiubiquitin chain assembly. *Cell*, 96, 635-644.

Laemmli, U.K. (1970) Cleavage of structural proteins during the assembly of the head of bacteriophage T4. *Nature*, 227, 680-685.

Lam, Y.A., Lawson, T.G., Velayutham, M., Zweier, J.L. and Pickart, C.M. (2002) A proteasomal ATPase subunit recognizes the polyubiquitin degradation signal. *Nature*, 416, 763-767.

Leggett, D.S., Hanna, J., Borodovsky, A., Crosas, B., Schmidt, M., Baker, R.T., Walz, T., Ploegh, H. and Finley, D. (2002) Multiple associated proteins regulate proteasome structure and function. *Mol Cell*, 10, 495-507.

References

Lewenhoeck, A. (1678) Observations D. Anthonii Lewenhoeck, de natis e'semine genetali Aminalculis. *Philos. Trans.*, Vol. 12, pp. 1040-1043.

Li, X. and Coffino, P. (1992) Regulated degradation of ornithine decarboxylase requires interaction with the polyamine-inducible protein antizyme. *Mol Cell Biol*, 12, 3556-3562.

Li, X. and Coffino, P. (1994) Distinct domains of antizyme required for binding and proteolysis of ornithine decarboxylase. *Mol Cell Biol*, 14, 87-92.

Lorick, K.L., Jensen, J.P., Fang, S., Ong, A.M., Hatakeyama, S. and Weissman, A.M. (1999) RING fingers mediate ubiquitin-conjugating enzyme (E2)-dependent ubiquitination. *Proc Natl Acad Sci U S A*, 96, 11364-11369.

Lu, Z., Xu, S., Joazeiro, C., Cobb, M.H. and Hunter, T. (2002) The PHD domain of MEKK1 acts as an E3 ubiquitin ligase and mediates ubiquitination and degradation of ERK1/2. *Mol Cell*, 9, 945-956.

Lum, R.T., Kerwar, S.S., Meyer, S.M., Nelson, M.G., Schow, S.R., Shiffman, D., Wick, M.M. and Joly, A. (1998) A new structural class of proteasome inhibitors that prevent NF-kappa B activation. *Biochem Pharmacol*, 55, 1391-1397.

Madura, K. (2004) Rad23 and Rpn10: perennial wallflowers join the melee. *Trends Biochem Sci*, 29, 637-640.

Mamroud-Kidron, E. and Kahana, C. (1994) The 26S proteasome degrades mouse and yeast ornithine decarboxylase in yeast cells. *FEBS Lett*, 356, 162-164.

Mamroud-Kidron, E., Rosenberg-Hasson, Y., Rom, E. and Kahana, C. (1994) The 20S proteasome mediates the degradation of mouse and yeast ornithine decarboxylase in yeast cells. *FEBS Lett*, 337, 239-242.

Matsufuji, S., Matsufuji, T., Miyazaki, Y., Murakami, Y., Atkins, J.F., Gesteland, R.F. and Hayashi, S. (1995) Autoregulatory frameshifting in decoding mammalian ornithine decarboxylase antizyme. *Cell*, 80, 51-60.

Maytal-Kivity, V., Reis, N., Hofmann, K. and Glickman, M.H. (2002) MPN+, a putative catalytic motif found in a subset of MPN domain proteins from eukaryotes and prokaryotes, is critical for Rpn11 function. *BMC Biochem*, 3, 28.

McGrath, J.P., Jentsch, S. and Varshavsky, A. (1991) UBA 1: an essential yeast gene encoding ubiquitin-activating enzyme. *Embo J*, 10, 227-236.

References

Megosh, L., Gilmour, S.K., Rosson, D., Soler, A.P., Blessing, M., Sawicki, J.A. and O'Brien, T.G. (1995) Increased frequency of spontaneous skin tumors in transgenic mice which overexpress ornithine decarboxylase. *Cancer Res*, 55, 4205-4209.

Meng, L., Kwok, B.H., Sin, N. and Crews, C.M. (1999) Eponemycin exerts its antitumor effect through the inhibition of proteasome function. *Cancer Res*, 59, 2798-2801.

Min, S.H., Simmen, R.C., Alhonen, L., Halmekyto, M., Porter, C.W., Janne, J. and Simmen, F.A. (2002) Altered levels of growth-related and novel gene transcripts in reproductive and other tissues of female mice overexpressing spermidine/spermine N1-acetyltransferase (SSAT). *J Biol Chem*, 277, 3647-3657.

Mitchell, J.L. and Chen, H.J. (1990) Conformational changes in ornithine decarboxylase enable recognition by antizyme. *Biochim Biophys Acta*, 1037, 115-121.

Mullis, K., Faloona, F., Scharf, S., Saiki, R., Horn, G. and Erlich, H. (1986) Specific enzymatic amplification of DNA in vitro: the polymerase chain reaction. *Cold Spring Harb Symp Quant Biol*, 51 Pt 1, 263-273.

Murakami, Y. and Hayashi, S. (1985) Role of antizyme in degradation of ornithine decarboxylase in HTC cells. *Biochem J*, 226, 893-896.

Murakami, Y., Matsufuji, S., Kameji, T., Hayashi, S., Igarashi, K., Tamura, T., Tanaka, K. and Ichihara, A. (1992) Ornithine decarboxylase is degraded by the 26S proteasome without ubiquitination. *Nature*, 360, 597-599.

Namy, O., Rousset, J.P., Napthine, S. and Brierley, I. (2004) Reprogrammed genetic decoding in cellular gene expression. *Mol Cell*, 13, 157-168.

Newman, R.M., Mobascher, A., Mangold, U., Koike, C., Diah, S., Schmidt, M., Finley, D. and Zetter, B.R. (2004) Antizyme targets cyclin D1 for degradation. A novel mechanism for cell growth repression. *J Biol Chem*, 279, 41504-41511.

Orlowski, M., Cardozo, C. and Michaud, C. (1993) Evidence for the presence of five distinct proteolytic components in the pituitary multicatalytic proteinase complex. Properties of two components cleaving bonds on the carboxyl side of branched chain and small neutral amino acids. *Biochemistry*, 32, 1563-1572.

Pamer, E. and Cresswell, P. (1998) Mechanisms of MHC class I--restricted antigen processing. *Annu Rev Immunol*, 16, 323-358.

References

Park, M.H., Wolff, E.C. and Folk, J.E. (1993) Is hypusine essential for eukaryotic cell proliferation? *Trends Biochem Sci*, 18, 475-479.

Peebles, C.L., Gegenheimer, P. and Abelson, J. (1983) Precise excision of intervening sequences from precursor tRNAs by a membrane-associated yeast endonuclease. *Cell*, 32, 525-536.

Pendeville, H., Carpino, N., Marine, J.C., Takahashi, Y., Muller, M., Martial, J.A. and Cleveland, J.L. (2001) The ornithine decarboxylase gene is essential for cell survival during early murine development. *Mol Cell Biol*, 21, 6549-6558.

Peters, J.M. (2002) The anaphase-promoting complex: proteolysis in mitosis and beyond. *Mol Cell*, 9, 931-943.

Pickart, C.M. (2001) Mechanisms underlying ubiquitination. *Annu Rev Biochem*, 70, 503-533.

Pickart, C.M. (2002) DNA repair: right on target with ubiquitin. *Nature*, 419, 120-121.

Pickart, C.M. and Cohen, R.E. (2004) Proteasomes and their kin: proteases in the machine age. *Nat Rev Mol Cell Biol*, 5, 177-187.

Pietila, M., Alhonen, L., Halmekyto, M., Kanter, P., Janne, J. and Porter, C.W. (1997) Activation of polyamine catabolism profoundly alters tissue polyamine pools and affects hair growth and female fertility in transgenic mice overexpressing spermidine/spermine N1-acetyltransferase. *J Biol Chem*, 272, 18746-18751.

Raasi, S., Schmidtke, G. and Groettrup, M. (2001) The ubiquitin-like protein FAT10 forms covalent conjugates and induces apoptosis. *J Biol Chem*, 276, 35334-35343.

Ramos, P.C., Hockendorff, J., Johnson, E.S., Varshavsky, A. and Dohmen, R.J. (1998) Ump1p is required for proper maturation of the 20S proteasome and becomes its substrate upon completion of the assembly. *Cell*, 92, 489-499.

Reinstein, E., Scheffner, M., Oren, M., Ciechanover, A. and Schwartz, A. (2000) Degradation of the E7 human papillomavirus oncoprotein by the ubiquitin-proteasome system: targeting via ubiquitination of the N-terminal residue. *Oncogene*, 19, 5944-5950.

Robzyk, K. and Kassir, Y. (1992) A simple and highly efficient procedure for rescuing autonomous plasmids from yeast. *Nucleic Acids Res*, 20, 3790.

References

Rock, K.L. and Goldberg, A.L. (1999) Degradation of cell proteins and the generation of MHC class I-presented peptides. *Annu Rev Immunol*, 17, 739-779.

Rosenberg-Hasson, Y., Bercovich, Z., Ciechanover, A. and Kahana, C. (1989) Degradation of ornithine decarboxylase in mammalian cells is ATP dependent but ubiquitin independent. *Eur J Biochem*, 185, 469-474.

Ruepp, A., Eckerskorn, C., Bogyo, M. and Baumeister, W. (1998) Proteasome function is dispensable under normal but not under heat shock conditions in Thermoplasma acidophilum. *FEBS Lett*, 425, 87-90.

Scheffner, M., Huibregtse, J.M. and Howley, P.M. (1994) Identification of a human ubiquitin-conjugating enzyme that mediates the E6-AP-dependent ubiquitination of p53. *Proc Natl Acad Sci U S A*, 91, 8797-8801.

Scheffner, M., Nuber, U. and Huibregtse, J.M. (1995) Protein ubiquitination involving an E1-E2-E3 enzyme ubiquitin thioester cascade. *Nature*, 373, 81-83.

Schwartz, B., Hittelman, A., Daneshvar, L., Basu, H.S., Marton, L.J. and Feuerstein, B.G. (1995) A new model for disruption of the ornithine decarboxylase gene, SPE1, in Saccharomyces cerevisiae exhibits growth arrest and genetic instability at the MAT locus. *Biochem J*, 312 (Pt 1), 83-90.

Seufert, W. and Jentsch, S. (1990) Ubiquitin-conjugating enzymes UBC4 and UBC5 mediate selective degradation of short-lived and abnormal proteins. *Embo J*, 9, 543-550.

Shantz, L.M., Feith, D.J. and Pegg, A.E. (2001) Targeted overexpression of ornithine decarboxylase enhances beta-adrenergic agonist-induced cardiac hypertrophy. *Biochem J*, 358, 25-32.

Shiba, T., Mizote, H., Kaneko, T., Nakajima, T. and Kakimoto, Y. (1971) Hypusine, a new amino acid occurring in bovine brain. Isolation and structural determination. *Biochim Biophys Acta*, 244, 523-531.

Sikorski, R.S. and Hieter, P. (1989) A system of shuttle vectors and yeast host strains designed for efficient manipulation of DNA in Saccharomyces cerevisiae. *Genetics*, 122, 19-27.

Skerra, A. (2000) Lipocalins as a scaffold. *Biochim Biophys Acta*, 1482, 337-350.

Tamori, A., Nishiguchi, S., Kuroki, T., Koh, N., Kobayashi, K., Yano, Y. and Otani, S. (1995) Point mutation of ornithine decarboxylase gene in human hepatocellular carcinoma. *Cancer Res*, 55, 3500-3503.

References

Tanaka, K., Suzuki, T. and Chiba, T. (1998) The ligation systems for ubiquitin and ubiquitin-like proteins. *Mol Cells*, 8, 503-512.

Tomitori, H., Kashiwagi, K., Sakata, K., Kakinuma, Y. and Igarashi, K. (1999) Identification of a gene for a polyamine transport protein in yeast. *J Biol Chem*, 274, 3265-3267.

Toth, C. and Coffino, P. (1999) Regulated degradation of yeast ornithine decarboxylase. *J Biol Chem*, 274, 25921-25926.

Treier, M., Staszewski, L.M. and Bohmann, D. (1994) Ubiquitin-dependent c-Jun degradation in vivo is mediated by the delta domain. *Cell*, 78, 787-798.

Uemura, T., Tachihara, K., Tomitori, H., Kashiwagi, K. and Igarashi, K. (2005) Characteristics of the polyamine transporter TPO1 and regulation of its activity and cellular localization by phosphorylation. *J Biol Chem*.

Unno, M., Mizushima, T., Morimoto, Y., Tomisugi, Y., Tanaka, K., Yasuoka, N. and Tsukihara, T. (2002) The structure of the mammalian 20S proteasome at 2.75 A resolution. *Structure (Camb)*, 10, 609-618.

van Daalen Wetters, T., Macrae, M., Brabant, M., Sittler, A. and Coffino, P. (1989) Polyamine-mediated regulation of mouse ornithine decarboxylase is posttranslational. *Mol Cell Biol*, 9, 5484-5490.

Verma, R., Aravind, L., Oania, R., McDonald, W.H., Yates, J.R., 3rd, Koonin, E.V. and Deshaies, R.J. (2002) Role of Rpn11 metalloprotease in deubiquitination and degradation by the 26S proteasome. *Science*, 298, 611-615.

Verma, R., Chen, S., Feldman, R., Schieltz, D., Yates, J., Dohmen, J. and Deshaies, R.J. (2000) Proteasomal proteomics: identification of nucleotide-sensitive proteasome-interacting proteins by mass spectrometric analysis of affinity-purified proteasomes. *Mol Biol Cell*, 11, 3425-3439.

Verma, R., Oania, R., Graumann, J. and Deshaies, R.J. (2004) Multiubiquitin chain receptors define a layer of substrate selectivity in the ubiquitin-proteasome system. *Cell*, 118, 99-110.

Volker, C. and Lupas, A.N. (2002) Molecular evolution of proteasomes. *Curr Top Microbiol Immunol*, 268, 1-22.

Wallace, H.M., Fraser, A.V. and Hughes, A. (2003) A perspective of polyamine metabolism. *Biochem J*, 376, 1-14.

References

Wang, C., Deng, L., Hong, M., Akkaraju, G.R., Inoue, J. and Chen, Z.J. (2001) TAK1 is a ubiquitin-dependent kinase of MKK and IKK. *Nature*, **412, 346-351.**

Xie, Y. and Varshavsky, A. (2001) RPN4 is a ligand, substrate, and transcriptional regulator of the 26S proteasome: a negative feedback circuit. *Proc Natl Acad Sci U S A*, **98, 3056-3061.**

Yao, T. and Cohen, R.E. (2002) A cryptic protease couples deubiquitination and degradation by the proteasome. *Nature*, **419, 403-407.**

Zhang, M., Pickart, C.M. and Coffino, P. (2003) Determinants of proteasome recognition of ornithine decarboxylase, a ubiquitin-independent substrate. *Embo J*, **22, 1488-1496.**

Zhu, C., Karplus, K., Grate, L. and Coffino, P. (2000) A homolog of mammalian antizyme is present in fission yeast Schizosaccharomyces pombe but not detected in budding yeast Saccharomyces cerevisiae. *Bioinformatics*, **16, 478-481.**

Zhu, C., Lang, D.W. and Coffino, P. (1999) Antizyme2 is a negative regulator of ornithine decarboxylase and polyamine transport. *J Biol Chem*, **274, 26425-26430.**

Appendix

APS	Ammoniumperoxodisulphate
bp	Basepair
BSA	Bovine serum albumin
cDNA	Complementary DNA
CEN	Centromer-Sequence
Cys	Cysteine
Da	Dalton
dNTP	Deoxynucleotide tri-phosphate
DNA	Deoxyribonucleic acid
DTT	Dithiothreitol
HA	Hemagglutinin influenza virus epitope tag
g	Relative centrifugal force
kDa	Kilodalton
Min	Minutes
OD	Optical density
ORF	Open reading frame
PCR	Polymerase chain reaction
pH	Negative log of hydrogen ion concentration
RNA	Ribonucleic acid
Sec	Seconds
ts	Temperature sensitive
RT	Room temperature
RNase	Ribonuclease

Acknowledgements

Eidesstattliche Erklärung

Ich versichere, daß ich die von mir vorgelegte Dissertation selbständig angefertigt, die benutzten Quellen und Hilfsmittel vollständig angegeben und die Stellen der Arbeit - einschließlich Tabellen, Karten und Abbildungen -, die anderen Werken im Wortlaut oder dem Sinn nach entnommen sind, in jedem Einzelfall als Entlehnung kenntlich gemacht habe; daß diese Dissertation noch keiner anderen Fakultät oder Universität zur Prüfung vorgelegen hat; daß sie - abgesehen von unten angegebenen Teilpublikationen - noch nicht veröffentlicht worden ist sowie, daß ich eine solche Veröffentlichung vor Abschluß des Promotionsverfahrens nicht vornehmen werde. Die Bestimmungen dieser Promotionsordnung sind mir bekannt. Die von mir vorgelegte Dissertation ist von Prof. Dr. R. Jürgen Dohmen betreut worden.

Köln,

März 2005.   **R. Palanimurugan**

Teilpublikationen im Rahmen dieser Arbeit:

Palanimurugan. R., Scheel. H., Hofmann. K, Dohmen. R.J.

Polyamines regulate their synthesis by inducing expression and blocking degradation of ODC antizyme.

EMBO J. 2004 Dec 8;23(24):4857-67.

Lebenslauf

Name: Palani Murugan, Rangasamy

Geburtsdatum: 01.05.1977

Geburtsort: Salem, TN, Indien

Staatsangehörigkeit: Indisch

1991-1992   Gymanasium (SSLC), Tamilnadu, Indien

1992-1994   Abitur (HSc), Tamilnadu, Indien

1994-1997   Bachelor of Science (B. Sc), University of madras, Indien

1997-1999   (Diplom) Master of Science (M. Sc), University of madras, Indien

1999-2001   Junior research fellow
                           Prof. R. Varadarajan's Lab
                           Indian institute of science
                           Bangalore, Indien

2001-2005   Doktorarbeit by Prof. Dr. R. Jürgen Dohmen am
                           Institüt für genetik,
                           Universität zu köln
                           Title: Regulation of polyamine biosynthesis
                                   in *Saccharomyces cerevisiae*

Köln
März 2005   Unterschrift